Analyzing individual-based models of microbial systems

Nabil Mabrouk

N d'ordre: D.U: 2008 EDSPIC: 474

Université Blaise Pascal - Clermont II

École Doctorale
Sciences Pour l'Ingénieur De Clermont-Ferrand

Thèse

Présentée par

Nabil MABROUK

Ingénieur en Industries Alimentaires

DEA en Modélisation en Hydraulique et Environnement

pour obtenir le grade de

Docteur d'Université

Spécialité: Informatique

Analyzing individual-based models of microbial systems

Soutenue publiquement le 7 janvier 2010 devant le jury:

Président :	**David Hill** Professeur, Université Blaise Pascal, Clermont-Ferrand
Rapporteur :	**Cristian Picioreanu** Professeur associé, Université Technique de Delft, Pays-Bas
	Jean-Daniel Zucker Directeur de Recherche, IRD, Paris
Examinateur :	**Théodore Bouchez** Chargé de Recherche, Cemagref, Antony
Directeurs de thèse :	**Guillaume Deffuant** Directeur de recherche, Cemagref, Clermont-Ferrand
	Claude Lobry Professeur, Université de Nice

Acknowledgment

I would like to express my gratitude to all who have contributed to the completion of this thesis in one way or another.

Special thanks go to

- Dr. Guillaume Deffuant and Prof. Claude Lobry for supporting me in the last years and for their guidance during my dissertation.
- Prof. David Hill, Dr. Cristian Picioreanu, Dr. Jean-Daniel Zucker and Dr. Theodore Bouchez who kindly accepted to review my dissertation.
- My colleagues and friends int the Laboratory of Engineering for Complex Systems and in the MERE team for their help and support.
- All the partners of the PATRES EU project for the interesting discussions and the nice moments I shared with them.
- My family and friends for their support during all these years.
- My lovely childrens, Anais, Adam and Léa to whome I dedicate this thesis.

Abstract

There is a debate in ecology between those favoring simple aggregated mathematical models containing only a few equations expressing a small number of general principles and those preferring complex individual-based models that are more structurally realistic with a more detailed representation of the basic processes and interactions at the level of the individuals. In this thesis we attempt to bridge these two approaches by deriving deterministic moment approximation models of microbial individual-based models. We illustrate the approach on the example of biofilm growth with immotile and motile bacteria. We show that moment model can capture the main features of spatial pattern that arise in simplified biofilm individual-based models. Finally we assess the limitation of moment models in capturing the effect of the local fluctuation of the individual's environment.

Résumé

Cette thèse s'inscrit dans le cadre du débat en écologie théorique entre ceux qui favorisent les modèles mathématiques agrégés contenant un nombre relativement faible d'équations exprimant quelques principes généraux et ceux qui préfèrent les modèles individus-centré (multi-agents) qui sont structurellement plus réalistes et comprennent une représentation détaillées des processus et interactions à l'échelle de l'individu. Dans cette thèse nous proposons d'établir un lien entre ces deux approches en dérivant des modèles déterministes basés sur les moments spatiaux et approximant la dynamique des modèles individus-centrés de systèmes microbiens. Nous illustrons cette approche sur l'exemple de croissance d'un biofilm formé par des bactéries mobiles ou immobiles. Nous montrons que les modèles des moments peuvent rendre compte des principales propriétés des structures spatiales obtenues par simulation individus-centrée. Enfin nous explorons les limites des modèles des moments notamment à rendre compte de l'effet des fluctuations locales de l'environnement des individus lorsque celles ci affectent la dynamique du système microbien simulé par le modèle individus-centré.

Contents

Chapter 1

Introduction

Individual-based models (IBMs) and aggregated mathematical models (AMMs) represent two different approaches for modeling ecological systems. There is a debate in ecology between those favoring simple AMMs containing only a few equations expressing a small number of general principles and those preferring complex IBMs that are more "structurally realistic" with a more detailed representation of the basic processes and interactions at the level of the individuals [Aumann 2007]. In this thesis we adopt a *double-modeling* strategy [Lobry 2003] [Deffuant 2004] by using (simple) AMMs to check, analyze and approximate the complex dynamic of IBMs of microbial systems.

1.1 Individual-based perspective of microbial systems

There is an increasing awareness in natural and social sciences that ecological as well as socio-economic systems share common characteristics of complex systems built of interacting individual agents [Levin 1998] [Arthur 1997] [Deffuant 2005] [Rammel 2007]. A major challenge in the study of these complex systems is to understand how seemingly organized collective behavior emerges out of the small-scale interactions between the individuals. Complex system research tends to adopt a bottom-up approach, describing kinds of agents and environments and then experimentally finding out what kind of complex dynamics are exhibited by the system agents [Railsback 2001]. Bottom-up models that represent the individuals and their interactions explicitly are broadly called individual-based models (IBMs).

Microbial ecosystems exhibit many features of such complex systems [Crawford 2005]. They are basically formed with individual microbial cells that encapsulate action, information storage and processing [Kreft 1998]. Because of their small size compared to the size of their environment, microbial cells have a local perception of their world. They react and adapt only to their local environment. The collective behavior that results from these local interactions may, however, exhibit several macroscale regularities and emergent properties.

A Microbial biofilm is one of the most remarkable examples of such a system. Biofilms are thin slimy layers formed by bacteria and their extracellular products on hydrated surfaces. They are ubiquitous in nature and represent the preferential growth mode of many bacterial species. Using advanced microscopy and molecular technologies, researchers have shown that biofilms represent a biological system with

a high level of organization where bacteria form structured, coordinated, functional communities [O'Toole 2000]. The formation of these organized "cities of microbes" is however to a large part mediated by local interactions between the individual cells and with their immediate surrounding environment. By viewing such systems as complex systems formed with locally interacting individuals, microbial ecology can take benefit from tools and approaches (like the individual-based modeling approach) developed to study comparable systems in other fields of science.

1.2 Individual-based modeling of microbial systems

The individual-based modeling approach attempts to capture the properties and dynamic of a population by describing all the actions of its constitutive individuals and their interaction with the environment and with each other. Since the individuals are represented explicitly in the model, the inherent heterogeneity of the population can be readily accounted for by explicitly modeling local differences in the environment and between the individuals [Murphy 2008] [Kreft 1999]. Grimm [Grimm 1999] defines IBMs in the ecological context as " simulation models that treat individuals as unique and discrete entities which have at least one property in addition to age that changes during the life cycle". Since microbe models do not include age (rather size) the definition is usually relaxed to include at least two independent properties (not counting position) [Hellweger 2009]. However, several bottom-up models used in ecology that do not entirely satisfy this definition are still referred to as IBM as long as they treat individuals as discrete entities [Dieckmann 2000].

A survey of the literature on the use of IBMs in microbial ecology shows that the approach is gaining a certain acceptance among microbiologists (see [Hellweger 2009] [Ferrer 2008] for a review). IBM approach has been applied for modeling bacteria systems that arise in wastewater treatment plants [Kreft 2001] [Gujer 2002][Picioreanu 2004][Picioreanu 2005] [Xavier 2005], medical and industrial settings, bacteria in food and other environments [Ginovart 2002][Dens 2005][Emonet 2005]. Hellweger and Bucci [Hellweger 2009] reviewed 46 published papers dealing with IBM application for microbial and phytoplankton systems. They noticed that the use of IBM approach is often motivated by the importance of the population heterogeneity(46%), emergence of population level patterns (24%), discreteness of the individuals (5%) and other reasons (26%) [Hellweger 2009]. The rapidly growing interest in the individual-based modeling approach is to a major part encouraged by the rapid increase in computing power and advances in molecular biology, biochemistry and confocal microscopy during the last 20 years. Powerful computers make it practical to simulate large numbers of individuals in virtual environments while the new experimental tools used in microbiology provide a detailed observation of the individual-level dynamics and raises new questions about the functioning and organization of microbial ecosys-

tems. Examples include the development of the complex structure of microbial biofilms as revealed by confocal microscopy observations and investigated using IBMs [Kreft 2001][Picioreanu 2004] or the adaptative and collaborating strategies of the individuals and their impact on the population level dynamics [Vlachos 2006].

Although IBMs enjoyed the claim of the latest generation models they face criticism as well [Laspidou 2009]. Some of the drawbacks of the IBM approach are simply due to the relatively young age of the approach which still misses a solid methodological framework for developing, implementing and validating IBMs. These issues have been addressed by several recent textbooks that proposed guidelines for building and using individual-based [Grimm 2006][Treuil 2008]. Other limitations however are inherent to the nature of the IBMs as stochastic simulation models. IBMs used in ecology often encompass the randomness of individual-level interactions and evolve in a large state and parameter space that can only be sampled. The complexity and limited generality are often quoted as the main limitations of individual-based modeling [Uchmanski 1996]. Grimm noticed that IBMs usually make more realistic assumptions than simple aggregated mathematical models, but it should not be forgotten that the aim of individual-based modeling is not 'realism' but modeling and that modeling must be guided by a problem or question about a real system, not just by the system itself [Grimm 2006].

1.3 Aggregated mathematical modeling of microbial ecosystems

Traditionally, microbial systems are modeled using aggregated mathematical models. Aggregated mathematical models often take the form of a set of differential and partial differential equations that describe the dynamic of aggregated system-level state variables. The notion of aggregated state variable implies some averaging or grouping of the microscale variables of a system. For instance a system formed with N discrete individuals each characterized by a real-valued state variable X_i, $i = 1..N$ is entirely described by the vector $(X_i)_{i=1..N}$. An aggregated mathematical model of this systems implies the reduction of the individual-based model to a smaller system described with new (aggregated) variables Y_j, $j = 1..M$ with $M << N$. The aggregated mathematical model is then formed with the set of differential (or partial differential) equations of the variables Y_j with the appropriate boundary and initial conditions.

A generic example of aggregated mathematical models used in microbial ecology can be derived for a simple system formed with N individuals each characterized with a mass m_i, $i = 1..N$. Rather than tracking the dynamics of each individual one can define a new aggregated variable Y_j, $j = 1$ corresponding to the total mass of the individuals and derive a differential equation that describe the dynamics of this

variable. The aggregated mathematical model then takes the form of a differential equation:

$$\frac{dY}{dt} = \Phi(Y)Y \tag{1.1}$$

Where $\phi(Y)$ is a function that describes the net growth rate of the population. Equations of this kind still play such a central role in microbial ecology, that many subsequent elaborations of theory have taken them as the starting point. Resource dynamics and spatial variation can be introduced and the models are sometimes interpreted as referring to individuals by assuming that the function $\Phi(Y)$ also describes the interactions at the level of the individual [McKane 2004]. However in most situations these models are generally derived without the need of a detailed knowledge of the interactions between the individuals and rely instead on the assumption that the terms which arise in the governing equations represent the net effects of individual interactions in some generic way [McKane 2004].

The relative simplicity and genericity of aggregated mathematical models from one side and the availability of a solid mathematical and numerical framework to analyze them on the other side have contributed to their successful establishment as a standard for modeling ecological systems. Additionally, for decades microbial ecology struggled as a scientific discipline because of the lack of reliable experimental tools to observe the individual-level structure of microbial ecosystems. Microbes were observed and quantified mainly at the population level [Hellweger 2009][Brehm-Stecher 2004]. For example the bacteria in a wastewater treatment bioreactor were quantified by measuring the volatile suspended solids. Thus, simple aggregated mathematical models were sufficient to exploit such data.

1.4 Debate between IBM and mathematical modeling

There is still an ongoing debate in ecology between those favoring simple system-level mathematical models containing only a few equations expressing a small number of general principles and those preferring complex simulation models that are more "structurally realistic" with a more detailed representations of the basic processes and interactions determining the system dynamic [Aumann 2007]. Grimm [Grimm 2005] noticed that strengths and weakness of IBMs and system-level mathematical models are to a large degree inversely related. Mathematical models are transparent and easy to communicate as they are by definition, formulated in the universal and unambiguous language of mathematics. They can make predictions, require less data for parameter estimation and model validation, may be less prone to error propagation and since they embody only a few heuristic principles, may be likely to lead to general causal understanding [Aumann 2007]. Mathematical models, however, have very limited ability to answer question about how system level behavior emerge out of local interactions. On the other hand, IBMs are designed

to answer such questions by explicitly representing the individuals and their interactions. They often encompass the randomness of individual-level interactions and thus yield realistic system-level patterns. However, one consequence of IBMs being less simple than classical mathematical models is that IBMs are not easy to communicate, analyze and learn from [Grimm 2005]. IBMs evolve in a large parameter state space which can only be sampled [Murrell 2000]. Consequently it is generally not known to what extent the outcome obtained for a set of parameters holds for other sets [Murrell 2000]. Furthermore, if the simulations are stochastic, the ecological signal may only emerge after averaging over a series of realizations, even with a particular parameter set, which may become computationally very expensive [Murrell 2000]. IBM advocate however claims that the approach is more than a new tool that adds to the toolbox of ecologists, but had a significant implication on the way we look to these complex system. By using IBMs the focus is shifted from populations to individuals and several IBMs have demonstrated the potential significance of individual characteristics to population dynamics and ecosystems processes [Grimm 2005].

1.5 Thesis scope

In this thesis, we move beyond the debate of whether of mathematical models or IBMs are more appropriate for representing microbial ecosystems, and concentrate on how the benefits of aggregated mathematical models can be combined with strengths of IBMs. We adopt a "double-modeling" strategy [Deffuant 2004] by using mathematical models along with IBMs in modeling microbial systems. Such an approach can help bridging the perceived gap between individual-based and classical approaches to microbial system modeling. We provide simple illustrations of how mathematical models can be used to analyze and approximate the dynamic of IBMs of microbial systems and assess their potential and limits in reproducing the rich and complex dynamic of the IBM.

We consider an IBM as "a virtual experimental system" designed to encompass the complexity of a microbial system by including features like the discreteness of the individuals, the stochasticity of their interactions, the heterogeneity of their traits and the heterogeneity of their local environment. Once constructed an IBM can be sampled by running computer simulations and/or "modeled" (in the sens of approximated) using aggregated mathematical models. Grimm and Railsback [Grimm 2006] noticed that the approximation of the IBM dynamic using aggregated mathematical models attempts to bridge the perceived gap between individual-based and classical approaches to ecological modeling and expands the ecologists' toolbox by deriving new aggregated mathematical models in which individual-level interaction are acknowledged.

1.5.1 Approximating spatially explicit IBMs with moment methods

We focus on approximating spatially explicit microbial IBM using moments approximation. Moment approximation has shown promise in deriving deterministic aggregated mathematical models that links individual-traits and local interactions to the population level dynamic [Dieckmann 2000][Murrell 2000] [Bolker 1997]. The approach provides a general framework for building direct deterministic approximations of the dynamic of stochastic IBMs if the latter are adequately simplified. There are in the literature several good examples demonstrating that moment models can accurately approximate the dynamic of many stochastic IBMs with the advantages of being deterministic, evolve in a tractable state parameter space and are computationally less expensive than IBMs. One of the aims of this thesis is to investigate whether this approach can also apply to spatially explicit IBMs used in microbiology and assess the potential and limits of the moment approach in capturing the main features of the IBM simulated microbial spatial patterns.

The essence of the moment approach is in deriving the dynamics of spatial moments by considering the processes affecting the spatial patterns and defined at the level of the individuals. They provide an alternative (or extension) to the mean-field approach as moment methods elegantly formalizes the notion of the "individual's-eye view" of the spatial heterogeneity. Consider a population of N individuals each characterized with a spatial location x in the space. The vector $(x_i)_{i=1..N}$ defines the spatial pattern of the population. If the individuals are not located at random in the domain, we refer to the population as having a spatial structure. The spatial pattern change through the individual-level stochastic events (birth, death, movement, ..) and an individual-based model simulation basically provides a realization of this pattern, whereas spatial moments provide a statistical description of the spatial pattern and moment models approximate the dynamic of these statistical quantities in time by considering the effect of the individual-level events.

Spatial moments are usually expressed in term correlation densities functions. The spatial pattern formed by the individuals can be defined by the list of the location of the individuals or in a continuous formulation using the density function $p(x)$ that is peaked at all locations occupied by individuals and is zero elsewhere. For a given spatial pattern p the first spatial moment is defined as:

$$N(p) = \frac{1}{A} \int p(x)dx \tag{1.2}$$

where A is the area of the considered domain. This corresponds to the mean density of individuals in the system. The second moment corresponds to the density of pairs formed by individuals that are vectorial distance ξ apart and is defined as:

$$C(\xi, p) = \frac{1}{A} \int p(x)p(x+\xi)dx \tag{1.3}$$

The third moment, denoted $T(\xi, \xi', p)$ corresponds to the density of triplet of individuals where the first pair in the triplet is separated with a vectorial distance ξ and the second pair with a vectorial distance ξ'. We can also define additional higher order spatial moment, but usually the moment approximation is restricted to the these three spatial moments.

The derivation of a tractable deterministic moment model from the stochastic rules of the IBM requires some level of approximation which are verified by confronting the moment model to the IBM simulations. The main approximation needed for in deriving the moment model is related to the cascade of hierarchy of spatial moment which at some level need to be cut off using a closure equation. Often moment models are limited to the first and second spatial moments and neglect the triple correlation between the positions of three individuals. The underlying assumption is that the probability of encountering a particular triplet configuration is fully given by pair densities [Van Baalen 2000]. Another important approximation is that the moment equation are based on the average neighborhood experienced by the individuals. Hence fluctuations experienced by the individuals are not considered in moment approximation models.

1.6 Methods and tools

1.6.1 IBM description

IBM description is often a critical step. While mathematical models are fully described with a set of equations, variable definitions and a parameter table, the description of an IBM usually requires a combination of mathematical equations, algorithmic rules (if .. then) and lengthy verbal description. This often makes the reproduction of an IBM difficult because of the ambiguity that may arise in the description of the model. Recently a standard protocol for describing IBMs called ODD (Overview, Design concepts and Details) has been proposed [Grimm 2006]. The protocol aims to structure the information about the IBM in a standard sequence (figure 5.1). The logic behind ODD is to provide first the context and general information (Overview), followed by more strategic considerations (Design concepts) and finally more technical details [Grimm 2006]. In this thesis we adopt the ODD framework to describe the IBMs.

1.6.2 IBM implementation

There are several flexible modeling environments for implementing individual-based models. Such environments include several utilities for storing the individuals, performing neighbor search, creating a graphical user interface, analyzing the simulation and tracking the state of the individuals. Agent-based modeling environment of this kind include NetLogo, Repast and Mason. In this work we used Mason library, an

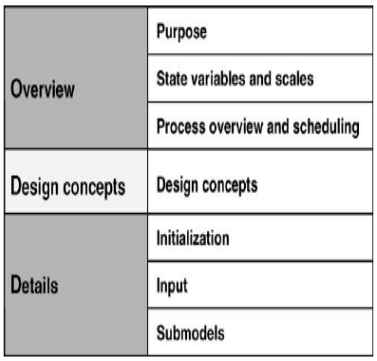

Figure 1.1: The seven elements of the ODD protocol for the description of individual-based models. The elements are grouped into the three blocks: Overview, Design concepts, and Details (reproduced from [Grimm 2006])

open source java-based event-driven library for implementing agent-based models [Luke 2004].

1.6.3 Exploring the IBMs using SimExplorer

We use SimExplorer to manage numerical IBM experimentations. SimExplorer is a framework designed for managing simulation experiments (see: www.simexplorer.org).

1.7 Report outline

The report is organized in six chapters (2-7) with an introductory chapter (chapter 1) and a concluding chapter (chapter 8). In chapter 2-4 we focus on a simple individual-based model of immotile bacteria while in chapters 5-7 we investigate the effect of adding bacteria motility on the observed patterns. Our methodological strategy consists in starting with a detailed IBM that mimics the observed behavior of the individuals, then simplify it to derive to a level that allows the derivation of an approximating aggregated mathematical models. We focus mainly on the derivation of moment approximation models that capture the main features of the spatial pattern dynamic. Nevertheless, we provide a comparison to a diffusion-reaction models in chapter 2.

- In chapter 2 we compare a simple spatially-explicit individual-based (IBM) for bacteria colony growth involving immotile bacteria with an equivalent diffusion-reaction model. Both model are extracted from the literature [Kreft 1998] for the IBM and [Eberl 2001] for the diffusion-reaction model. Our aim behind this comparison is to illustrate the potential and limit of each approach.

- In chapter 3 we simplify the colony growth IBM and approximate the simplified IBM with an aggregated mathematical moment model.
- In chapter 4 we investigate the stationary patterns that arise in a system with immotile bacteria and compare these patterns to those yielded by an approximating moment model.
- In chapter 5 to 7 we focus on a new individual-based model that includes bacteria surface-associated motility. The originality of this model is in assuming that the excretion of exopolymeric substances by the bacteria tend to reduces their migration capacity yielding a rich variety of spatial patterns. In chapter 5 we present the detailed individual-based model
- In chapter 6 we provide a first simplification of the detailed individual-based model in which we keep the exopolymeric substance dynamic and approximate the simplified model using moment approximation techniques
- In chapter 7 we provide a further simplification of the model that still allow to reproduce the main patterns observed in the previous models. We compare the simplified IBM results to those obtain with an approximating moment model.
- Finally, in chapter 8 we summarize the main results and propose some perspectives.

Chapter 2

Microbial colony growth: comparison of an individual-based model and diffusion-reaction model

Contents

Diffusion-reaction models (DRM) are traditionally used for simulating the formation of spatial patterns in biological systems [Murray 2001]. A vast mathematical theory for DRMs and a considerable body of literature of their applications in biology and microbial systems now exist. In this chapter we compare an individual-based model (IBM) adapted from [Kreft 1998] and a diffusion-reaction model described in [Eberl 2001]. Both models represent the core of several more complex microbial biofilm models involving multiple microbial groups and metabolites [Kreft 2001][Eberl 2001][Picioreanu 2004][Xavier 2005]. We use both models to simulate the growth of a microbial colony initiated with a single cell located at the center of a squared two-dimensional domain. The cell grows by uptaking a diffusive nutrient which concentration is imposed at the domain boundary. We propose to compare the spatial patterns of the simulated colonies yielded by both models in two different growth regimes: the 'reaction-limited' regime where the growth of the

bacteria is limited by their nutriment uptake capacity and the 'diffusion-limited' regime in which the bacteria growth is limited by the nutrient transport. Through this comparison, we aim to illustrate the potential and limitation of each approach.

The chapter is organized in six sections. The first section introduces the problem of modeling microbial spatial patterns using IBMs and DRMs. In the second section we present the IBM using the ODD (Overview, Design Concepts and Details) protocol recommended in [Grimm 2006]. In the third section we simulate the growth of a colony in the 'reaction-limited' and the 'diffusion-limited' regimes. In the fourth section we present the aggregated diffusion-reaction model. In the fifth section we compare the diffusion-reaction model pattern to the average pattern yielded by the IBM. Finally we discuss the limitation and potential of each approach.

2.1 Modeling microbial spatial patterns

The problem of aggregation of microbial cells, in particular bacteria, is a central one in microbial ecology. Depending on the bacterial species and the culture conditions, individual cells can form colonies [Ben-Jacob 2000], flocs [Schmid 2003], granules [Morgenroth 1997] and biofilms [Costerton 1995] that exhibit a great diversity of forms. Such patterns are often observable at the level of the population but are to a large extent mediated by the processes taking place at the level of the individual cells. Much effort is dedicated to explore the linkage between these levels. In particular how changes in individuals' responses to their environment translate into changes in observable patterns and conversely how the emergence of these spatial structures affect the dynamic of the individuals.

IBMs and aggregated mathematical models based on the diffusion-reaction equation framework have both been extensively used to investigate how these spatial structures form and evolve in time [Grimson 1994] [Kreft 2001] [Picioreanu 2004] [Lacasta 1999][Eberl 2001][Cogan 2004][Alpkvist 2007]. While IBMs attempt to simulate the development of microbial patterns by specifying the behavioral and interactions rules at the level of the discrete individuals, diffusion-reaction models represent the pattern as an entity (a density field) and attempt to capture how this entity evolve in time. The diffusion-reaction model is usually considered as the continuum limit of the IBM when the number of the individuals is large. This implies that the diffusion-reaction model can be derived rigorously from the rules stated in the IBM. However in practice, the derivation of the diffusion-reaction equation from rigorous considerations of the individual-level rules is often complex and feasible only for some ideal systems. Consequently, and as will be illustrated in this chapter (section 3), assumptions and simplifications have to be made in the development of the diffusion-reaction model and comparison of the diffusion-reaction model to the IBM can be helpful to measure the impact of these simplifications.

Kreft *et al.* [Kreft 1998] proposed an original IBM (called Bacsim) involving discrete representation of the individual cells and an explicit description of their processes (growth, division, shoving). The shoving process, a mechanisms by which the individuals push each others to relax overlapping, is the main process responsible of the colony expansion. In the diffusion-reaction mathematical model proposed in [Eberl 2001] the bacteria spatial distribution is represented with a biomass concentration field which dynamic is given by a diffusion-reaction mass balance equation. The nutrient dynamic in both models is represented identically using a diffusion-reaction mass balance equation. The models differ essentially by the way they represent the biomass (discrete versus continuous) and the biomass-related processes, especially biomass redistribution. The growth of the bacteria increases the local density of the biomass which needs to be redistributed over space. In the IBM rules are set to place the newborn cell close to the mother cell and the final distribution of bacteria results from the self-organization of the individuals through a shoving process. This mechanisms is described in the AMMs proposed in [Eberl 2001] as a density-dependent diffusion. The biomass diffusion increases with the increase of the local density of biomass.

We shall note that an alternative to the aggregated diffusion-reaction mathematical model proposed in [Eberl 2001] is to consider the biomass as a viscous fluid as in the Dckery-Klapper model [Dockery 2001][Cogan 2004]. The biomass is then described with a density and a pressure fields. The growth of the biomass increases the local pressure inducing an advective transport of the biomass. The biomass advective vector u is linked to the local pressure gradient ∇p through the Darcy law:

$$u = -\lambda \nabla p \tag{2.1}$$

where λ is the Darcy constant. Compared to the DRM proposed by Eberl [Eberl 2001], this model is much more accepted and has been extended to multiple microbial types [Alpkvist 2007] The Dockery-Klapper model [Dockery 2001] however involves an additional state variable (pressure p) and more complex boundaries conditions at the biofilm/bulk interface. For simplicity we consider the Eberl model in this chapter.

2.2 Individual-based model

We describe an IBM for a system initially formed with a bacterial cell located in the center a two dimensional squared domain. The model is a simplified version of Kreft's IBM Bacsim simulating the growth of a single *Escherichia coli* cell into a colony[Kreft 1998].

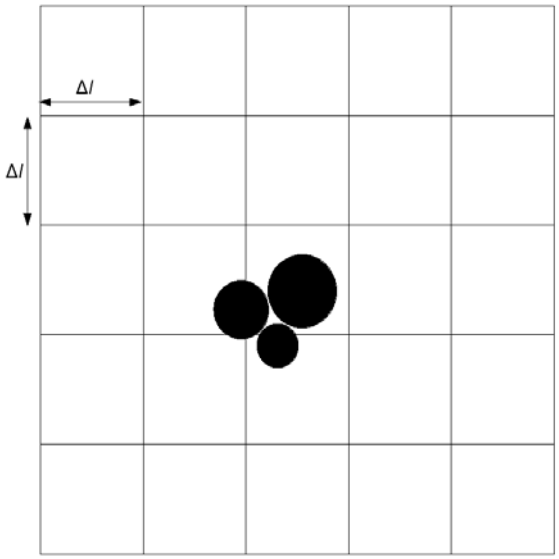

Figure 2.1: Zoomed view of the IBM spatial domain: bacterial cells (discs) and patches (squares with a side Δl). A bacterium with continuous coordinates x,y is contained in the patch $i = floor(x/\Delta l)$, $j = floor(y/\Delta l)$.

2.3 Model description

2.3.1 Overview

2.3.1.1 Purpose

The aim of the model is to investigate how colony patterns emerge from the local interactions between the individual cells.

2.3.1.2 State variables

The model is a two-dimensional representation of a domain and comprises two entities: bacterial cells and their local environment (patches) (figure 2.1). Bacterial cells are represented as discs. They are characterized by the state variables: continuous position (x, y), individual mass (m) and individual substrate uptake rate (r)(table 2.1).

A patch (i, j) is characterized by two state variables: substrate concentration $(s(i, j))$ and a substrate uptake rate $(r_s(i, j))$. The later corresponds to the sum of uptake rates of the individual cells contained within the patch (table 2.1).

2.3.1.3 Process Overview and scheduling

We consider a virtual population of bacterial cells initiated with a single cell in the center of squared domain. We suppose that the domain holds an initial stock of a

	Variable	Description
Bacterium state	x, y	Continuous position of the center of the bacterium
	m	Mass
	r	Individual substrate uptake rate
Patch state	s	Substrate concentration
	r_s	Reaction rate (sum of substrate uptake rates of the individual cells contained within the patch)

Table 2.1: State variables of the individual-based model

Parameters	Description	Unit	Value
s_0	Initial substrate concentration	kg/m^2	1.0
N_0	Initial number of individuals		1
m_0	Initial mass of the individual	kg	10^{-9}

Table 2.2: Individual-based model initialization

diffusive substrate consumed by the bacteria. In the model, an individual bacterial cell grows by uptaking substrate from its local environment at a rate that depends on the local substrate concentration and on its individual mass. If the mass of the individual becomes higher than a critical value, the individual divides into two identical adjacent individuals.

2.3.2 Design Concepts

- **Emergence**: the spatial pattern of the colony emerges out of the local interaction between the individuals and between the individuals and their environment.
- **Interaction**: individuals interact with the environment by up-taking substrate. They compete with each others for substrate and for space.
- **Stochasticity**: the only stochastic process that we included in the model is the selection of the location of the newborn individual after a division event.

2.3.3 Details

2.3.3.1 Initialization

We initialize the model with a single individual $N_0 = 1$ located at the center of the domain $x_0 = L/2, y_0 = L/2$ and having an initial mass m_0. Initially, the substrate is uniformly distributed over the domain. The initial substrate concentration is s_0 for all spatial patches (i, j).

2.3.3.2 Submodels

- **Bacteria growth model:** growth is modeled by allowing the individuals mass to increase proportionally to individuals nutrient uptake rate. As the nutrient has to be taken up through the cell's surface, it is straightforward to assume that uptake is proportional to surface area [Button 1993] [Kreft 1998]. The changes of surface-to-volume ratio during the cell cycle would result in non-exponentiality of the cell's growth curve if uptake limits growth [Kreft 1998]. However, after a long controversy, it is now generally assumed that the growth of a single cell does not deviate significantly from the exponential growth law [Koch 1993]. Thus, we suppose that an individual cell uptakes substrate proportionally to its mass and according to Monod growth kinetic. The net growth rate of an individual cell is then given by:

$$\frac{dm}{dt} = m\mu_{max}\frac{s}{s+k_s} \tag{2.2}$$

  where m is the mas of the individual, s is the substrate concentration in the spatial patch corresponding to the cell position, μ_{max} is the maximum growth rate, k_s is the affinity factor or the half-saturation constant as k_s corresponds to the substrate concentration for which the growth rate of the individual is $\mu_{max}/2$.

- **Bacteria division:** one of the simplest way to model bacteria division with any pretense to reality is to make the individual cell divide once its mass reaches a critical value (denoted $m_d c$). The mother cell is divided into two daughter cells each having a mass corresponding to half of the mass of the mother cell. One of the daughter cells is placed at the position of the mother cell while the second one is placed randomly in an adjacent position.

- **Shoving relaxation model:** adjacent bacteria may overlap when their size increase or after a division event. The overlap of the individual is relaxed using an algorithm that mimics a shoving mechanism adapted from [Kreft 1998]. If a bacterium with radius a is overlapped with n neighboring cells, it is displaced with a shoving vector d calculated using the following equation adapted from [Kreft 2001]:

$$d = \sum_{k=1:n} \frac{a + a_k - d_k}{2} u_k \tag{2.3}$$

  a_k is the radius of the neighbor cell k, d_k is the Euclidean distance from the center of the bacterium to the center the k^{th} neighboring cell and u_k is a vector directed from the center of neighbor bacterium k towards the center of the bacterium and having a unitary norm.

- **Local reaction rate calculation:** an individual located within a patch consumes an amount of the substrate available within the patch. If a patch

contains more than one individual, then we calculate the patch reaction rate by summing the uptake rates of the individuals contained within the patch:

$$r_s(i,j) = \frac{1}{\Delta A} \sum_{k=1}^{N_k} \left(\frac{dm}{dt} \right)_k \tag{2.4}$$

where ΔA is the area of the patch, N_k the number of individuals within the patch

- **Substrate mass balance:** we suppose that the substrate is provided to the domain through the boundary by fixing a constant level of substrate at the boundary. Inside the domain, we suppose that the substrate is transported by diffusion. The substrate spatial distribution can be obtained obtained by solving the diffusion-reaction equation:

$$\frac{\partial s}{\partial t} = D_s \nabla^2 s - r_s \tag{2.5}$$

where D_s is the nutrient diffusion factor and r_s the nutrient consumption rate. Equation eq:substrate is complemented with the a uniform initial conditions $s(x,t,t=0) = s_0$ and imposed substrate concentration s_{bound} on the boundary. Equation 2.5 cannot be solved analytically but rather is discretized with respect to time and space which yields the following set of algebraic equations:

$$\begin{aligned} s^{t+dt}(i,j) &= s^t(i,j) + \frac{dtD}{\Delta l^2}[s^t(i-1,j) + s^t(i+1,j) + \\ &\quad + s^t(i,j-1) + s^t(i,j+1) - 4s^t(i,j)] - dtr(i,j) \end{aligned} \tag{2.6}$$

where i,j are the coordinates of the internal patches, $s^t(i,j)$ and $s^{t+dt}(i,j)$ are the substrate concentrations within the patch (i,j) at time t and $t+dt$ respectively. Equation gives the new spatial distribution of substrate as a function of the substrate spatial distribution and the bacteria uptake rates in the previous time-step.

2.3.4 Model parameters

Unless explicitly specified we consider the values of the IBM parameters are reported in table 2.3

2.4 Individual-based model simulation

We explore the colony spatial pattern for two colony growth regimes, namely the 'reaction-limited' and the 'diffusion-limited' regimes. The 'reaction-limited' regime implies that the growth of the individuals in the colony is limited by their growth

Parameters	Description	Unit	Value
Spatial domain	-	μm x μm	201 x 201
Δx	Spatial discretization	μm	5
Δt	Time step	s	*variable*
μ_{max}	Maximum growth rate	s^{-1}	10^{-4}
k_s	Affinity factor	kg/m^2	0.01
D_s	Substrate diffusion constant	m^2/s	*variable*
S_{bound}	Imposed boundary substrate concentration	kg/m^2	1.0
m_d	Mass of the bacterium at divison	kg	2.0 10^{-9}
ρ	areal density of a bacterium	kg/m^2	290.0

Table 2.3: Individual-based model parameters. The substrate diffusion factor is varied to switch from the 'reaction-limited' and the 'diffusion-limited' cases. The time-step is adapted consequently to ensure the convergence of the explicit Euler time discretization scheme of the substrate mass balance equation

parameters rather than by the nutrient availability. In this regime, the nutrient is transported at a sufficient rate from the boundary of the domain to the locations of the bacteria . To obtain this regime we set the nutrient diffusion rate to a relatively high value $D_s = 10^{-10} m^2/s$. Conversely, in the 'diffusion-limited' regime, the growth of the bacteria is limited by the nutrient availability. In this regime, the bacteria experience low nutrient concentrations and their growth rate is much lower than their maximum growth rate (given by μ_{max}). The 'diffusion-limited' regime can be obtained by setting the substrate diffusion rate to a low value ($D_s = 10^{-12} m^2/s$ in our case). Figure 2.2 and figure 2.3 show the time evolution of the spatial pattern of the colony simulated by the IBM for 'reaction-limited' an 'diffusion-limited' regimes respectively. In the case of the 'reaction-limited' regime the formed colony has a regular rounded shape while in the case of 'diffusion-limited' regime the shape of the colony is irregular and shows the formation of 'fingers'. Cells that are closer to the boundary than their neighbors either due to stochastic positioning of daughter cells after a division event or due to the individuals shoving each others have a competitive advantage as they are likely to experience a higher substrate concentration than their neighbors and thus grow at a higher rate. It is interesting to note that the shape of the colony is not coded in the dynamic of the individuals but is an emergent population-level property. In the next sections of this chapter we investigate whether these patterns can be yielded by the aggregated mathematical model proposed by in [Eberl 2001].

2.5 Aggregated mathematical model

Eberl *et al.* [Eberl 2001] proposed a continuum deterministic model based on the diffusion-reaction framework for modeling microbial biofilms. The model represents

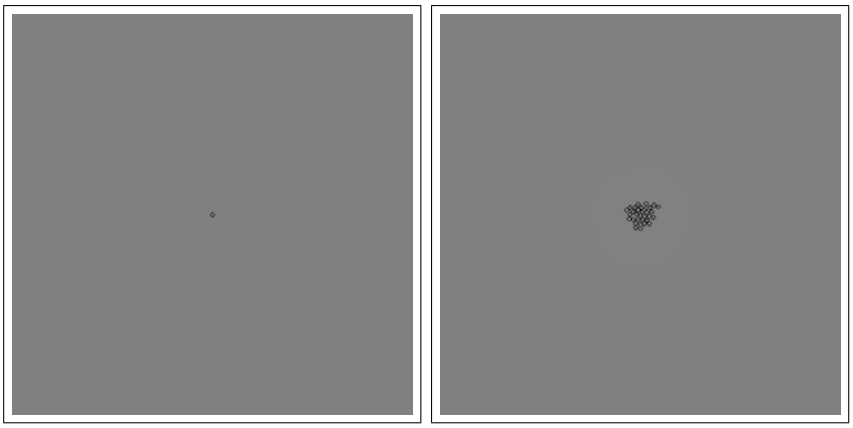

(a) IBM $time = 0h$ (b) IBM $time = 10h$

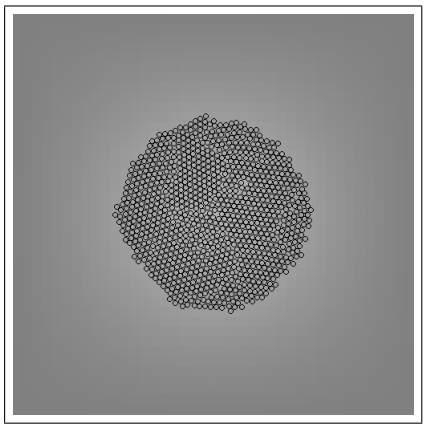

(c) IBM $time = 20h$

Figure 2.2: Time evolution of the colony pattern simulated using the IBM in the case of a 'reaction-limited regime'. Simulation conducted with $D_s = 10^{-10} m^2/s$ and $dt = 0.05s$. The gray scale indicates the nutrient concentration (Dark gray: $s = 1.0 kg/m^2$, white: $s = 0$)

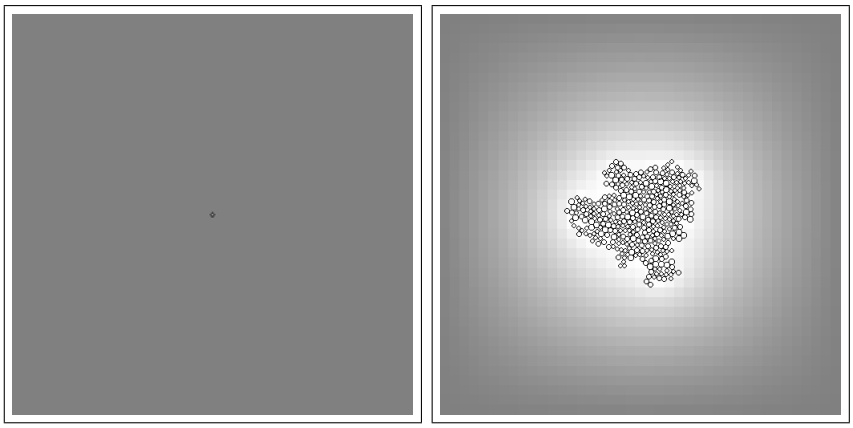

(a) IBM $time = 0h$ (b) IBM $time = 10h$

(c) IBM $time = 20h$

Figure 2.3: Time evolution of the colony pattern simulated using the IBM in the case of a 'diffusion-limited regime'. Simulation conducted with $D_s = 10^{-}12m^2/s$ and $dt = 0.5s$. The gray scale indicates the nutrient concentration(Dark gray: $s = 1.0kg/m^2$, white: $s = 0$)

the individuals and the substrate with two density fields denoted respectively $s(x, y)$ and $c_b(x, y)$.

Compared to the IBM that we presented above, the diffusion-reaction model that we describe in this section is an aggregated mathematical model. The notion of *aggregated model* implies the use of *aggregated state variables* which provide a macroscale description of the state of the bacteria. In a diffusion-reaction model the aggregated state variable is biomass density field which determines the expected mass density of bacteria in any location x, y of the domain.

The diffusion-reaction model for the bacteria has the following general form:

$$\frac{\partial c_b}{\partial t} = \nabla^2(D_b c_b) + r_b c_b \tag{2.7}$$

The first term in the right-hand side accounts for the diffusion of the biomass and the second term for the production of biomass. The first term expresses how the mass of the bacteria is redistributed over neighboring patches. This term provides a rough approximation at the macro-level of the shoving process described in the IBM. The expansion of the colony depends on the local density of bacteria and takes place only if the biomass density approaches a prescribed maximum value which establishes an upper bound [Eberl 2001]. Elberl et al. [Eberl 2001] proposed a density-dependent expression for the diffusion factor D_b that satisfies this condition. The expression takes the following generic form:

$$D_b = D_0 \frac{c_b^\alpha}{(C_{bmax} - c_b)^\beta} \tag{2.8}$$

with $\alpha, \beta > 1$ and D_0 three parameters and C_{bmax} the maximum local density of biomass. The physical interpretation of this equation is that the biomass diffusivity vanishes as c_b becomes small but increases as c_b grows due to substrate uptake. Equation 2.7 is coupled to the following diffusion-reaction equation of the substrate:

$$\frac{\partial s}{\partial t} = D_s \nabla^2 s - r_b \tag{2.9}$$

where s is the concentration of substrate, D_s the diffusion factor of the substrate and r_b the substrate uptake rate. Assuming a Monod kinetic as in the IBM, the substrate uptake rate is given by:

$$r_b = \mu_{max} \frac{s}{s + k_s} c_b \tag{2.10}$$

where μ_{max} is the maximum growth rate of the bacteria and k_s the half-saturation Monod constant. Additionally, we consider the same boundary and initial conditions for the substrate as those that we used in the IBM (fixed concentration of substrate at the boundary and uniform initial distribution of the substrate). For the biomass we consider periodic boundary conditions and we suppose that an initial

Parameters	Description	Unit	Value
Spatial domain		μm x μm	201 x 201
Δl		μm	5
Δt		s	variable
μ_{max}	Maximum growth rate of the individuals	s^{-1}	10^{-4}
k_s	Affinity factor	kg/m^2	0.01
D_s	Substrate diffusion constant	m^2/s	variable
C_{bmax}	Maximum local density of biomass	m^2/s	10^{-12}
α		dimensionless	4.0
β		dimensionless	4.0
D_0		m^2/s	variable

Table 2.4: Diffusion-reaction model parameters

seed of biomass is located in the central patch of the domain. The model parameters are reported in table 2.4.

2.6 Comparing the IBM with the diffusion-reaction model

We compare the simulation results of both models for the two colony growth regimes. The diffusion-reaction model proposed in [Eberl 2001] is not derived rigorously from the microscale dynamic that we considered in the IBM. It uses an *ad-hoc* approximation of these microscale processes based on a density-dependent expression of the biomass diffusion. This function requires four parameters α, β, D_0 and C_{bmax} and one of the difficulties that arises when we attempt to compare the DRM with the IBM is to assign appropriate values to these parameters. The parameter C_{bmax} (the maximum local density of biomass) can be deduced from the IBM simulations by taking the maximum measured local density of biomass. For the parameters α and β we use the values suggested by Eberl *et al.* [Eberl 2001]. The parameter D_0, which is the maximum value of the biomass diffusion factor is calibrated (manually) to obtain the best fit between the patterns yielded by both models. A high value of D_0 yields a simulated colony that expands faster than in the IBM.

Figure 2.4 compares the snapshots of the colonies simulated with the IBM and the diffusion-reaction model in the case of a 'reaction-limited' regime. Both models yield rounded shaped colonies that expand equally in all directions. The fluctuations in the colony simulated with the IBM are due to the stochastic positioning the newborn individuals. The length scale of these fluctuations is relatively small compared to the size of the colony, and a small number of simulations is sufficient to extract the

deterministic limit yielded by the diffusion-reaction model.

We compare the shape of the simulated colonies in the case of 'diffusion-limited' regime. In this case, the individuals experience significant heterogeneities in the substrate concentration and consequently grow at different rate depending on their location in the colony. Individuals located at the edge of the colony tend to have high growth rates in comparison to the individuals located at the center of the colony. Figure 2.5 compares snapshots of the simulated colony patterns. The IBM pattern is averaged over 20 IBM simulations run with with the same parameter and different seeds for the random number generator. In the diffusion-reaction model the colony expands forming fingers that are directed towards the closest distances to the boundary of the domain where the substrate concentration is the highest. While 'fingers' are also formed in each of the IBM simulations, they are not observed in the average pattern and are not likely to be directed towards any preferential direction. They seems to occur at random and the average pattern shows a round-shaped colony. The closest distance to the boundary is not necessary the one with the steepest nutrient gradient as the nutrient distribution is heterogeneous and can be affected with the irregular shape of the colony.

We assessed the sensitivity of the DRM pattern to the variation of the parameter D_0. Figure 2.6 shows the average pattern obtained with the IBM at an intermediate time $t = 71h$ and the pattern yielded by the DRM for three values of the parameter D_0. The increases of D_0 increases the size of the colony and reduced it areal biomass density (vertical axis). The shape of the colony however still have the star-like shape with fingers directed towards the closest boundary.

2.7 Discussion

IBM and DRM are two commonly used modeling approaches for simulating microbial spatial patterns formation. In this chapter we compared these two approaches by considering a simple case of the a mono-species colony growing on a diffusive substrate. Both models yield comparable results for the case of 'reaction-limited' regime but show significant differences in the case of 'diffusion-limited' regime. While , int he 'diffusion-limited' regime each realization of the IBM yields a pattern with an irregular shape and 'finger-like' structure the average pattern yields a round shaped colony suggesting the 'fingers' have no preferential direction. The direct averaging of spatial patterns obtained through the replication of a simulation is often an inappropriate approach as some important features of the pattern (irregular shape, finger formation) that has an impact on the local environment of the individuals are lost during the averaging exercise.

The DRM captures the formation of 'fingers' in the case of the 'diffusion-limited' regime. The DRM pattern is symmetric and the fingers directed towards the closest

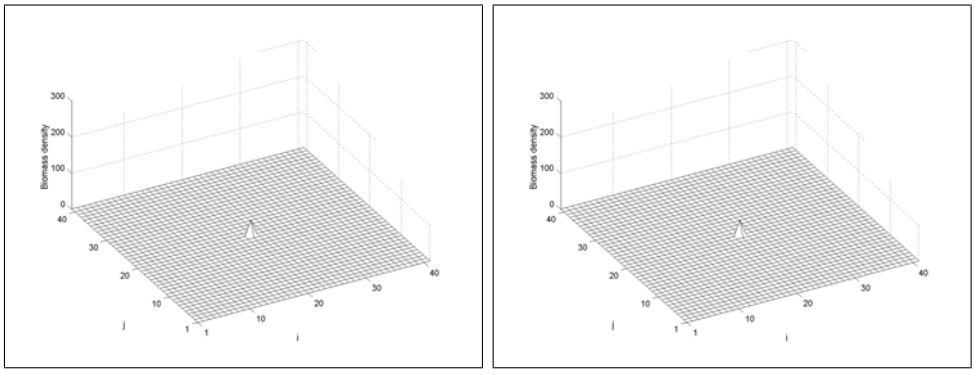

(a) IBM $time = 0$ (b) DR $time = 0$

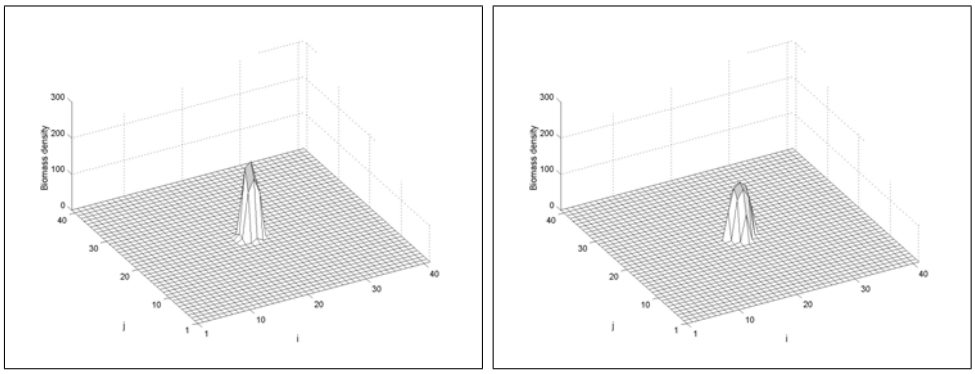

(c) IBM $time = 10h$ (d) DR $time = 10h$

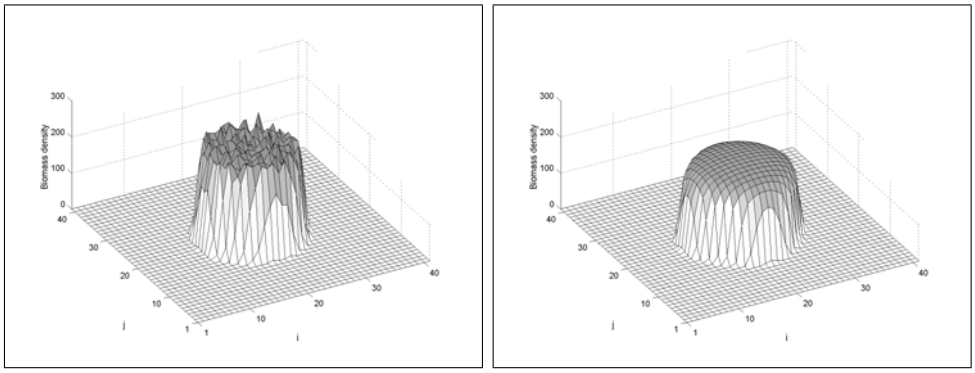

(e) IBM $time = 20h$ (f) DR $time = 20h$

Figure 2.4: Comparison of the colony pattern simulated by the IBM and by the diffusion-reaction model in the case of a 'reaction-limited regime'. DRM simulation conducted with $D_0 = 10^{-14}\ m^2/s$

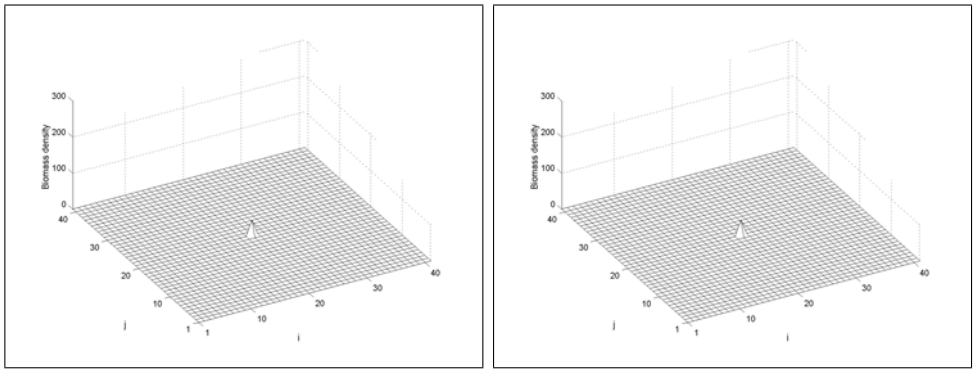

(a) IBM $time = 0$ (b) DR $time = 0$

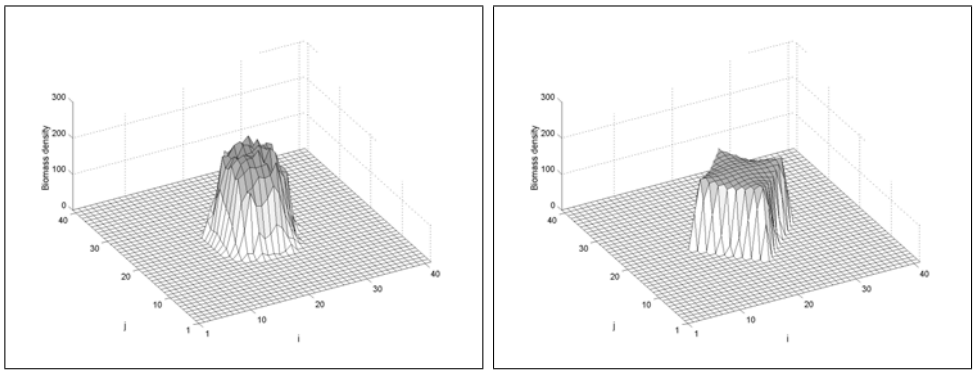

(c) IBM $time = 50h$ (d) DR $time = 50h$

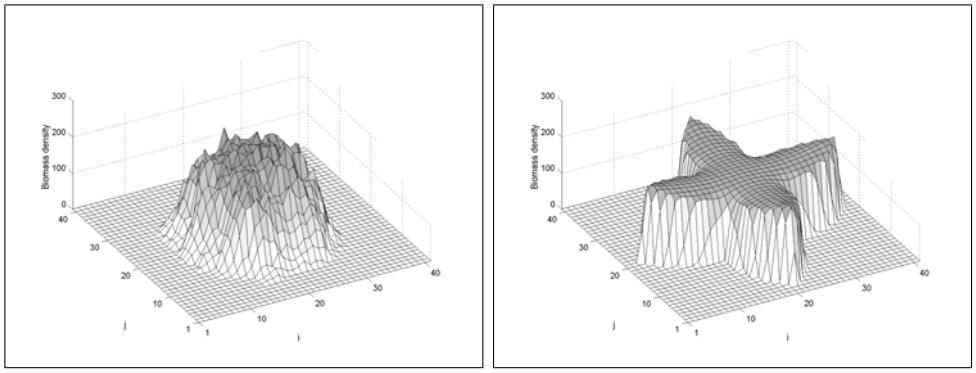

(e) IBM $time = 100h$ (f) DR $time = 100h$

Figure 2.5: Comparison of the colony pattern simulated by the IBM and by the diffusion-reaction model in the case of a 'diffusion-limited regime'. DRM simulation conducted with $D_0 = 10^{-16}\ m^2/s$

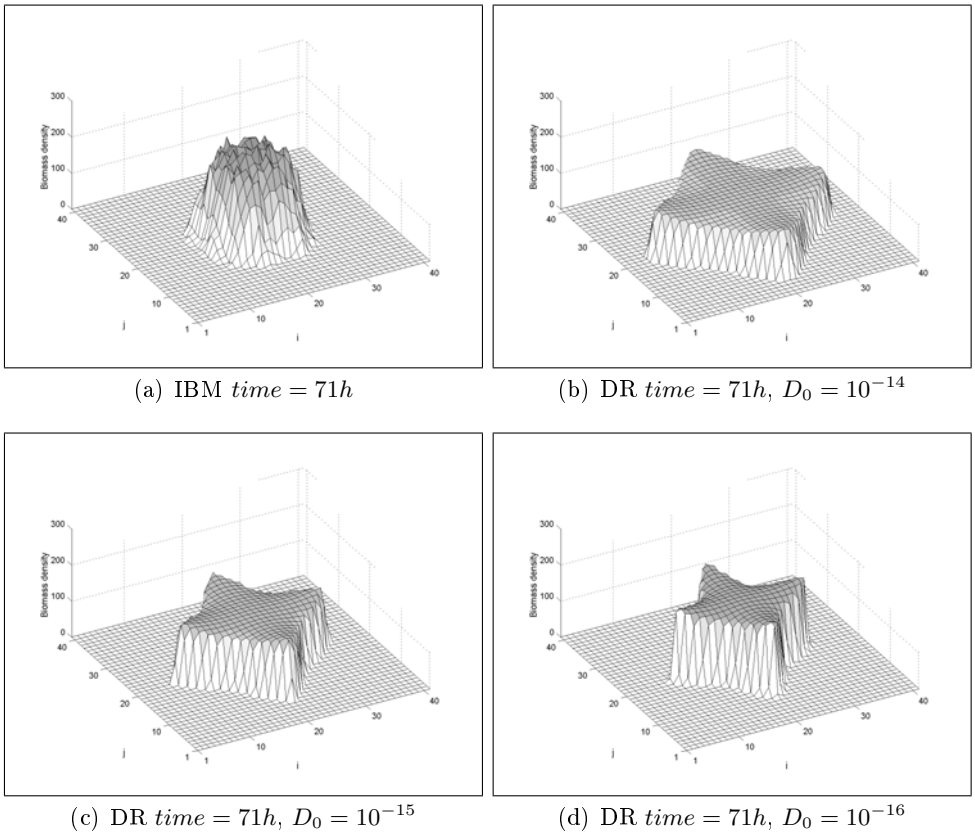

(a) IBM $time = 71h$ (b) DR $time = 71h$, $D_0 = 10^{-14}$

(c) DR $time = 71h$, $D_0 = 10^{-15}$ (d) DR $time = 71h$, $D_0 = 10^{-16}$

Figure 2.6: Comparison of the average pattern yielded by the IBM (a) and the pattern simulated with DRM (b)-(d) for different values of D_0

boundary. One of the limitations of the DRMs is the identifiability of the model parameters. As these models are rarely rigorously derived from the microscale dynamic of the individuals they imply the use of ad-hoc approximations involving several parameters. These parameters encompass the complexity of the microscale interaction and may lack physical meaning. Thus their values may be difficult to obtain from laboratory experiments.

Applying both approaches to a same problem may be very helpful. DRM provide a deterministic reference to which the IBM simulations can be compared while the IBM may help in assessing the quality of the approximations needed in the DRM and in the identifiability of the DRM parameters.

Chapter 3

Moment approximation of a microbial IBM for colony growth

Contents

In the previous chapter (chapter 2) we investigated how a spatially explicit individual-based model for simulating the growth of a microbial colony compares to diffusion-reaction models. In this chapter we are concerned with another class of aggregated mathematical models, namely spatial moment approximation models. Spatial moments models were originally developed in statistical physics and have been applied during the last decade to the approximation of individual-based models that arise in several ecological systems of plants and animals [Dieckmann 2000]. In this chapter we discuss the extension of the approach to modeling microbial systems and illustrate with the example of microbial colony growth with a slight difference compared to the previous chapter. Here we will consider systems initialized with $n_0 > 1$ individuals randomly distributed rather than with one individual located in the center of the domain.

The derivation of the moment approximating model from the detailed IBM including individuals with variable sizes and complex shoving process is quiet difficult. Thus our approach consist in first simplifying the detailed IBM than approximate the simplified IBM using moment techniques.

The chapter in organized in three parts: the first part is dedicated to the simplification of the colony growth IBM. In the second part we derive a moment approximation model of the simplified IBM. In the third part we compare the moment model and the simplified model to assess the quality of the approximations considered in the moment model. We conclude this chapter by discussing the relevance of the spatial moment method in approximating microbial IBMs and the possible extensions of the approach.

3.1 Description of the simplified individual-based model

We describe in Chapter 2 an IBM for the growth of a colony in which the individual cells are represented as discs with variable diameters. The individuals grow and divide while uptaking a diffusive substrate. They shove each others making the size of the colony to increase. The individuals compete for the nutrient and the increase of their local density decreases the level of nutrient and reduces their growth rate. This phenomena is somehow comparable to a density-dependent growth process. When the local density of the bacteria increases their individual growth rate decreases because of the decrease of the local substrate concentration perceived by the bacteria. We propose to construct a simple IBM that captures this density-dependant growth without considering the variability in individual size and the explicit dynamic of the substrate. We also simplify the shoving process by using instead a uniform dispersion kernel. We assess how this simplification affect the shape of the colony. In this section we propose to describe the simplified IBM using the ODD protocol.

3.1.1 Overview

3.1.1.1 State variables and scales

We consider a sessile community of individual bacterial cells living in a two-dimensional space. The individual cells are considered as point particles entirely characterized by their location $x = (x_1, x_2)$ in this plane. The abiotic environment is homogeneous in space.

3.1.1.2 Process overview

The community changes through two stochastic events acting on the individuals: division and lysis (or death). We suppose that individuals divide with a probability that decreases with the increase of the local density of individuals and die with a constant probability. The local density is measured using an interaction kernel

specifying how neighboring individuals affect the division rate of a focal individual. During a division event we suppose that the parent individual generates an offspring which position is randomly selected within a neighborhood of its parent.

3.1.1.3 Scheduling

The temporal behavior of the simplified IBM is governed solely by the stochastic division and death events. To simulate the temporal evolution of such system we need to specify when the next event will occur, what kind of event it will be and which individual will be concerned with the event. Gillespie [GIllespie 1976] proposed a Monte Carlo procedure for simulating comparable stochastic processes that arise in chemical reaction research. The procedure can easily be extended to a stochastic birth-death model in which the individuals experience different birth and death probabilities [Dieckmann 1999]. The procedure iterate over the following steps:

1. Set the time to $t = 0$
2. Calculate the division and death rates $b_i(p)$ and d_i of each individual $i = 1..n$ where p is the spatial pattern at time t
3. Calculate the sums $r_b = \sum_{i=1}^{n} b_i(p)$ and $r_d = \sum_{i=1}^{n} d_i$. The rate at which an event (division or death) occurs is given by $r(t) = r_b(t) + r_d(t)$
4. Choose the waiting time τ for the next event to occur according to $\tau = -\frac{1}{r} \ln \lambda$ where $0 < \lambda \leq 1$ is a uniformly distributed random number
5. Choose a division or death event with a probability r_b/r and r_d/r respectively
6. Choose an individual k with a probability b_k/r_b (if the event is division) or d_k/r_d if the event is death, where b_k and d_k are the respectively the division and death rates of the individual k
7. Perform the selected event on the individual k
8. Update time according to $t = t + \tau$
9. Continue from step 2 until $t < t_{end}$

3.1.2 Design concepts

- Stochasticity: all the processes (division and death processes)are stochastic.
- Emergence: the spatial pattern emerges from the iteration of division and death processes of the individuals.

3.1.3 Details

3.1.3.1 Initialization

The model is initialized with $N_0 = 100$ cells distributed uniformly over the domain.

3.1.3.2 Submodels

- Division: we suppose that the probability per unit of time that an individual i in position x_i produces a new cell located in position x' is given by:

$$B(x_i, x') = [b_1 - b'_1 p_{loc}(x_i)] K\left(\frac{||x_i - x'||}{w_b}\right) \tag{3.1}$$

  The parameters b_1 and b'_1 are the density-independent and the density-dependant division rates respectively. The term $p_{loc}(x_i)$ is the local density (defined in more details below) perceived by the individual in x_i. $K(||x_i - x'||/w_b)$ is a dispersion kernel (we call it also birth or division kernel). The dispersion kernel gives the probability that the newly formed individual disperses instantaneously after the division event to the location x'. For simplicity we use a uniform dispersion kernel. In some way, the dispersion kernel translates the observation that daughter cells are located randomly in the neighborhood of their mother cells.

- Calculation of the perceived local density: in a system containing N individuals, each individual has at maximum $N - 1$ neighbors. However, as we suppose that individuals perceive only their local environment. They are likely to be affected only by the neighbors located in their immediate surrounding environment. In order to calculate this perceived local density of neighbors we use a uniform interaction kernel, denoted $K(||x_i - x_j||/w_d)$. The interaction kernel measures the contribution of the individual j in x_j to the local density perceived by the individual i in x_i. The perceived local density is then calculated using the following expression:

$$p_{loc}(x) = \sum_{j=0, j\neq i}^{j=n} K\left(\frac{||x_i - x_j||}{w_d}\right) \tag{3.2}$$

- Death process: we suppose that the individuals die at a constant rate d_1. The death probability of an individual per unit of time is supposed to be independent from the local density of individuals.

3.1.4 Parameters

The model parameters are summarized in table 1.

Parameters	Description	Value	Unit
L	Side of the squared spatial domain	101x 101	$\mu m \times \mu m$
b_1	Density-independent division rate	0.1	h^{-1}
b_1'	Density-dependant division rate	*variable*	$h^{-1}\mu m^2/\#$
d_1	Density-independent detachment rate	0.1	h^{-1}
w_b	Side of the uniform dispersion kernel	5	μm
w_d	Side of the squared uniform interaction kernel	5	μm

Table 3.1: Model parameters. (The # symbol denotes for the dimension on the number of individuals)

3.1.5 Model outputs

The model output is a list containing the positions of the individuals. The list defines the spatial pattern and changes when an individual event (division or death) occurs. We analyze these spatial pattern by measuring two statistical quantities defining the first and second spatial moments:

- the average density of individuals, denoted $N(t)$ (number of individuals divided by the area L^2 of the domain)
- the pair correlation density function denoted $C(\xi, p)$ and defined as the density of pairs of individuals separated with a vectorial distance $\xi = (\xi_1, \xi_2)$.

3.1.6 Comparison of the simplified IBM with the detailed IBM

We propose to assess the impact of simplifying the spatial extent of the individuals on the shape of the simulated colonies. In the detailed IBM that we presented previously (see chapter 2) we represented the individuals as discs shoving each others and having variable sizes. This is simplified in the IBM described in this chapter and the individuals are represented as particles without a spatial extent. By taking this simplifying assumption we also neglect the processes induced by the spatial extent of the bacteria like the shoving process. Consequently in the simplified IBM the only mechanism that makes the size of the colony to increase is the dispersion of daughter cells after division. We modeled this dispersion using a uniform dispersion kernel.

Another important difference between the simplified model and the detailed one is related to the substrate and the growth functions of the individuals. In the detailed model we suppose that the individuals grow by uptaking a nutrient which dynamics is explicitly considered in the model (using a diffusion-reaction mass balance). The growth rate of the individuals in the detailed IBM is a non-linear function of the local nutrient concentration (Monod equation). In the simplified model we do not

account explicitly for the nutrient dynamic. The division rate of the individual is a decreasing linear function of the local density of the individuals.

Figures 3.1 and 3.2 show colony patterns simulated with both models in the case of a 'reaction-limited' and 'diffusion-limited' regimes. We switch from the 'reaction-limited' regime to the 'diffusion-limited' regime by decreasing the nutrient diffusion factor in the detailed model and by increasing the value of the density-dependent growth parameter b_1' in the simplified model. The patterns yielded by both models shows similarities and differences. First the simplified model reproduces quiet well the circular and irregular shapes observed in the detailed model. The distribution of the individuals within the colony are however different in the pattern yielded by both models. In the original model the individuals are tightly packed where as in the simplified model they are dispersed within the colony. This is due to the simplification of the mechanical pushing process (shoving process) considered in the detailed model. Shoving process rearranges the position of the individual in the colony simulated with the detailed IBM and relax overlapping of neighboring cells. In the detailed IBM the cells continuously shove each others and their position in slightly modified after each time step while in the simplified IBM the position of the daughter cell is fixed after the division event and do not change in time. The effect of shoving can be included in the simplified IBM by adding a density-dependent motility process where individuals become motile when the local density of neighbors increases. However for simplicity we do not include this effect and consider that the simplified IBM already captures the main features of colony shape. Another form of density-dependent motility will be studied in more detail in chapter 5 to 7.

Finally, substrate dynamic can also be included in the simplified IBM by representing substrate as particles undergoing a Brownian motion. The division rate of the bacteria can be expressed as a function of the local density of substrate particles, and substrate consumption can be modeled as predation process. However this adds some complexity to the individual-based model and some algebra to the moment approximation model. We consider that at least qualitatively the effect of the substrate is implicitly included in the simplified IBM through the use of density-dependent growth function.

3.1.7 Moment approximation of the simplified IBM

Now we propose to derive a deterministic mathematical model approximating the dynamic of the simplified IBM using moment approximation techniques. The principle of the moment approximation technique is to derive the equations that describe the dynamic of the first and second spatial moments. The first moment is the average density and contains no spatial information about the pattern. The second moment measure the variation of the density of individuals in space and is represented by the density of pairs of individuals separated with vectorial distance ξ. We first start by defining these moments for a set of n individuals that inhabit

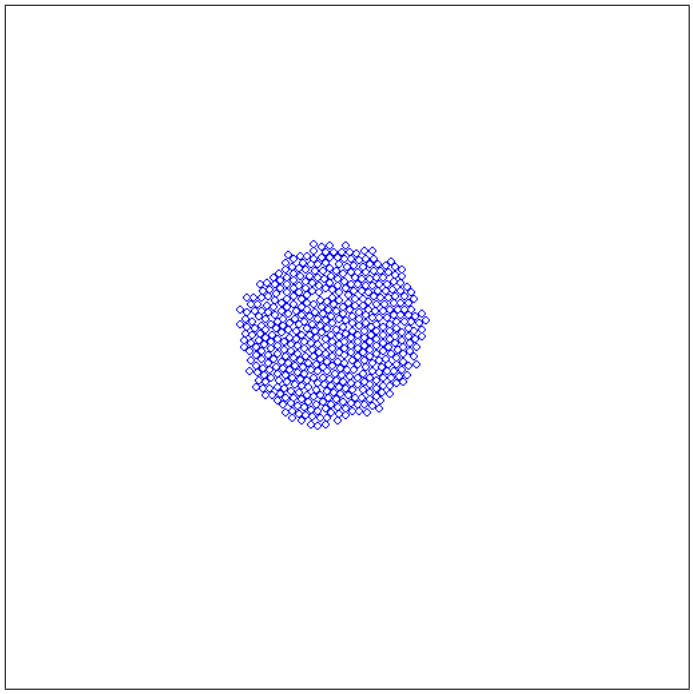

(a)

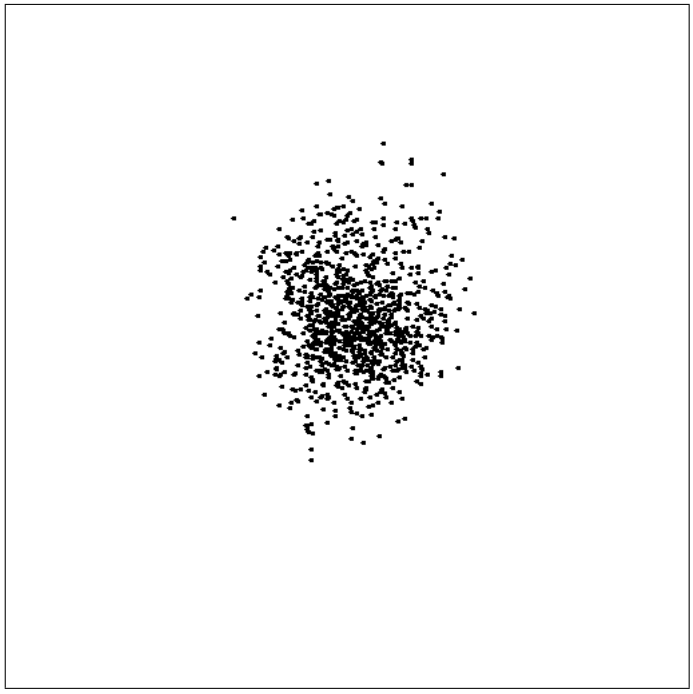

(b)

Figure 3.1: Comparison of colony pattern simulated with the detailed IBM (a)) and the simplified IBM (b) in the case of 'reaction-limited' regime

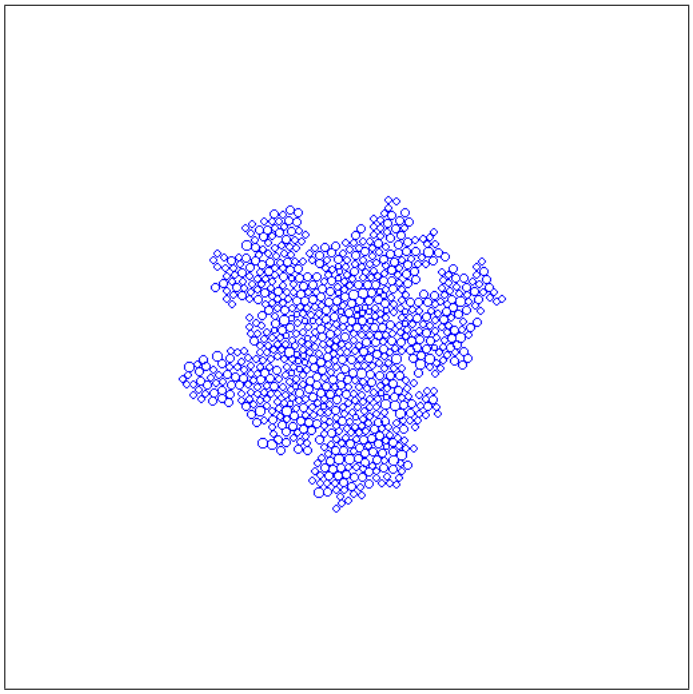

(a)

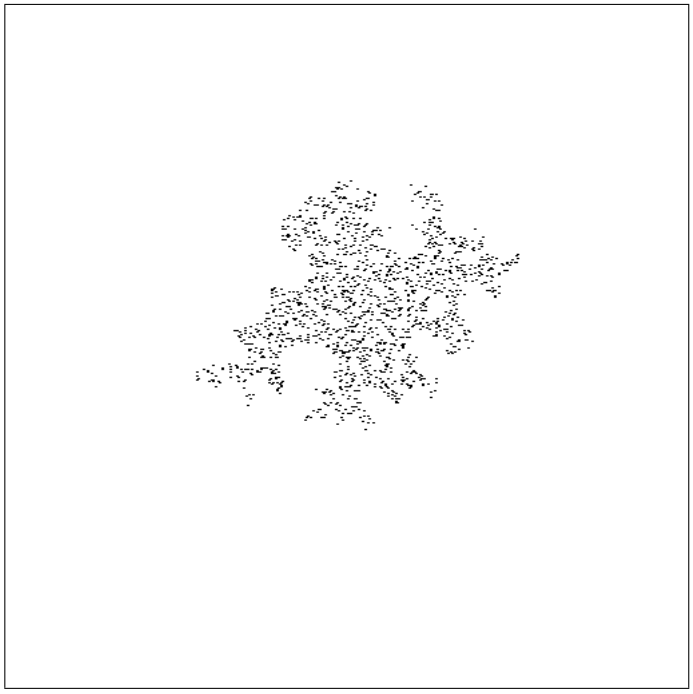

(b)

Figure 3.2: Comparison of colony pattern simulated with the detailed IBM (c)) and the simplified IBM (d) in the case of 'diffusion-limited' regime

a continuous space and occupying continuous positions x_i, $i = 1..n$ then we derive their dynamical equations.

The first and second moments can be calculated on the pattern yielded by the IBM and compared to those obtained by solving numerically the moment model equations. The calculation of the first moment from the IBM simulation results is performed simply by counting the number of individuals and dividing by the domain area to get an average density over the domain. The second spatial moment is measured through the pair correlation function. The pair correlation function $C(\xi)$ gives the average density of individuals located at a vectorial distance ξ from a focal individual. We calculate the pair correlation density function for a given pattern p formed with n individuals as in [Dieckmann 2000] by counting for a focal individual at location $x = (x_1, x_2)$, the number of paired individuals within the square $(x_1 + \xi_1, x_1 + \xi_1 + d\xi_1) \times (x_2 + \xi_2, x_2 + \xi_2 + d\xi_2)$, using a sufficiently small spatial resolution $d\xi = (d\xi_1, d\xi_2)$. We repeat this procedure for each individual in turn being the focal one and dividing the total count by the domain area L^2 and by $d\xi_1 d\xi_2$ yields the pair density at distance ξ. The result is a matrix. The central value of the matrix corresponds to the average density of individuals experienced by a focal individual at distances smaller than the spatial resolution $d\xi$. The matrix can be understood by imagining that a virtual focal individual is located in the center. The matrix than correspond to the average 'individuals'eye view' of its environment.

Figure 3.3 shows two snapshots of an IBM simulation of two colonies. The colonies show different shapes. The bacteria in the first seems distributed uniformly where as they are organized in small groups in the second pattern. Figure 3.4 reports the corresponding pair correlation functions ($C(\xi)$ matrices plotted using Matlab). The matrices should not be confused with the colony pattern itself. The matrices describes the average local environment experience by an individual within the colony at different distances. A peak in the center of the matrix indicates that the individuals experience a high density of neighbors at short distances. These densities tend to vanish at higher distances. The matrices are normalized such that a value of 1 corresponds to a Poisson-like patterns where the individuals are uniformly distributed over the domain. Values higher than one indicates an aggregated pattern meaning that the density experienced by the individuals is higher than what would be expected if the individuals were distributed uniformly. The comparison of the pair correlation matrices confirm that the individuals within the colonies in figure 3.3 experience different local conditions in term of neighbor densities. The profiles of the Cartesian pair correlation function plotted in figure 3.4 that the pair correlation function takes values close to 1 for the first colony indicating the absence of any spatial structure, whereas the second function peaked at short distance and vanished to one at large distances. The peak at short distances indicates that the individuals are likely to experience higher densities of neighbors than what would be experienced in the absence of any spatial structure. The pair correlation function

captures well the heterogeneities experienced by the individuals.

3.1.7.1 Deriving the dynamic equations of the first and second moment

The dynamic of the first moment (mean density of individuals) is given by the following equation:

$$\frac{dN}{dt} = (b_1 - d_1)N - b_1' \int C(\xi) K\left(\frac{||\xi||}{w_d}\right) d\xi \tag{3.3}$$

The first term on the right-hand side is neighborhood-independent components of divisions and death, and the second term is the neighborhood-dependent components of divisions. The integral term involve the pair density function $C(\xi)$ and the interaction kernel $K(||\xi||/w_d)$. This term encompass the effect of the local environment on the mean density of individuals which is the result of the spatial structure, as given by $C(\xi)$, and on the extent the individuals experience the effect of this structure as given by $K(||\xi||/w_d)$. Note that if the side of the uniform interaction kernel, w_d, is equal to the side L of the domain than equation 3.3 can be simplified to a simple non spatial Lotka-voltera equation [Law 2000]:

$$\frac{dN}{dt} = (b_1 - d_1)N - b_1' N^2 \tag{3.4}$$

In this case the division rate of any individual is equally affected by all the other individuals. However in most microbial system the individuals perceive only their local environment. The dynamic of the second moment accounts for the processes (division and death) that affect the density of pairs separated with a vectorial distance ξ.

$$\frac{dC(\xi)}{dt} = \left(\frac{dC(\xi)}{dt}\right)_{division} + \left(\frac{dC(\xi)}{dt}\right)_{death} \tag{3.5}$$

The terms in the right-hand side denote respectively the effect of division and death events on the density of pairs $C(\xi)$. The effect of the death is straightforward. Consider a pair of individuals separated with a distance ξ. If one of these two individual dies than we loose a pair of individuals separated with a distance ξ. The rate at which we loose pairs of individual separated with a distance ξ is given by:

$$\left(\frac{dC(\xi)}{dt}\right)_{death} = -2d_1 C(\xi) \tag{3.6}$$

The effect of the individual division events on the density of pairs at distance ξ is more complicated and is given by the following equation:

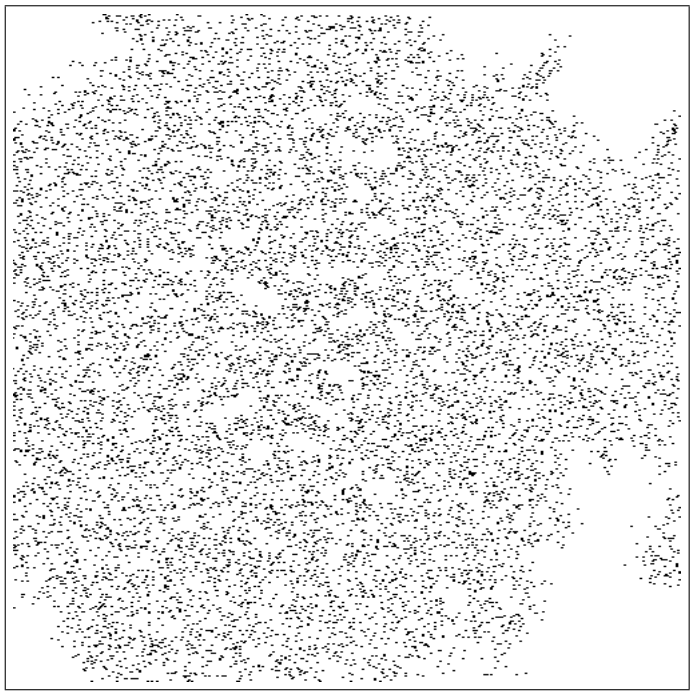

(a)

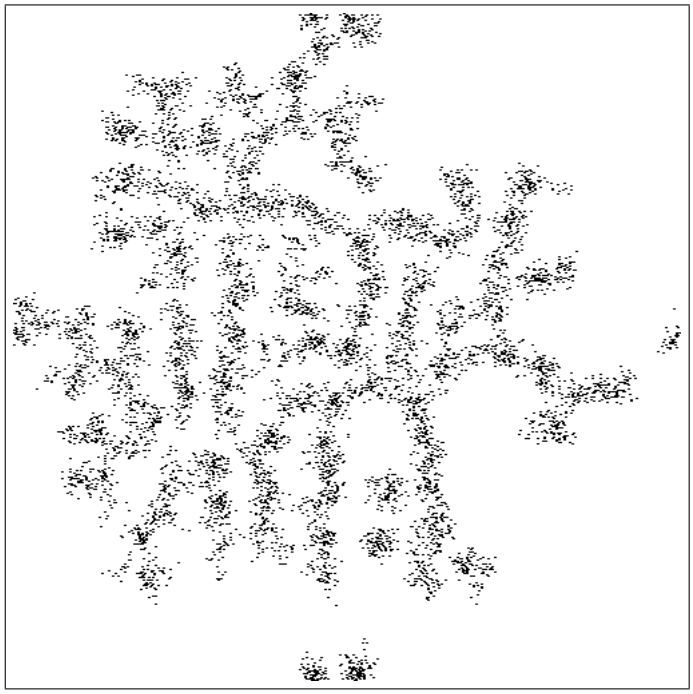

(b)

Figure 3.3: Examples of colony patterns both initialized with a single cell in the center of the domain.

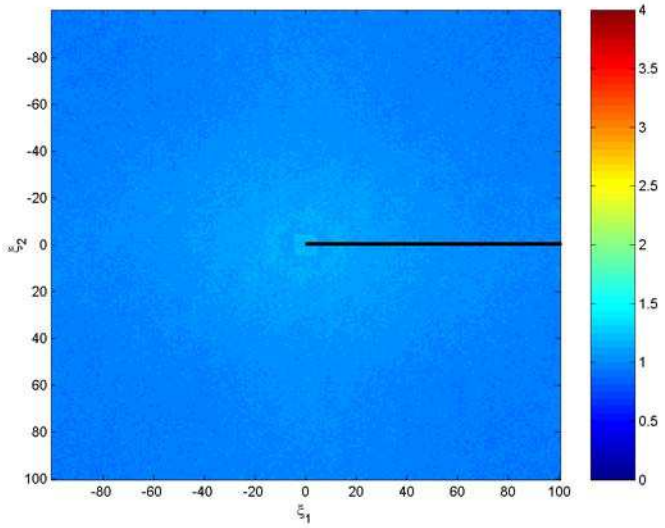

(a)

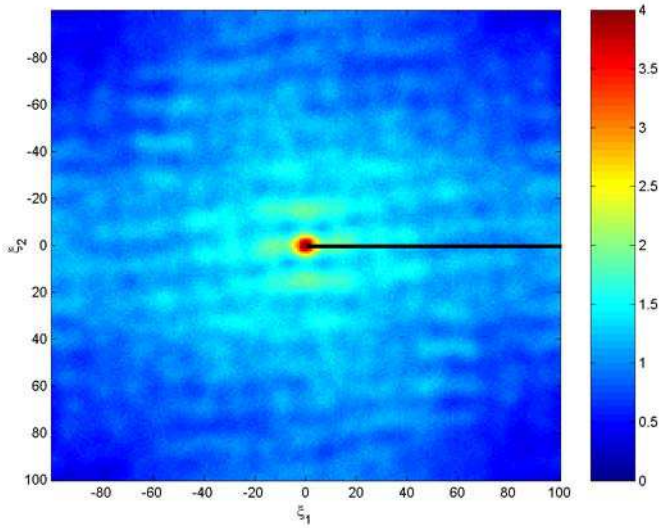

(b)

Figure 3.4: Cartesian pair correlation functions (matrices $C(\xi)$) corresponding to the patterns in figure 3.3. The black lines indicates the radial profiles that are plotted in the next figure (figure 3.5)

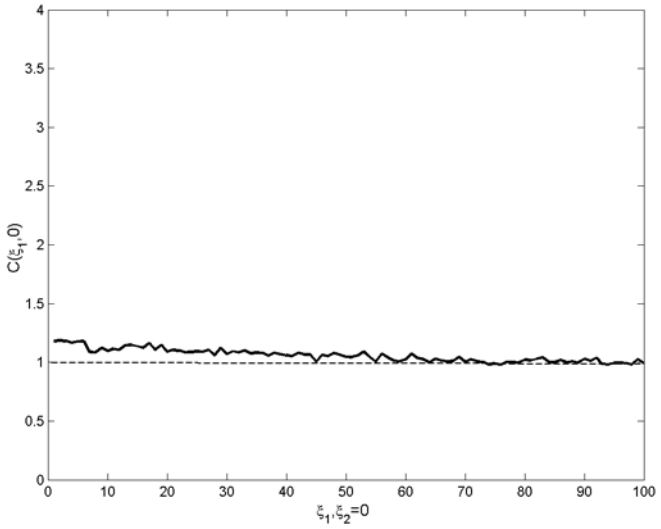

(a)

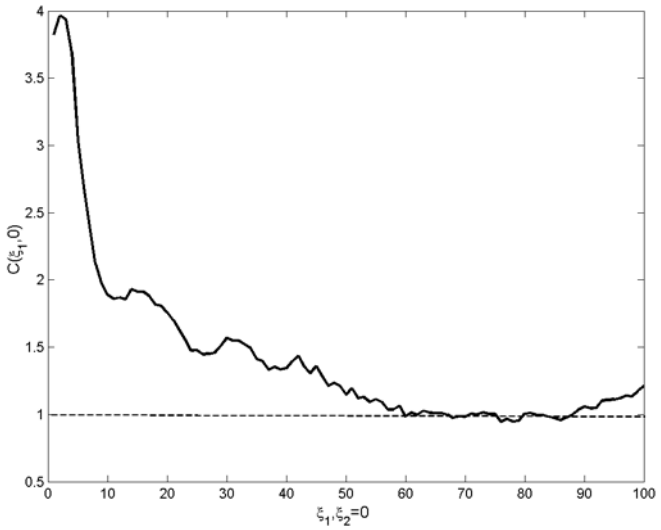

(b)

Figure 3.5: Radial profiles of the Cartesian pair correlation function (black lines in figure 3.4)

$$\left(\frac{dC(\xi)}{dt}\right)_{division} = \\ +2b_1 NK\left(\frac{||\xi||}{w_b}\right) \\ -2b_1' K\left(\frac{||\xi||}{w_b}\right)\int K\left(\frac{||\xi''||}{w_d}\right)C(\xi'')d\xi'' \\ +2b_1\int C(\xi+\xi')K\left(\frac{||\xi'||}{w_b}\right)d\xi' \\ -2b_1'\int\int K\left(\frac{||\xi'||}{w_b}\right)K\left(\frac{(||\xi''||}{w_d}\right)T(\xi+\xi',\xi'')d\xi' d\xi'' \\ -2b_1'\int C(\xi+\xi')K\left(\frac{(||\xi+\xi'||}{w_d}\right)K\left(\frac{(||\xi'||}{w_b}\right)d\xi' \qquad (3.7)$$

The right-hand side is formed with five terms that describe the variation in the density of (i,j) pairs at vectorial distance ξ resulting from division events. To understand the precise interpretation of each term we proceed as in [Dieckmann 2000] by focusing on the individual i of the (i,j) pair.

- the first term accounts for the density-independent division of an individual i producing a new individual j located at a vectorial distance ξ. Multiplying the mean density of individuals N and by the independent per capita division rate b_1 gives the rate of of division events. Then we multiply by the probability that the newly formed cell is located at distance ξ from the parent position. The factor 2 accounts for newly formed individuals that disperse to distance $-\xi$ which also form a new pair (j,i) at distance ξ

- the second term corrects the independent division rate calculated by the first term by taking into account the negative effect of the possible presence of neighbors around the individual i. The average local density of neighbors experienced by the individual i is given by the integral $\int K(||\xi''||/w_d)C(\xi'')d\xi''$. Multiplying by the density-dependent division rate b_1' and by $2K(||\xi||/w_b)$ gives the density-dependent correction of the first term.

- the third term also accounts for the density-independent division, but focuses on the new pair that the offspring of an individual i forms with and individual j located at a distance $\xi+\xi'$ from i. The per capita rate of density-independent rate of division is b_1, the density of (i,j) pairs is $C(\xi+\xi')$ and the spatial density of offspring settling around the i parent is $K(||\xi'||/w_b)$. Multiplying these three factors and integrating over all possible distances ξ' of offspring dispersal yields the third term.

- the fourth term is a correction of the density independent third term to account for the effect of neighbors of the individual i that reduces its rate of producing new individuals. The division rate of the individual i in the pair (i,j) at

distance $\xi + \xi'$ can be modified by the presence of a neighbor k located at distance ξ'' from i. The density of triplet of individuals (i, j, k) is $T(\xi + \xi', \xi'')$, the interaction kernel for the (i, k) pair yields $K(||\xi''||/w_d)$ and the spatial density of offspring around the individual i is $K(||\xi'||/w_b)$. Multiplying these factors with the density dependent birth rate and integrating over all possible distances ξ' and interaction distances ξ'' gives the forth term.

- the fifth term accounts for the effect of triplet (i, j, k) but do not include the effect of the individual j on the division rate of the individual i. Thus the fifth term adds this correction by multiplying the density of pairs (i, j) separated with a distance $\xi + \xi'$ with the interaction kernel $K(||\xi + \xi'||/w_d)$. The correction term is obtained by integrating over all possible distances ξ' and by multiplying by the probability density $K(||\xi'||/w_b)$ of having an offspring at distance ξ' from i and the density dependent division rate b_1'

In the three last terms we focused on the individual i. Analogous events can occur to the individual j. We take this in consideration by multiplying these terms by a factor 2. The dynamic of the first moment involve the second moment, that of the second moment involves the density of triplet denoted $T(\xi + \xi', \xi'')$. We can in principle continue with the dynamic of the third moment (triplet densities) which should involve the higher order moments. To escape this cascade of dependencies Dieckmann and Law [Dieckmann 2000] proposed to truncate the moment hierarchy by expressing the third moment in terms of the second and first moment. Such expression are called moment closures and should satisfy a number of conditions detailed in [Dieckmann 2000]. The choice of the moment closure may have an impact on the quality of the approximation of the underlying individual processes. This is often assessed by comparing the moment model to the dynamic of the underlying individual-based model [Dieckmann 2000]. We use the following approximation closure equation which expresses the third moment as a function of the second and first moments:

$$T(\xi, \xi') = \frac{C(\xi)C(\xi')}{N} \tag{3.8}$$

3.1.8 Solving the moment approximation model

The system formed with equations 3.3, 3.7 and 3.8 can be solved assuming periodic boundary conditions and taking as initial conditions an initial density $N(t = 0)$ of individuals distributed uniformly which yields an initial pair correlation density function $C(\xi, t = 0) = N^2$. The system can be solved in the Cartesian coordinates or in the radial coordinates (because of the isotropy of the domain and the radial symmetry of all the processes). For the radial formulation of these equations refer to the Annexe A of this chapter. We present here the procedure for solving the moment dynamic equation in the Cartesian coordinates.

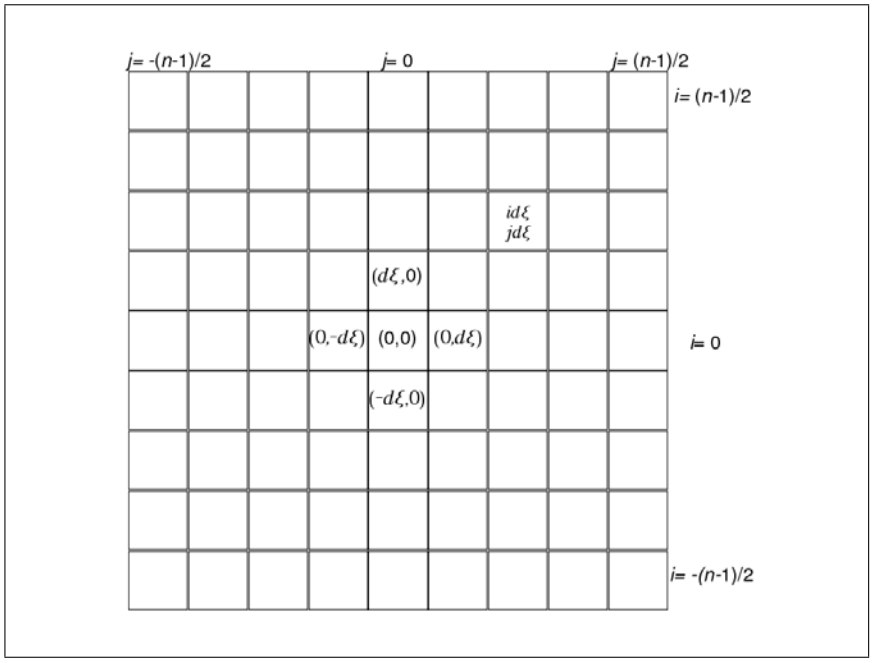

Figure 3.6: Discretization of the vectorial distance ξ separating two individuals

The state variables of the moment model are the first and second spatial moments $N(t)$ and $C(\xi, t)$. The first moment $N(t)$ is a real value (density of individuals). The second moment $C(\xi, t)$ is a function that gives the density of pairs of individuals separated by a vectorial distance $\xi = (\xi_1, \xi_2)$. To solve the moment dynamic model we start by discretizing the equation 3.3 and 3.7 with respect to space and time.

- **Spatial discretization** We discretize the vectorial distance $\xi = (\xi_1, \xi_2)$ into $\xi(i, j) = (\xi_1(i), \xi_2(j))$ with $i, j = -(n-1)/2..(n-1)/2$ (see figure 3.6). The function $C(\xi, t)$ is evaluated only in these discretized points and takes the form of a $n \times n$ square matrix $C(i, j, t)$ with $i, j = -(n-1)/2..(n-1)/2$

  For the calculation of the integral terms in equations 3.3 and 3.7 we need to discretize the kernels $K(||\xi||/w_b)$ and $K(||\xi||/w_b d)$. We use the same spatial resolution $d\xi$. Note that the spatial resolution $d\xi$ depends on the size of the interaction and dispersion kernels. As these kernels define the spatial distance over which local interactions take place, the spatial resolution $d\xi$ should be small compared to the size of these kernels. A typical resolution to discretize Gaussian kernels is $d\xi = ((min(w_b, w_d)/5, min(w_b, w_d)/5)$ where $min(w_b, w_d)$ is smallest value between w_b and w_d. In this work we considered identical uniform kernels (see figure 3.7).

- **Time discretization** We discretize time derivatives in equation 3.3 and 3.7 using an explicit Euler scheme with a time step $\Delta t = 1$

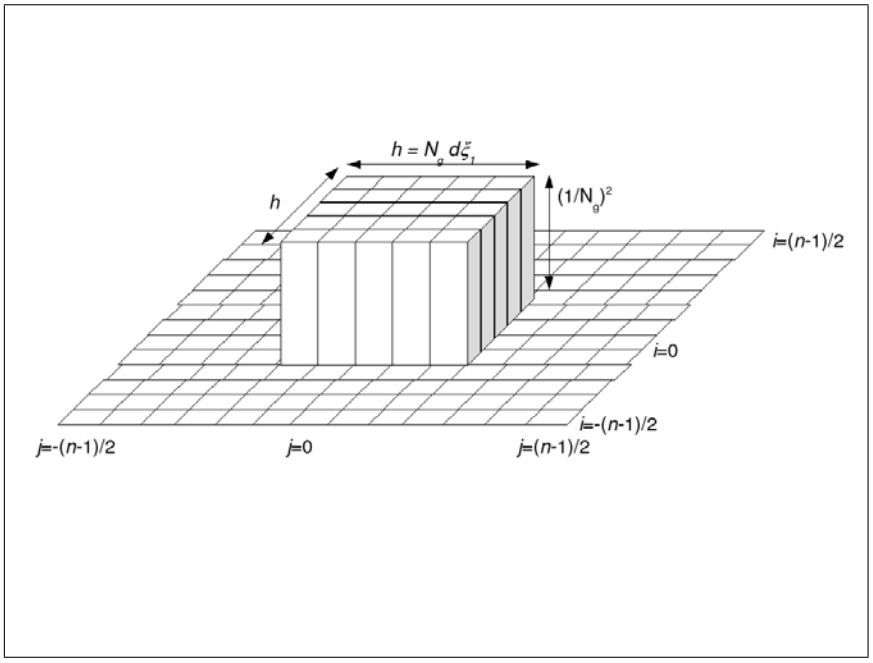

Figure 3.7: Discretization of interaction and dispersion kernels $K(||\xi||/w_b)$ and $K(||\xi||/w_d)$. Both kernels are uniform with a window width $w_b = w_d = h = 5d\xi$

The discretized system is formed with $n^2 + 1$ algebraic equations where the unknowns are the density of individuals N and the n^2 elements of the matrix $C(\xi)$.

3.2 Comparison of the moment model with the simplified IBM

We compare the simulation results the simplified IBM and the moment model or the case of density-independent growth ($b_1' = 0$) and density-dependant growth ($b_1' > 0$).

3.2.1 Density independent growth model ($b_1' = 0$)

The case of density independent growth implies that the spatial pattern has no impact on the average density of individuals. This can be seen from equation 3.3. By setting the density-dependent growth parameter to zero $b_1' = 0$ the equation simplifies to a classical non spatial mean field equation:

$$\frac{dN}{dt} = b_1 N - d_1 N \tag{3.9}$$

As we assumed that $b_1 = d_1$, the average density of individuals is constant (if N_0 is the initial density of individuals, than $N(t) = N_0$). Figure 3.10 compares the average densities of individuals yielded by both models for the case $b_1' = 0$ and shows

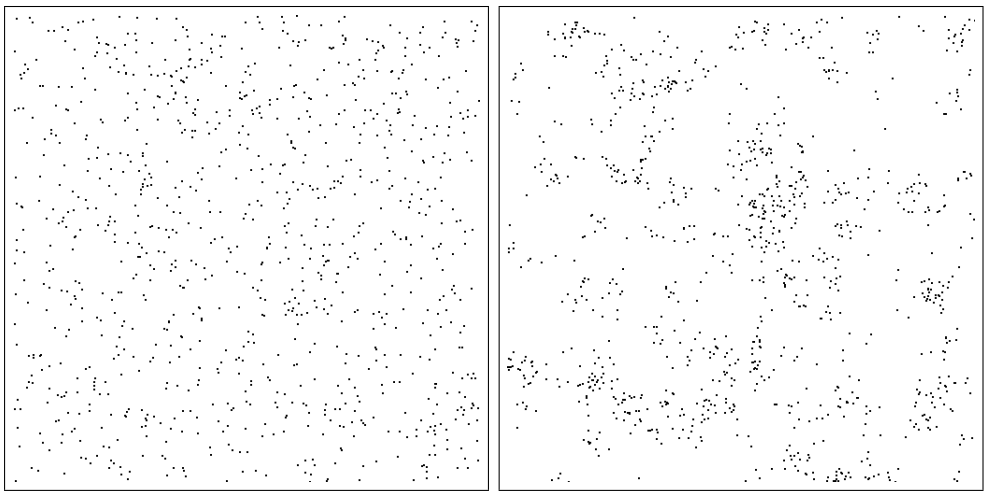

(a) Time=0 (b) Time=50

(c) Time=100

Figure 3.8: Individual-based simulation of pattern formation for $b_1 = d_1 = 0.1$, $b_1' = 0.0$

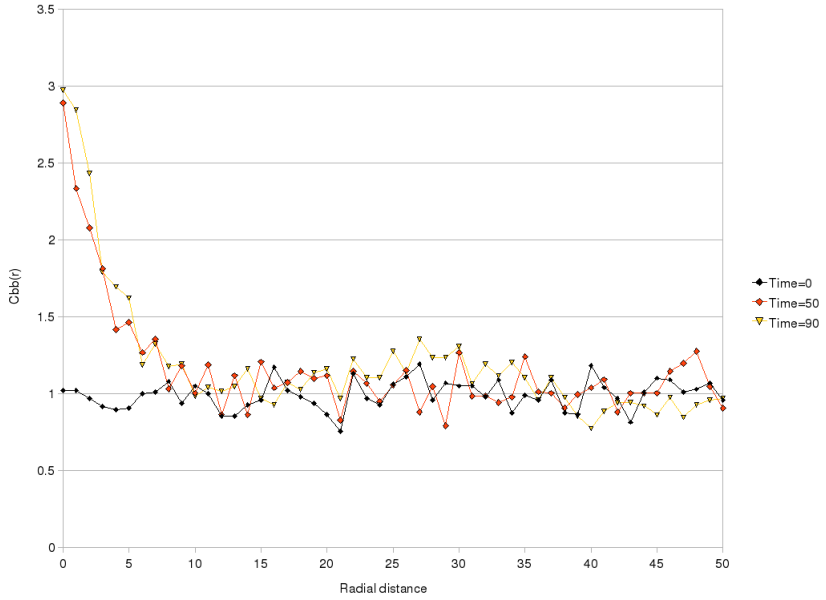

Figure 3.9: Radial pair correlation function yielded by the IBM for $b_1 = d_1 = 0.1$, $b_1' = 0.0$

that the average density of individuals remains constant in the moment model and that it fluctuates around the initial value in the IBM.

The moment model and IBM encompass additional informations about the spatial pattern. As we mentioned before, the assumption that daughter cells are located in the neighborhood of the mother cells is sufficient to produce spatial patterns. Figure 3.8 shows an illustration of such patterns. The initial uniform distribution of individuals in figure 3.8(a) evolves towards and aggregated patterns (figure 3.8(b)). The comparison of figure 3.8(b) and 3.8(c) shows that the pattern is dynamic and that aggregates change continuously in size and position due to the stochastic division and detachment events. This simulation illustrates one of the limitation of the IBM approach. The ecological signal is often blurred by stochastic fluctuations. Thus checking the model or its implementation is a non trivial task.

We use the pair correlation function as a measure to characterize the aggregated patterns yielded by the IBM. The function, measuring the average density of bacteria located at different vectorial distance from a focal individual, takes the form of a matrix. The matrix is radially symmetric and the center of the matrix correspond to the average density of neighbors at a distance smaller than the spatial resolution $d\xi$. Figure 3.9 shows the radial pair correlation function (extracted from the central row of the Cartesian pair correlation function). As the initial distribution of individuals is uniform the initial pair correlation function takes values close to one. However

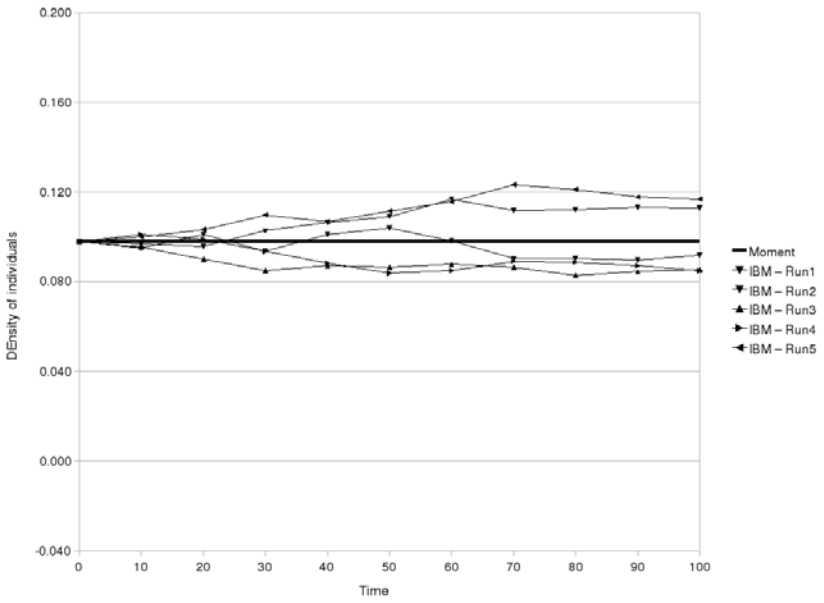

Figure 3.10: Time evolution of the simulated density of individuals calculated using the moment approximation model and the individual-based model (5 runs)

when pattern start to form, the function peaked at small distances indicating the formation of aggregates. The function reaches a pseudo-stationary (see figure 3.9 time = 50 and 90) and vary slightly due to random fluctuations.

Moment model attempts to capture the deterministic dynamic of the pair correlation function. Figure 3.11 compares the pair correlation function obtained by solving the moment model and the IBM. The results of the moment model are in accordance with those of the IBM. This shows that the moment model can help in extracting the deterministic ecological 'signal'. The moment model capture the main deterministic features of the spatial pattern simulated with the IBM.

3.2.2 Density dependant division model ($b_1' > 0$)

In the density-dependent division model, the division rate of the individuals is reduced by the formation of colonies. The spatial pattern is then expected to have an impact on the time course of the average density of individuals. In order to assess the impact of the spatial pattern, we use the non spatial mean-field model as a reference to which we compare the results of the IBM and the moment model. The mean-field limit is given by:

$$\frac{dN}{dt} = (b_1 - d_1)N - b_1' N^2 \tag{3.10}$$

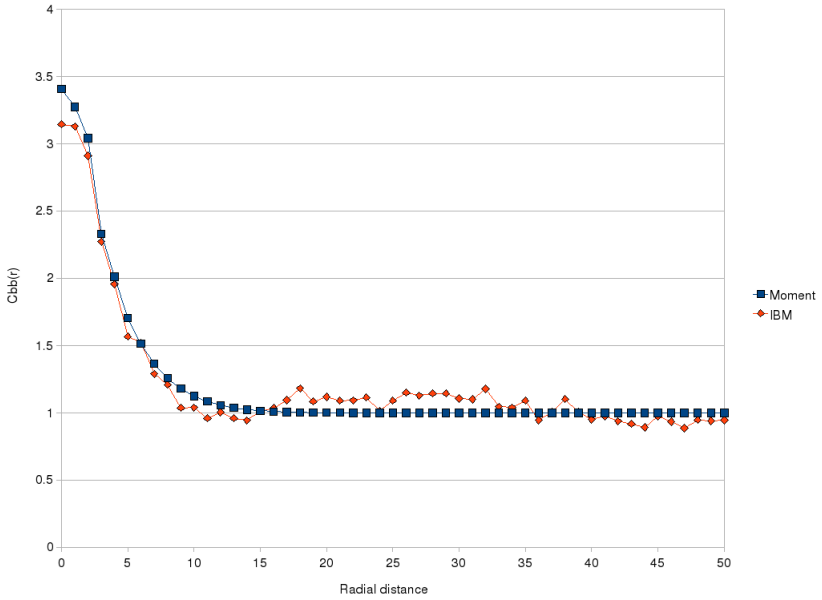

Figure 3.11: Comparison of the moment approximation model to the individual-based model. The individual-based results are averaged over 5 simulations

The stationary solutions are $N^* = 0$ or $N^* = (b_1 - d_1)/b_1'$. Note that if $b_1 = d_1$ than $N^* = 0$. For the simulations with the density-dependent model we consider the case where $b_1 > d_1$ and $b_1' > 0$. Figure 3.11 compares the time course of the average densities yielded by the IBM and the moment model for $b_1 = 0.1$, $d_1 = 0.05$ and $b_1' = 0.2$. The corresponding stationary solution obtained with the non spatial model is $N^* = 0.25$. Figure 3.12 shows that both the IBM and the moment models yields equilibrium values of the density of individuals lower than that yielded by the non spatial model. The formation of colonies reduces the division rate of the individuals compared to the case of uniform distribution of individuals.

Figure 3.13 shows the time evolution of the central element value of the Cartesian pair correlation function. The moment model captures well the dynamic of the local neighborhood simulated by the IBM.

3.3 Discussion

Our results on the density-dependent division-death model confirm that moment approximation can capture the deterministic average behavior of stochastic IBMs. IBMs used in microbiology are often complex and include several details about the shape and dynamic of the individuals. They can only explored numerically and are difficult to approximate with deterministic mathematical models. There are certainly research questions that require such a level of details. For instance detailed IBM may be needed for simulating the fine scale structure of biofilms and calculating

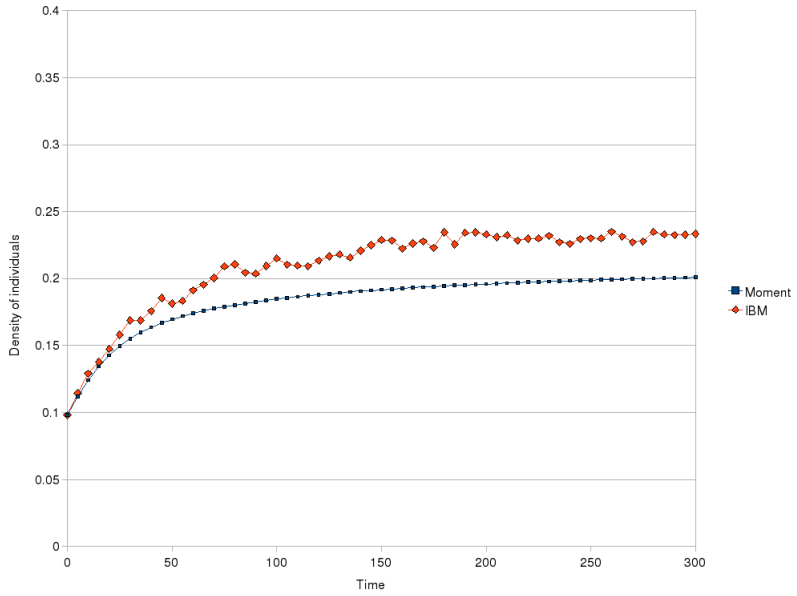

Figure 3.12: Time evolution of the average density of individuals : $b_1 = 0.1$, $b_1' = 0.2$ and $d_1 = 0.05$

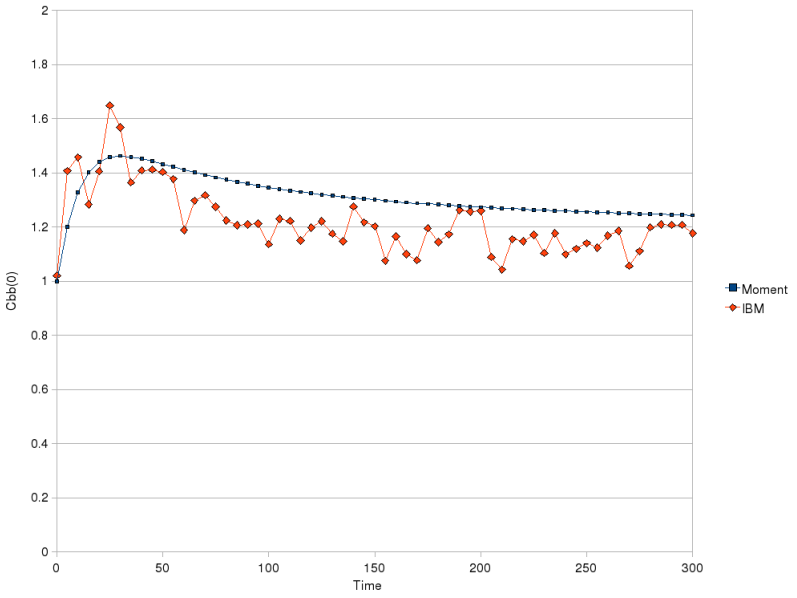

Figure 3.13: First point (at distance 0) of the radial pair correlation function: $b_1 = 0.1$, $b_1' = 0.2$ and $d_1 = 0.05$

physical and mechanical properties. However, if the focus is on understanding how spatial patterns affect the average population densities of microbial species, the detailed IBM can be simplified which yields less realistic fine scale structures but tractable models that can be approximated with moment techniques.

Deterministic approximation of IBMs has several advantages. First it is often easier to analyze a mathematical model than a stochastic IBM. Moment models are more computationally more performent than IBM. Second it is often difficult to check that IBMs implementation into a computer code is error free. Thus deterministic approximation may provide a reference to which the IBM results can be compared. Third, several questions which are important in ecology are difficult to answer on the sole basis of stochastic simulation. Example includes the characterization of the long-run patterns and the identification of stationnary states. Finally, IBM often have a large parameter state space that can only be sampled and it is difficult to determine the effect of varying parameters or initial conditions on the qualitative and quantitative outcome of the IBM.

The reduction of an IBM to a small set of equations require a number of approximation. Birch *et al.* [Birch 2006] showed that moment methods are reductions of the master equation. The master equation contains complete and detailed information concerning all of the statistical properties of an IBM but it is often very complicated to derive and to solve. Moment approximation is an alternative approach based on an unclosed hierarchy of spatial moments [Birch 2006]. Moment models are often limited to the first and second spatial moments and use approximative closure relation expressing the third moment as a function of the second and first moments. The closure expression implies that the positions of triplet and higher number of individuals are not correlated. This is an approximation that need to be assessed by comparing the moment model to the IBM simulation.

Another important approximation relies on the use, in the moment model, of the average local environment of the individuals. In moment models the average local environment is often expressed with the integral of the pair correlation densities weighted with an interaction kernel:

$$\int K\left(\frac{||\xi||}{w_d}\right) C(\xi) d\xi \tag{3.11}$$

However in the IBM the local environment of the individuals is variable. Thus if the local environment varies within a wide range individuals may experience local densities that are very different from the average. This may cause the failure of the moment model in capturing the individual-based dynamic as will be illustrated in chapter 6

Finally, the assessment of the quality of the approximation made in the moment model are often performed by comparing the IBM and the moment model simulations. The simulations are run for particular set of parameters and it is not clear whether a comparison of the results over a small set of parameters is sufficient to assess the quality of the approximation.

3.4 Annexe A: expressing the moment model in radial coordinates

Solving the moment approximation moment involves the calculation of two-dimensional convolutions having the following form:

$$(C \star m)(\xi) = \int_{\xi'} C(\xi + \xi')m(\xi')d\xi' \tag{3.12}$$

As ξ and ξ' are defined as vectorial distances which, when expressed in Cartesian coordinates write : $\xi = (\xi_1, \xi_2)$ and $\xi' = (\xi'_1, \xi'_2)$), the integral over the ξ' is a double-integral:

$$(C \star m)(\xi_1, \xi_2) = \int_{\xi'_1} \int_{\xi'_2} C(\xi_1 + \xi'_1, \xi_2 + \xi'_2)m(\xi'_1, \xi'_2)d\xi'_1 d\xi'_2 \tag{3.13}$$

The convolution can be also expressed in polar coordinates as:

$$(C \star m)(r) = \int_{r'} \int_{\theta} C(r')m(R(r, r', \theta))r'dr'd\theta \tag{3.14}$$

where $R(r, r', \theta) = (r^2 + r'^2 - 2rr'\cos\theta)^{1/2}$

Chapter 4

Moment approximation of a simplified biofilm IBM with detachment

Contents

4.1 Introduction

In this chapter we propose to derive a moment model approximating a simplified individual-based model (IBM) of microbial biofilms development. The IBM is basically an extension of the colony growth IBM presented in chapter 3 by considering a multi-colonies system and including a biofilm detachment process. Our aim is first to explore the different spatial patterns yielded by the IBM under different division and detachment conditions. We characterize these patterns using the first and second spatial moments introduced in the previous chapter. Second, we propose to approximate the dynamic of these aggregated descriptors using the moment approximation approach and compare the result of the aggregated mathematical moment model to the IBM simulations.

The chapter is organized in four sections. The first section is dedicated to the description of the simplified biofilm individual-based model where the individuals are subject to a density-dependent detachment process. In the second section we propose to explore the spatial patterns yielded by the IBM when the spatial ranges of the division and detachment kernels are varied. We derive a moment approximation model in the third section of the chapter. Finally we compare the moment model

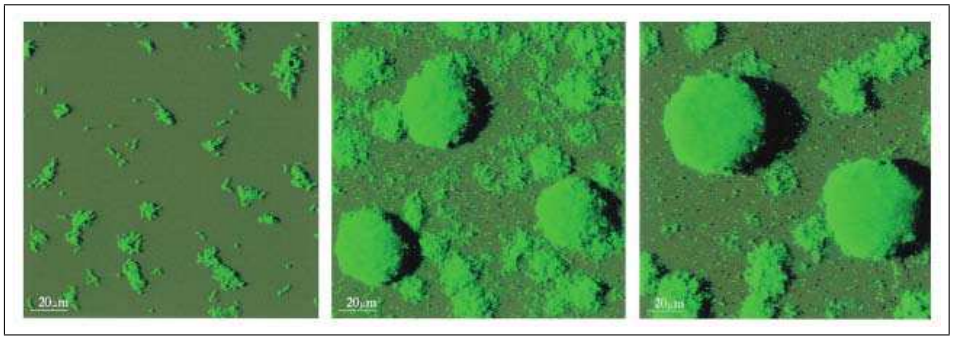

Figure 4.1: The spatial structure in a developing biofilm as revealed by advanced microscopy techniques (CSLM) [Tolker-Nielsen 2000]. The initial pattern formed with a small number of cells adsorbed on a surface (left) evolves toward a multi-colonies pattern (middle and right)

and the IBM in the fourth section and assess the capacity of the aggregated model in reproducing the main features of the simulated patterns.

4.2 A simplified biofilm IBM with detachment

Bacteria attach to hydrated surfaces and develop biofilms. Biofilms development is a complex and sequential process often initiated by the adsorption of a small number of cells on a surface. Through binary fission and a number of other mechanisms including surface migration, exopolymer production and detachment the initial colonizers develop progressively complex and sophisticated structures. Figure 4.1 shows an example of biofilm development process (under specific laboratory conditions) where a small number of cells develop into a multi-colonies biofilm.

The accumulation of the microorganisms on the colonized surface may be restricted by nutrient availability (treated in chapter 2 and 3) and/or counterbalanced by the detachment process. The term detachment here refers to different mechanisms by which bacterial particles are transported from the (attached) biofilm to the surrounding fluid phase. Different processes are responsible for detachment of biomass from biofilms and four categories can be distinguished [Morgenroth 2000][Stewart 1993]: (1) abrasion, (2) erosion, (3) sloughing and (4) predator grazing. Abrasion and erosion both refer to the removal of small groups of cells from the surface of the biofilm while sloughing refers to the detachment of relatively large portions of the biofilm [Morgenroth 2000].

In this section we describe a simplified IBM of biofilm development under different growth and detachment conditions. The model is basically an extension of the IBM that we presented in chapter 3 with the following three modifications:

- we assume that the division rate of the individuals is balanced exclusively by the detachment process rather than by the competition on the nutrient. Thus in this model we assume that an individual located in $x = (x_1, x_2)$ divides at a constant probability rate b_1. The probability that the individual in x produces a new born located in x' is given by:

$$B(x, x') = b_1 K\left(\frac{||x - x'||}{w_b}\right) \tag{4.1}$$

where $K(||x - x'||/w_b)$ is a birth kernel. As in chapter 3 we consider for simplicity a uniform kernel defined by:

$$K\left(\frac{||x - x'||}{w_b}\right) = \begin{cases} 1/w_b & \text{if} \quad ||x - x'|| < w_b \\ 0 & \text{else} \end{cases} \tag{4.2}$$

- we model the detachment process as a density-dependent process where the removal probability $D(x)$ of an individual located in x increases with the increase of the local density of individuals. The removal probability $D(x)$ is given by:

$$D(x) = d_1 + d_1' p_{loc}(x, w_d) \tag{4.3}$$

d_1 is a constant death rate and d_1' is the density dependent detachment rate. $p_{loc}(x, w_d)$ denotes the local density of individuals in x calculated using a uniform interaction kernel $K(||x-x'||/w_d)$ with size w_d. The interaction kernel measures how the individual in x perceives the effect of a neighbor individual located in x'. We obtain the local perceived density if x by summing the effect of all the neighbors:

$$p_{loc}(x, w_d) = \sum_{i=1}^{N} K\left(\frac{||x - x_i||}{w_d}\right) \tag{4.4}$$

The birth kernel measures the instantaneous dispersion of the daughter cell at a certain distance from the location of the mother cell. Taking large birth kernels would yield a rapid extension of the colony because the newly divided cells disperse over large distances. For detachment, a small detachment kernel can be considered as a proxy to model small biofilm fragment detachment as individuals separated with a short distance (with the order of the radii of the detachment kernel) are likely to experience the same the local density p_{loc} and would detach with the same probability.

Parameters	Description	Value
L	Domain size	201×201
ΔL	Spatial discretization	1
b_1	Density-independent bacteria division rate	0.12
d_1	Density-dependent detachment rate	0.02
d_1'	Density-dependent detachment rate	0.4
w_b	Size of the birth kernel	variable
w_d	Size of the detachment kernel	variable

Table 4.1: Individual-based model parameters

The assumption that the biofilm detachment probability (or rate) increases with the increase of the local density of individuals (or biofilm thickness in some models) is encountered in many biofilm detachment models. Implicitly we suppose that the biofilm detachment rate increases when the biofilm grows in the vertical dimension (though not considered explicitily in this model) due to an increased hydrodynamic shear stress.

The choice of the birth and detachment kernels may have an effect on the system dynamics [Hernàndez-Garcià 2004][Birch 2006]. With regard to density-dependent processes, the use of a uniform kernel embodies the assumption that all the individuals within the kernel window have an equal effect on the focal individual. A Gaussian interaction kernel would give a higher weight to the closest neighbors. This may have an effect on the observed patterns and on the dynamic of the population density. We discuss this briefly in the last section of this paper.

4.2.1 Individual-based model parameters

The model parameters are summarized in table 4.2.1.

4.3 IBM simulation results

To explore the patterns yielded by the IBM described above we start by considering the mean-field limit. In this case, all the individuals experience the same average conditions. This limit is obtained by setting the birth and detachment kernel sizes to relatively large values. A large birth kernel would mean that the individuals divide and disperse instantaneously over a large distance. This tends to prevent the formation of aggregates. Starting from this case, we progressively reduce the size of the birth kernel and explore the effect on the emergent spatial pattern. Figure 4.2 shows the (quasi) stationary spatial patterns yielded by the IBM for a large birth kernel ($w_b = 19$) and different sizes of the detachment kernel ($w_d = 3$ and $w_d = 19$). A large value of the birth kernel seems to prevent colony formation yielding a Poisson-like pattern where the individuals are uniformly distributed over the

domain. However, for small birth kernels (figure 4.3) we observe the formation of colonies spaced with a regular distance. The distance between the colonies corresponds approximatively to the radii of the detachment kernel as illustrated in figure 4.4 showing the stationary patterns for a small birth kernel $w_b = 3$ and two different detachment kernels $w_d = 19$ and $w_d = 31$. The increase of the size of the detachment kernel induced an increase in the spacing between the colonies. The pattern of isolated colonies in figure 4.4 is a typical example of a system-level behavior that emerges out of the local interactions. The pattern minimizes the competition between the colonies with regard to detachment. If the colonies were too close to each other, the individuals in each colony would experience a higher local density than the local densities experienced if the colonies were isolated. By keeping a distance between the individuals corresponding approximatively to the radii of the detachment kernel, the individuals within each colony experience only the effect of their neighbors in the colony.

4.4 Deriving the moment approximation model

We propose to approximate the dynamic of the average density of individuals and the pair correlation function using moment approximation technique and compare the results with those measured on the IBM patterns. The state variable of the moment model are the average density of individuals N (the first spatial moment) and the pair correlation function $C(\xi)$ (the second spatial moment) where $\xi = (\xi_1, \xi_2)$ is a vectorial distance. The dynamic of these variables is given by:

$$\frac{dN}{dt} = b_1 N - d_1 N - d_1' \int K\left(\frac{||\xi||}{w_d}\right) C(\xi) d\xi \tag{4.5}$$

The first and second terms on the right-hand side (RHS) are relative to the neighborhood-independent division and detachment processes. The third term in the RHS is the neighborhood-dependent component of the detachment process. The integral term involves the pair density function $C(\xi)$ and the interaction kernel $K(||\xi||/w_d)$. This term accounts for the effect of the local environment on the mean density of individuals which is the result of the spatial structure, as given by $C(\xi)$, and on the extent the individuals experience the effect of this structure as given by $K(||\xi||/w_d)$. Note that if the side of the uniform interaction kernel, w_d, is equal to the side L of the domain than equation 4.5 can be simplified to the mean-field equation:

$$\frac{dN}{dt} = (b_1 - d_1)N - d_1' N^2 \tag{4.6}$$

We suppose however that the detachment kernel is relatively small ($w_d = 3$ to 31) compared to the size of the domain ($L = 201$). The dynamic of the pair correlation function is given by:

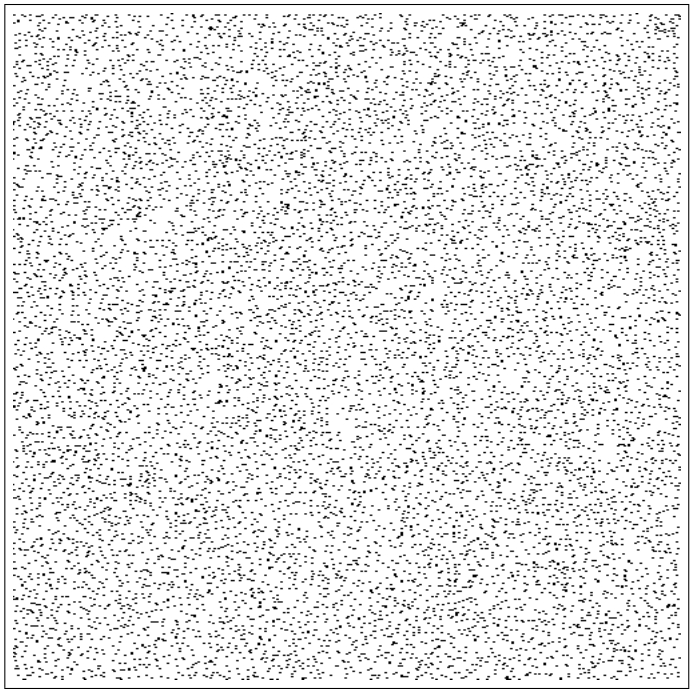

(a) $w_d = 3$

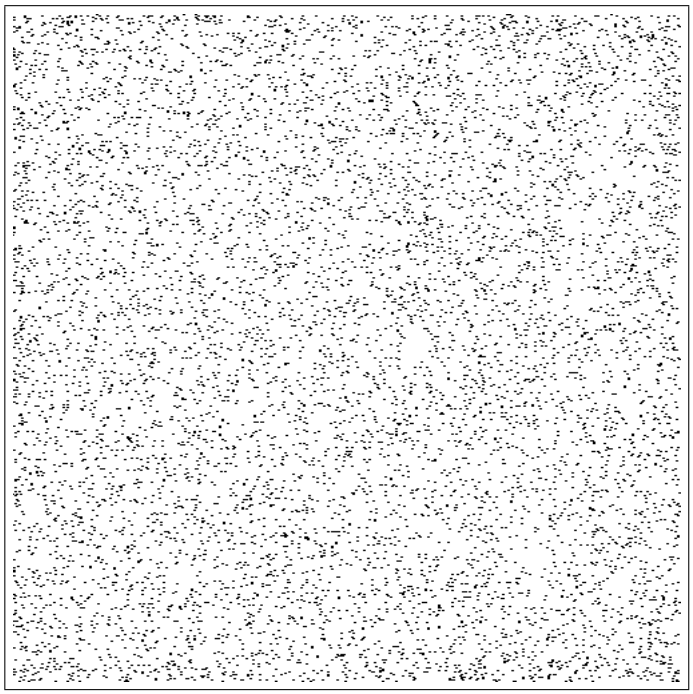

(b) $w_d = 19$

Figure 4.2: (Quasi) stationary spatial patterns yielded by the IBM for $w_b = 19$ and variable w_d

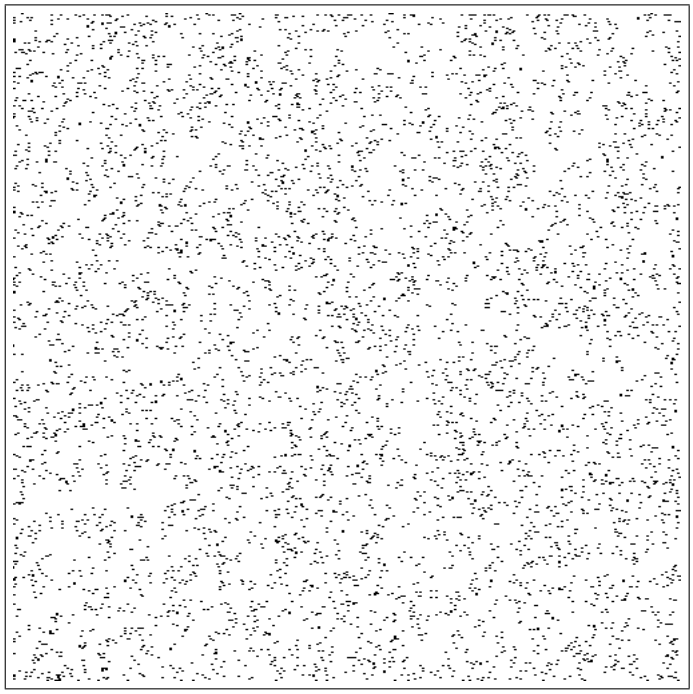

(a) $w_d = 3$

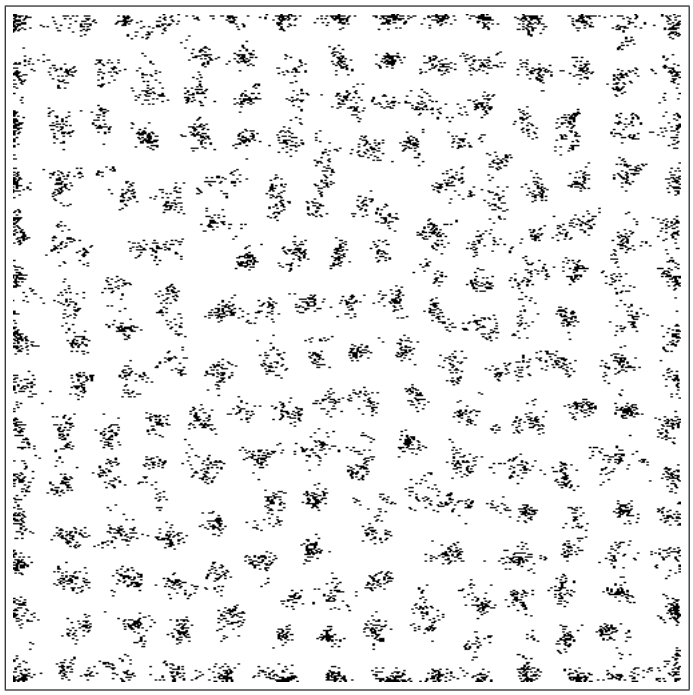

(b) $w_d = 19$

Figure 4.3: (Quasi) stationary spatial patterns yielded by the IBM for $w_b = 3$ and variable

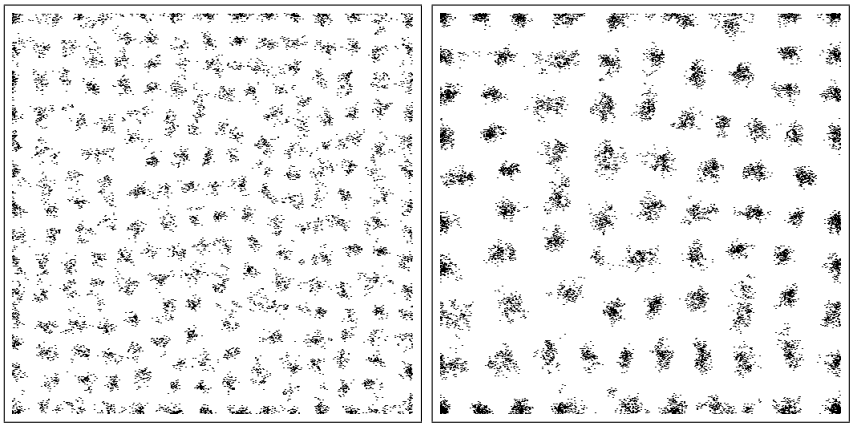

(a) $w_d = 19$ (b) $w_d = 31$

Figure 4.4: (Quasi) stationary spatial patterns yielded by the IBM for $w_b = 3$ and large detachment kernels

$$\begin{aligned}\frac{dC(\xi)}{dt} &= 2b_1 NK\left(\frac{||\xi||}{w_b}\right) + 2b_1 \int K\left(\frac{||\xi'||}{w_b}\right) C(\xi+\xi')d\xi' \\ &- 2d_1 C(\xi) - 2d_1' K\left(\frac{||\xi||}{w_d}\right) C(\xi) - d_1' \int K\left(\frac{||\xi''||}{w_d}\right) T(\xi,\xi'')d\xi'' - \\ &- d_1' \int K\left(\frac{||\xi''||}{w_d}\right) T(-\xi,\xi'')d\xi''\end{aligned} \tag{4.7}$$

The first and second terms on the right-hand side account for the formation of new pairs at distance ξ through division events and are explained in the previous chapter. The third to sixth terms account for the effect of detachment. These last three terms are negative as detachment eliminates pairs. Following is a more detailed description of these six terms:

- the first term accounts for the density-independent division of an individual i producing a new individual j located at a vectorial distance ξ. Multiplying the mean density of individuals N by the independent per capita division rate b_1 gives the rate of division events. Then we multiply by the probability that the newly formed cell is located at distance ξ from the parent position. The factor 2 accounts for newly formed individuals that disperse to distance $-\xi$ which also form a new pair (j,i) at distance ξ.

- the second term also accounts for the density-independent division, but focuses on the new pair that the offspring of an individual i forms with and individual j located at a distance $\xi+\xi'$ from i. The per capita rate of density-independent division is b_1, the density of (i,j) pairs is $C(\xi+\xi')$ and the spatial density of

offspring settling around the i parent is $K(||\xi'||/w_b)$. Multiplying these three factors and integrating over all possible distances ξ' of offspring dispersal yields the second term.

- the third term accounts for ij pairs that are lost due to the density-independent death of the individual i in the pair (respectively j).
- the fourth term corrects the death rate of the individual i in the pair ij by adding the effect of the individual j on the death rate of the individual i.
- the fifth and sixth terms correct the death rate of the individual i in the pair ij by adding the effect of neighbors (other than j) located at a distance ξ'' from i. The density of this triplet configuration is given by the triple density function $T(\xi, \xi'')$ and $T(-\xi, \xi'')$ We multiply by the detachment kernel calculated at distance ξ'' and integrate over all possible neighbors (or all distances ξ'').

The system formed with equations 4.5 and 4.7 involves the third spatial moment $T(\xi, \xi')$. To close this system we need to express the third moment as a function of the first and the second moments. We use the following closure expressions [Dieckmann 2000]:

$$T(\xi, \xi') = \frac{C(\xi)C(\xi')C(\xi' - \xi)}{N^3} \tag{4.8}$$

As will be detailed in the next paragraph the choice of the closure expression can have a significant impact on the simulated pattern. This choice is guided by the comparison of the moment and the individual-based model patterns. A good closure is the one that allows the moment model to capture the main features of the patterns and dynamics yielded by the individual-based model.

We solve the moment model formed with equations 4.5, 4.7, 4.8 and **??**, as detailed in the previous chapter, by discretizing the vectorial distances ξ with a spatial resolution $d\xi = (d\xi_1, d\xi_2)$ and time with a constant time step Δt. We use an explicit Euler scheme for descritizing the time derivative. The resultant algebraic system is formed with $n_x^2 + 1$ equation (where n_x is the size of discretized $C(\xi)$ expresses the density of individuals N and the pair correlation matrix $C(\xi)$ at the instant $t + \Delta t$ as a function of N and C at the previous instant t.

4.5 Comparison of the moment model and the IBM

We compare the time course of the average density of individuals yielded by the IBM and the moment model (figure 4.5) and the stationary radial pair correlation function (figure 4.6). For a large birth kernel $w_b = 19$, the IBM and the moment models yields comparable results to those obtained with the mean-field limit (dashed line in figure 4.5(a)). In this case where the distribution of the individuals is uniform as can be seen from the pair density correlation functions in figure 4.6(a)which take values close to 1 in both models indicating that the local density of pairs is almost

equal to N^2 (the average density of pairs in the system) For small birth kernels however, the density of individuals increases in both models beyond the stationary value yielded by the mean-field model. This is a counter intuitive result as one may expect that the formation of aggregates would increase the detachment rate of the individuals yielding lower equilibrium density than what would be obtained in the case of a uniform distribution. The organization of the individuals with a regular distance is likely to induce a lower average detachment rate as this arrangement seems to minimize the competition with regard to detachment between the colonies.

The pattern of isolated colonies yields an oscillating radial pair correlation function. The first peak is due to the high density of neighbors within the colony (short distance). the waves are due to the regular arrangement of the colonies. The peaks in the IBM are lower than those yielded by the moment model and the wavy radial pair correlation function seems to vanish to 1 in the IBM for large distances. This is due to the fluctuations around the colonies simulated by the IBM. The individuals are in majority enclosed within the colonies but some of them are still between the colonies due to the stochastic division and detachment process. This blurs the deterministic ecological signal as revealed by the moment model.

4.6 Discussion

We approximated the dynamic of a simplified IBM with a population of individuals inhabiting a two-dimensional domain. The individuals are subject to division events and a density-dependent detachment process. The numerical exploration of the IBM shows for large birth kernels the newborn cells disperse over large distances preventing the formation of colonies. In this case the average density yielded by the IBM evolve as in the mean-field limits.

However when we reduce the size of the birth kernel, patterns with isolated microcolonies may emerge and can be observed especially when the size of the detachment kernel is higher than that of the birth kernel.

We approximated the IBM with a moment model. Moment model attempts to capture how the local environment of the individuals evolve in time and how it affects the average density of individuals. The derived moment model is globally in a good agreement with the IBM. Moment model predicts a Poisson-like distribution in the case of large birth kernels and an oscillating radial pair correlation function, in the case of small dispersion and large detachment kernel, with a period approximatively corresponding to the size of the detachment kernel. The peaks in the oscillating pair correlation function however are high in the moment model than in the IBM. This may be explained by the choice of the closure. The closure expresses the the third moment in term of first and second moments. The moment model results can be very sensitive to the choice of the closure expression. For instance the classical second order closures ($T(\xi, \xi') = C(\xi')C(\xi)/N$) fails in predicting the wavy strcture of the pair correlation while the third order closure overestimates the hight of the

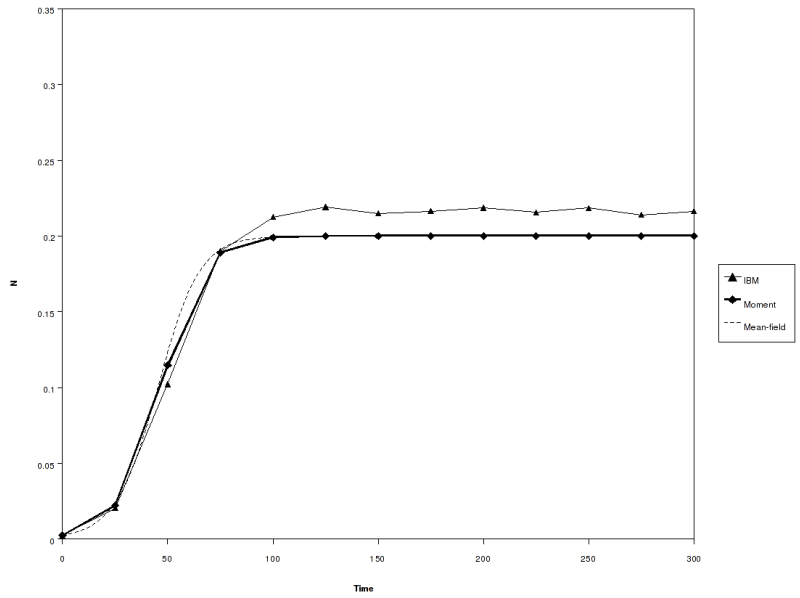

(a) $w_b = 19, w_d = 19$

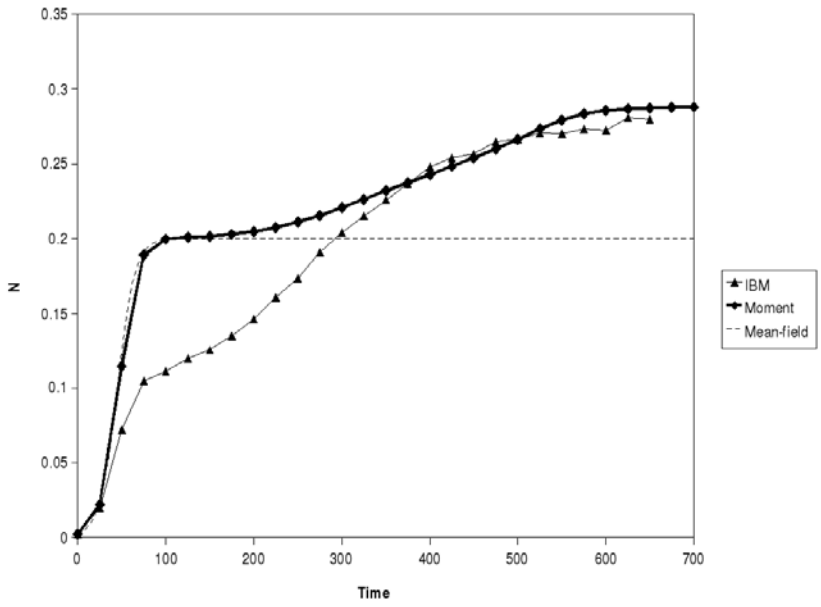

(b) $w_b = 3, w_d = 19$

Figure 4.5: Comparison of the average densities of individuals (first spatial moment) calculated with the moment model and simulated with the IBM for different birth kernel sizes: $w_b = 19$ and 3 (Domain size 201×201 and $w_d = 19$)

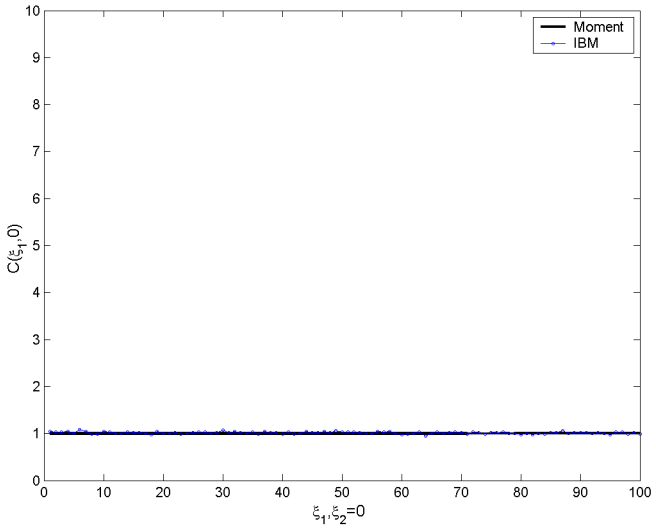

(a) $w_b = 19$

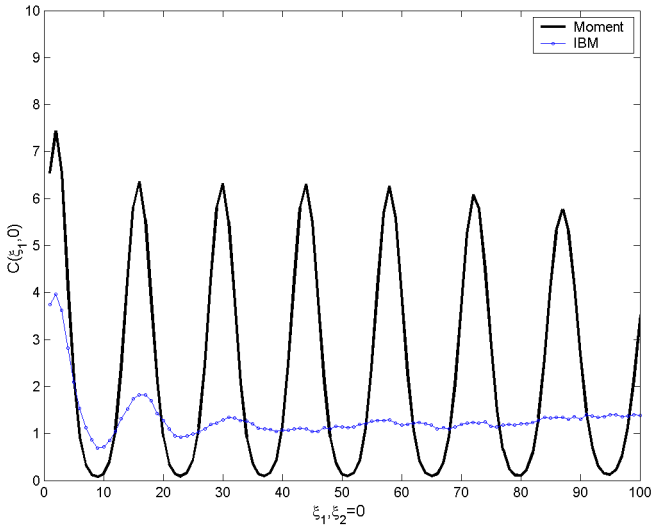

(b) $w_b = 3$

Figure 4.6: Comparison of the radial pair yielded by the IBM and the moment model for $w_d = 19$ and different sizes of the dispersion kernel

peaks.

This is one of the limtations of moment models which provide deterministic approximations of the dynamic of the individual-based model. The quality of the approximation need to be assessed through comparison to the individual-based model simulations and improved by selecting the best closure expression.

Chapter 5

A detailed individual-based model of biofilm formed with motile bacteria

Published in Theory in Biosciences: Mabrouk, N., Deffuant,G.,Tolker-Nielsen,T., Lobry,C.: Bacteria can form interconnected microcolonies when a self-excreted product reduces their surface motility: evidence from individual-based model simulation. DOI: 10.1007/s12064-009-0078-8

Contents

We propose to analyze using numerical experimentations a new individual-based model of a microbial system formed with surface-associated motile bacteria which motility is reduced by a self-excreted substance. The model is inspired from recent experimental observations of *Pseudomonas aeruginosa*, a model bacterium in biofilm research that have been shown to bind, under specific growth conditions, to self-excreted DNA. These experimental observations also showed that *Pseudomonas aeruginosa* forms interconnected microcolonies and presumed a possible involvement of the extracellular DNA in the formation of these patterns. In this chapter, we use an individual-based model to assess the involvement of bacteria motility and interaction with self-excreted extracellular substance in the formation of patterns with interconnected microcolonies. Our analysis is based on numerical experimentations using the IBM and starting with obvious cases than moving progressively to the case of interest.

5.1 Background

Many bacteria have an innate propensity to form biofilms: they build structured multicellular communities attached to solid surfaces. Microscopic examination of biofilms formed by Pseudomonas aeruginosa, a model bacterium in biofilm research [Costerton 1995][Davey 2000], reveals a wide diversity of spatial patterns which, depending on the growth conditions, range from a flat thin layer of cells to a patchy pattern with interconnected microcolonies having complex tower or mushroom like shapes [Klausen 003b][Barken 2008]. At least some explanation for the different biofilm patterns formed under different conditions relates to surface motility. Conditions that promote extensive surface motility can lead to the formation of flat, homogeneous biofilms, whereas biofilms characterized by aggregates result from at least a subpopulation of the community ceasing to move at an early stage of biofilm formation [Parsek 2008]. In *P. aeruginosa* biofilms, formation of initial microcolonies (stalks) that subsequently become colonized by cap-forming bacteria is necessary for the formation of mushroom-shaped multicellular structures [Klausen 003a][Klausen 003b]. These multicellular structures often provide important benefits such as a higher tolerance to adverse conditions [Parsek 2008], and can be crucial in industrial processes. Therefore, much experimental and theoretical effort is currently devoted to understand their mechanisms of formation.

The formation of spatial patterns in *P. aeruginosa* biofilms involves a complex interplay between cell proliferation, surface-associated motility and the production of extracellular macromolecules that form a structural matrix (for a review see [Parsek 2008]). Evidence has been provided that arrest of type IV pili-mediated motility (twitching motility) plays a role in the formation of the initial microcolonies in P. aeruginosa biofilms, whereas flagella- driven motility (swarming motility) plays a role in the subsequent formation of the cap-portion of the mushroom-shaped structures [Klausen 003a][Klausen 003b][Barken 2008]. The early stages of biofilm development by *P. aeruginosa* is dependent on extracellular DNA [Whitchurch 2002], which is known to bind with high affinity to type IV pili [Aas 2002][Van Schaik 2005], a fimbrae extending from the cell body and mediating surface-associated twitching motility. Hence it may be assumed that initially motile bacteria stop and form microcolonies in the regions of abundant extracellular DNA. Recently, Allesen- Holm et al. [Allesen-Holm 2006] visualized the spatial distribution of extracellular DNA and bacteria in P. aeruginosa biofilms, grown in flow chambers on minimal glucose medium. In 2-day-old biofilms the extracellular DNA was present inside the small microcolonies, but accumulated mainly in the outer layer of the microcolonies and between the microcolonies forming a grid-like structure. Zoomed views of the microcolonies revealed that they were often interconnected with thin strands of extracellular DNA covered with bacteria (see figure 5.1). In 4-day-old biofilms cap- like multicellular structures had formed on top of the initial small microcolonies, and the highest concentration of extracellular DNA was present between the stalk- portion and the cap-portion of the mushroom-shaped

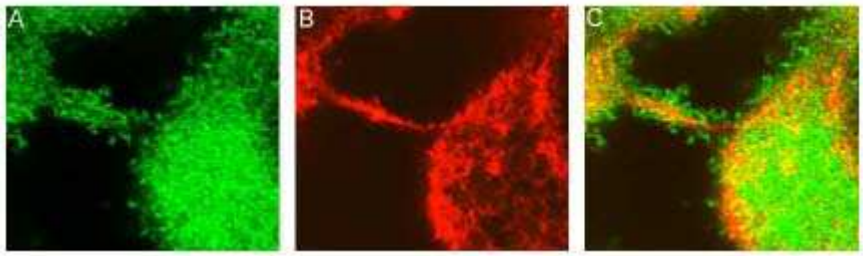

Figure 5.1: Horizontal confocal laser scanning microscope section acquired in a 2-day- old DDAO-stained biofilm formed by Gfp-tagged *P. aeruginosa* PAO1. The images show the green fluorescent bacteria (A), the red fluorescent extracellular DNA (B), and an overlay of the two (C). Reproduced from Molecular Microbiology 59: 1114-1128

multicellular structures.

The factors involved when bacteria shift from being motile to sessile in biofilms are currently not fully understood. In the present article we present a simple spatially explicit individual-based model in which bacterial motility is reduced by a self-produced extracellular substance.

IBMs have been widely used for modeling spatial organization of bacteria within colonies [Kreft 2001] [Ginovart 2002] and biofilms [Kreft 2001][Xavier 2005] (for a review see [Ferrer 2008] and [Hellweger 2009]). Recently, an individual-based model of surface associated populations of *P. aeruginosa* has been presented [Picioreanu 2007]. The model involves a three-dimensional space and aims to provide a proof-of- principle of the implication of motility in the formation of biofilm structure. It reproduces qualitatively the tendency of motile bacteria to form flat biofilms and that of immotile bacteria to form microcolonies by clonal growth, and proposes detachment and reattachment processes of the motile bacteria as possible mechanisms yielding the formation of complex mushroom-shaped microcolonies. In our model, we focus on the interplay between extracellular DNA production and bacterial motility. We show that a model where bacterial migration is stopped due to adherence to self-produced extracellular DNA can produce complex patterns of interconnected microcolonies.

5.2 Model description

We describe the model through the ODD protocol (Overview, Design concepts and Details) [Grimm 2006].

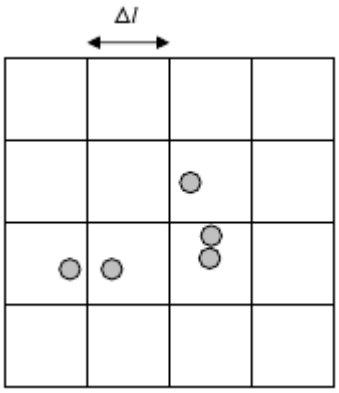

Figure 5.2: Schematic representation of the model entities: bacterial cells (discs) and patches (squares with a side Δl). A bacterium with continuous coordinates x,y is contained in the patch $i = floor(x/\Delta l)$, $j = floor(y/\Delta l)$.

5.2.1 Purpose

The model we propose is intended to qualitatively explore the role of surface-motility reduction by self-produced macromolecules in biofilm pattern formation. We address this question at a rather abstract level, and the model results are not compared to specific experimental results.

5.2.2 State variables and scales

The model is a two-dimensional representation of a biofilm system and comprises two entities: bacterial cells and their local environment (patches) (figure 5.2). Bacterial cells are represented as discs. They are characterized by the state variables: continuous position (x, y), individual mass (m), individual diffusion factor (D_f) and individual substrate uptake rate (r)(table 5.1). A Patch (i, j) is characterized by the state variables: substrate concentration (s), extracellular substance concentration (p) and a substrate uptake rate (r_s). The later corresponds to the sum of uptake rates of the individual cells contained within the patch (table 5.1).

5.2.3 Scales

We simulated the first day of the biofilm development. We discretized time with a constant time step, denoted $\Delta t = 1s$. A spatial patch has a size of 5×5 μm and the whole domain contains 400×400 patches (spatial domain side $l = 2000\mu m$). Bacterial cells have variable diameters ($\sim 2\mu m$) depending on their masses.

5.2.4 Process overview and scheduling

In the IBM, bacteria move stochastically along a 2-D surface while consuming substrate, growing and reproducing by binary fission and excreting a product. Bac-

	Variable	Description
Bacterium state	x, y	Continuous position of the center of the bacterium
	m	Mass
	D_f	Diffusion factor
	r	Individual substrate uptake rate
Patch state	s	Substrate concentration
	p	Excreted product concentration
	r_s	Reaction rate (sum of substrate uptake rates of the individual cells contained within the patch)

Table 5.1: State variables of the individual-based model

teria movement is then slowed down through interactions with the excreted product yielding different patterns of microcolonies.

At each time step the following processes are performed sequentially:

- Bacteria growth: for each individual cell we (1) calculate and individual substrate uptake rate (r) which depends on the mass of the cell and the local substrate concentration. (2) We use the calculated uptake rate to update the mass of the cell.

- Substrate uptake rates for patches: given the uptake rates of each individual cell, we calculate an uptake rate (r_s) for each patch by taking the sum of the uptake rates of the individual cells contained within it.

- Division: for each individual cell we compare the cell mass to a critical value. If the cell mass is higher than the critical value than the cell is divided into two daughter cells. One the daughter cells takes the position of the mother cell while the second is placed at random around the mother cell position at a distance (d) corresponding to the diameter of the daughter cell.

- Surface motility: we model bacteria translocation as a Brownian process using an diffusion factor (D_f) proper to each individual. For each individual cell, including newly formed cells, we calculate a diffusion factor (D_f) using a decreasing function of the local product concentration and then move the individual cell accordingly.

- Shoving: bacteria division and motion may produce cells overlaps. In this case cells are displaced using an algorithm proposed by [Kreft 2001]that mimics a shoving process.

- Substrate and excreted product mass balances: we modeled the substrate and the excreted product dynamics using two diffusion-reaction equations discretized on the lattice formed by the patches. The reaction terms in these equations are calculated using the substrate uptake rate (r_s) previously calculated for each patch.

5.2.5 Design Concepts

- Emergence: the IBM is designed such that the spatial pattern of bacteria and product distribution emerge from local interactions.
- Sensing: in our model, a bacterium senses the substrate and product concentration within the patch corresponding to its position. The substrate concentration affects the growth rate of the bacterium whereas the product concentration affects the motility of the bacteria.
- Stochasticity: bacteria motility and the positioning of the daughter cells after a division event are the only stochastic processes that we considered in the IBM.
- Observation: at each time step the state variables for bacteria and patches are recorded.

5.2.6 Submodels

5.2.6.1 Bacteria growth

We calculate the individual substrate uptake rate ($r(t)$) of a cell located in (x, y) and having a mass m using the following Monod-like kinetic equation:

$$r(t) = \mu_{max} m \frac{s(i,j,t)}{s(i,j,t) + k_s} \tag{5.1}$$

Where $s(i,j,t)$ is the substrate concentration at patch (i,j) with $i = floor(x/\Delta l)$ and $j = floor(y/\Delta l)$ and μmax and ks are Monod kinetic parameters. The growth rate of the bacterium is given by:

$$\frac{dm}{dt} = Y_b r(t) \tag{5.2}$$

Where Yb is the biomass yield (expressed in mass of bacteria per mass of consumed substrate). The time derivative is discretized using an Euler explicit scheme and the new mass of the cell is calculated by:

$$m(t + \Delta t) = m(t) + \Delta t Y_b r(t) \tag{5.3}$$

With Δt the time step. The product excretion rate $rp(t)$ of the considered individual cell is given by:

$$r_p(t) = Y_p r(t) \tag{5.4}$$

5.2.6.2 Substrate Uptake rates

For each patch we calculate a substrate uptake rate $rs(t,i,j)$ by summing the individual substrate uptake rates of the cells contained within the patch:

$$r_s(t,i,j) = \frac{1}{\Delta l^2} \sum_k r_k(t) \tag{5.5}$$

where k is the number of cells in patch i,j.

5.2.6.3 Bacteria division

If the mass of a focal individual (a mother cell) becomes greater than twice the initial mass of an individual ($2m_0 \leq m$) it divides into two daughter cells each with a mass $m/2$. The first daughter cell takes the position of the mother cell while the second daughter cell is placed randomly at a distance d (distance between the centers of both cells) corresponding to the diameter of the daughter cells (both daughter cells have the same diameter).

5.2.6.4 Bacteria motility

The motility of the cells is modeled as a Brownian motion process with an apparent diffusion factor (Df) which is specific to each individual cell. For a given bacterium located at x,y at time t, the position of the bacterium at the instant $t+\Delta t$ is given by:

$$\begin{aligned} x(t+\Delta t) &= x(t) + \sqrt{2D_f(x,y)\Delta t}N(0,1) \\ y(t+\Delta t) &= y(t) + \sqrt{2D_f(x,y)\Delta t}N(0,1) \end{aligned} \tag{5.6}$$

where $N(0,1)$ draws a number from a centered normal distribution of standard deviation 1 (generated using the Mersenne Twister pseudo-random number generator). As we assumed that bacteria motility was reduced by the excreted product, we calculate diffusion factor (D_f) as a decreasing function of the excreted product concentration in the corresponding patch (i,j). We use the following function:

$$D_f = D_{fmax}\frac{1}{1+\beta p(i,j,t)} \tag{5.7}$$

Where D_{fmax} is the maximum diffusion factor of the bacterium, β is a binding affinity factor and $p(i,j,t)$ is the product concentration at patch (i,j). The parameter β rules the sensitivity of Df to the variation of $p(i,j,t)$ as shown by figure 5.3.

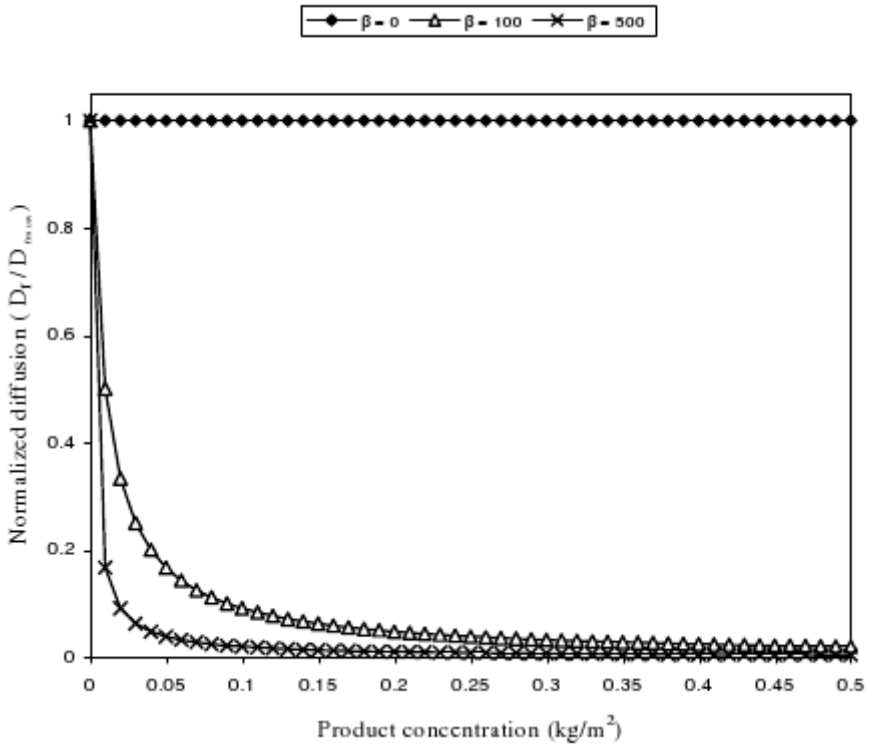

Figure 5.3: Motility dependence on the excreted product concentration for different values of β

5.2.6.5 Bacteria shoving

Bacteria shove each other when they overlap. If a bacterium with radius a is overlapped with n neighboring cells, it is displaced with a shoving vector d calculated using the following equation adapted from [Kreft 2001]:

$$d = \sum_{k=1:n} \frac{a + a_k - d_k}{2} u_k \tag{5.8}$$

a_k is the radius of the neighbor cell k, d_k is the Euclidean distance from the center of the bacterium to the center the kth neighboring cell and u_k is a vector directed from the center of neighbor bacterium k towards the center of the bacterium and having a unitary norm.

5.2.6.6 Substrate and excreted product mass balance equation

The distribution of the substrate is the solution of the following continuous diffusion-reaction equation:

$$\frac{\partial s}{\partial t} = D_s \nabla^2 s - r_s \tag{5.9}$$

with periodic boundary conditions:

$$s(t, x = 0, y) = s(t, x = l, y) \tag{5.10}$$

$$s(t, x, y = 0) = s(t, x, y = l) \tag{5.11}$$

and having as initial conditions:

$$s(t = 0, x, y) = s_0 \tag{5.12}$$

The excreted product dynamic is also given by a diffusion-reaction equation:

$$\frac{\partial p}{\partial t} = D_p \nabla^2 p + Y_p r_s \tag{5.13}$$

with periodic boundary conditions:

$$p(t, x = 0, y) = p(t, x = l, y) \tag{5.14}$$

$$p(t, x, y = 0) = p(t, x, y = l) \tag{5.15}$$

and having as initial conditions

$$p(t = 0, x, y) = 0 \tag{5.16}$$

Y_p in (equation 5.13) is the product yield expressed in mass of excreted product per mass of consumed substrate. We discretize substrate and product mass balance equations with respect to space on the lattice formed with the patches using a four-point scheme. The reaction term has already been calculated for each patch (equation 5). We discretize time derivative term in the substrate and the product mass balance equations using an implicit scheme for the diffusion term. Note that the reaction term is calculated on the basis of an explicit scheme. The obtained discretized system is a sparse linear system that we solve using an explicit Euler method. This gives the new substrate and product concentrations in each patch.

Parameter	Description	Units	Value
l	Domain size	(μm)	2000 (*)
Δl	Spatial step	(μm)	5 (*)
D_s	Diffusion constant for the substrate	(m^2/s)	10^{-10} (**)
D_p	Diffusion constant for the product	(m^2/s)	10^{-16} (*)
D_{fmax}	Maximum diffusion factor for the bacteria	(m^2/s)	10^{-12} (**)
μ_{max}	Maximum growth rate	$kg_{substrate}/(kg_{biomass}\ s)$	10^{-4} (**)
k_s	Affinity constant	$kg_{substrate}/m^2)$	0.01 (**)
Y_p	Product yield	$kg_{biomass}/kg_{substrate}$	0.1 (*)

Table 5.2: Table 2 Individual-based model parameters. Source: (*)Assumed - (**)Adapted from [Picioreanu 2007]

Parameter	Description	Units	Value
s_0	Initial substrate concentration in all patches	kg/m^2	10.0
p_0	Initial product concentration in all patches	kg/m^2	0.0
N_0	Initial number of bacterial cells	–	100
m_0	Initial mass of a bacterium	kg	10^{-15}

Table 5.3: Initial conditions of the individual-based model

5.2.6.7 IBM parameters

Unless explicitly specified, we use the parameters values in table 5.2 for the individual-based model.

5.2.6.8 Initialization

We initialize all simulations with:

- a uniform initial substrate concentration s_0
- a uniformly null concentration of excreted product
- N_0 bacterial cells drawn at random in the domain each with the same initial mass m_0.

Initial conditions are detailed in table 5.3.

5.2.6.9 Model implementation

We implemented the model using the Java programming language and the Mason framework. Mason is a discrete event multiagent simulation library code developed at the George Mason University for implementing multi-agent models [Luke 2004].

5.3 Results

We simulate the patterns formed by the spatial distribution of bacteria and the excreted product displayed after 9 and 18 hours for different values of β (the parameter determining the impact of the excreted product on bacteria motility) and for the case of immotile bacteria. Two extreme cases can be identified. In the first case, bacteria are motile and their motility is independent from the excreted product ($\beta = 0$) while in the second case bacteria are immotile $D_{fmax} = 0$. Figures 4 and 5 show the patterns obtained in these limiting cases. Motile cells disperse over the spatial domain (Fig. 4) in contrast with immotile cells that form isolated microcolonies (Fig. 5). These results are consistent with previous theoretical [Picioreanu 2007] and experimental [Klausen 003b] studies of *P. aeruginosa* showing that motile cells tend to form flat biofilms while immotile bacteria form round shaped microcolonies.

We also simulated intermediate cases where the bacteria motility depends on the local concentration of the excreted product. Figure 6 and 7 show examples of spatial pattern obtained after 9 and 18 hours for a small and a large value of the parameter β respectively. As the system evolves over time, the patterns of microcolony formation under the two parameterizations begin to diverge. A large value of β results in microcolonies that are more spatially discrete with higher densities of individuals within them (Figure 5.7), while the smaller value of β results in a pattern of microcolonies that are more amorphous in size and shape, are more connected with each other, and densities of bacteria within them are lower (Figure 5.6).

In our simulations, microcolony formation is initiated by the local accumulation of the product excreted by the cells along their Brownian trajectories. The product excretion rate is maximal ($\sim Y_p \mu_{max}$, see Equations 5.1 and 5.7) at the beginning of the simulation when the substrate ($S >> k_s$ in Equation 1) is abundant and accumulates due to its low diffusion factor. For large values of β bacteria are rapidly entrapped within the locations containing the excreted product and their daughter cells tend to accumulate locally yielding dense and discrete microcolonies. In the opposite for small values of β, bacteria and their daughter cells tend to disperse and the yielded microcolonies have amorphous shape. Analogously, simulation with different values of the product excretion ratio Y_p (Equation 5.7), at a constant value of β, between the two extreme cases of $Y_p = 0$ (no product excretion) and $Y_p = 1.0$ (no growth, all the substrate is released back on the form of product) yields patterns that vary respectively from uniform distribution of the bacteria to the formation of isolated, round-shaped microcolonies (data not shown). This suggests that the binding affinity factor (β) and the product excretion rate may have a significant impact on the patterns of spatial distribution of the bacteria. In our model, the substrate concentration impacts the rate of product excretion. An initial low substrate level yields low rates of product excretion of the individuals which may not be sufficient to reduce the motility of the bacteria and the formation of microcolonies. In our simulation the initial substrate level is relatively high and

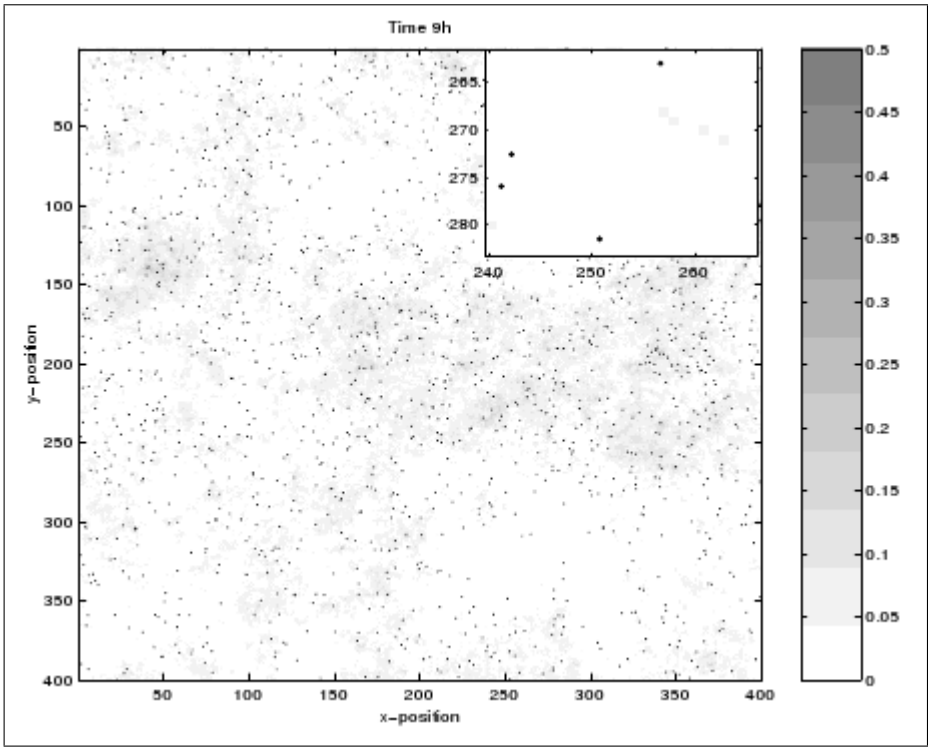

(a) $time = 9hours$

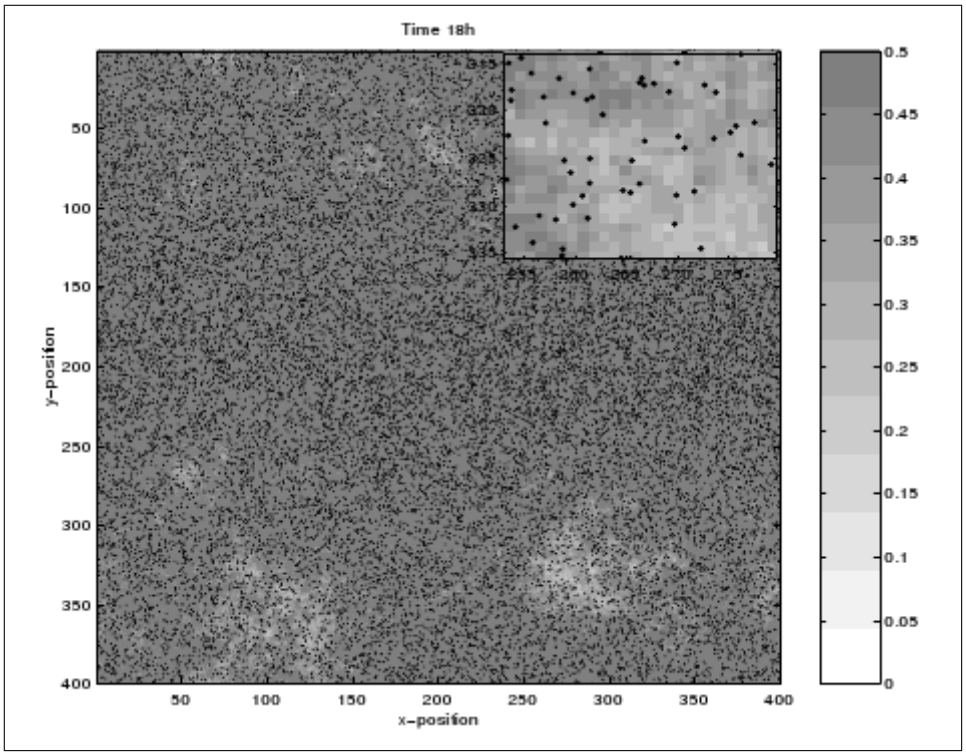

(b) $time = 18hours$

Figure 5.4: Overall and zoomed view of the spatial pattern formed by the bacteria (black dots) and the excreted macromolecules (gray scale) for motile bacteria ($\beta = 0$)

only 90% of this initial stock is consumed by the end of the simulation.

We investigate how the interconnections between the microcolonies form in the case of large value of binding affinity parameter ($\beta = 500$). Figure 5.8 shows a zoomed view of the formation of the interconnection between two neighboring microcolonies.

The interconnection seems to be created by bacteria which go from a microcolony to a neighboring one, and which progressively accumulate excreted product on the path. The resultant pattern is formed with dense and discrete microcolonies interconnected with relatively thin strands of bacteria and excreted product.

5.4 Discussion

In this work we abstract experimental observations on *P. aeruginosa* biofilm development [Whitchurch 2002] [Klausen 003a] [Klausen 003b] [Allesen-Holm 2006][Barken 2008]in an individual-based model and investigate how bacteria motility reduction due to a self-produced substance yields different spatial patterns during the early stages of biofilm development. Our simulation results suggest that self-produced substance-mediated motility reduction does play a role in microcolony formation. Furthermore, in some cases, these simulated microcolonies build interconnections, similar to interconnected microcolonies observed during the early stages of *P. aeruginosa* biofilm development in flow chambers[Allesen-Holm 2006], and also in biofilms formed by Pseudomonas species in marine environments [Dalton 1994][Dalton 1996].

Several authors already explored the mechanisms yielding microcolonies in biofilms[Alpkvist 2006][Picioreanu 2007]. However, the pattern of interconnected microcolonies cannot be obtained with these usual mechanisms: immotile bacteria form isolated microcolonies and constantly motile bacteria form flat biofilms. Based on experimental data and computer simulations we suggest a mechanism that could be responsible for the observed patterns. Our model shows that microcolonies may result from bacteria motility reduction by self-produced macromolecules. The analysis of the simulation results suggests that cells on the edge of a microcolony occasionally detach and undergo a surface-associated motility until being captured by a neighboring microcolony. The path of the migrating cell is marked by the excreted macromolecules and is progressively reinforced by other migrating cells. This results in the formation of an interconnection between the neighboring microcolonies. However, more investigation is necessary to strengthen or falsify this hypothesis.

This investigation could be important for a better understanding of biofilm functions. Indeed, it is well accepted that the presence of different subpopulations in microcolonies can favor the survival of one or more subpopulations under adverse

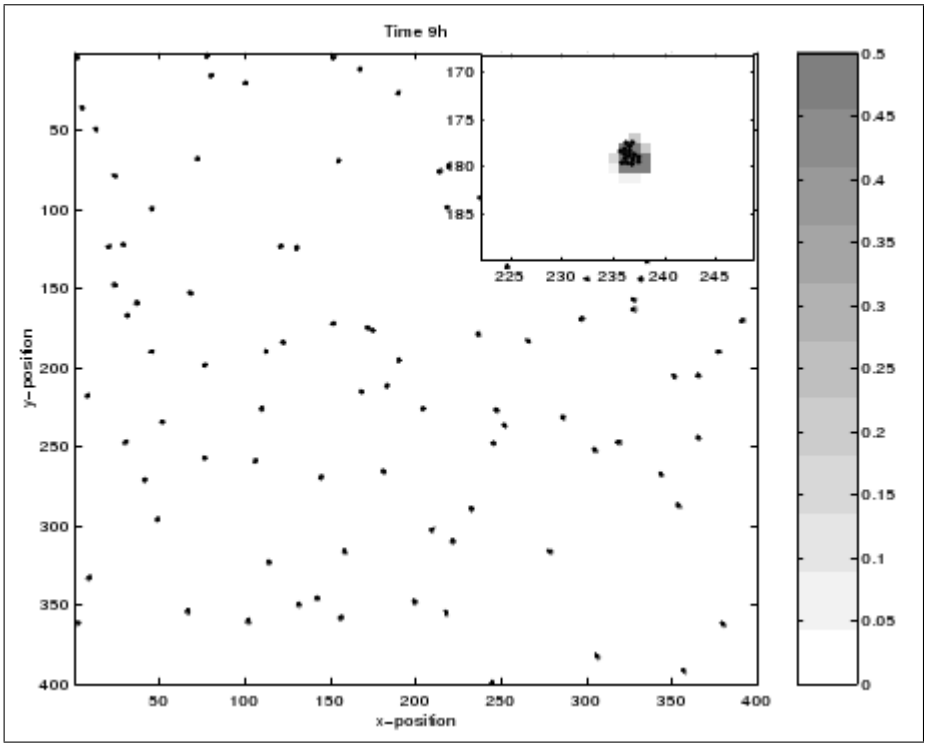

(a) $time = 9hours$

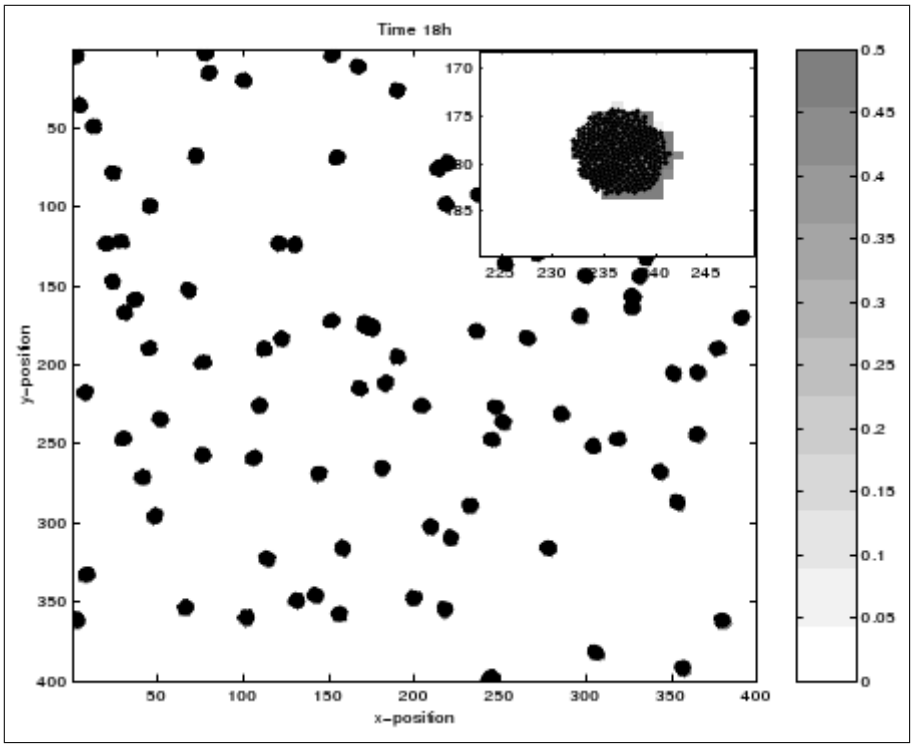

(b) $time = 18hours$

Figure 5.5: Overall and zoomed view of the spatial pattern formed by the bacteria (black dots) and the excreted macromolecules (gray scale) for immotile bacteria

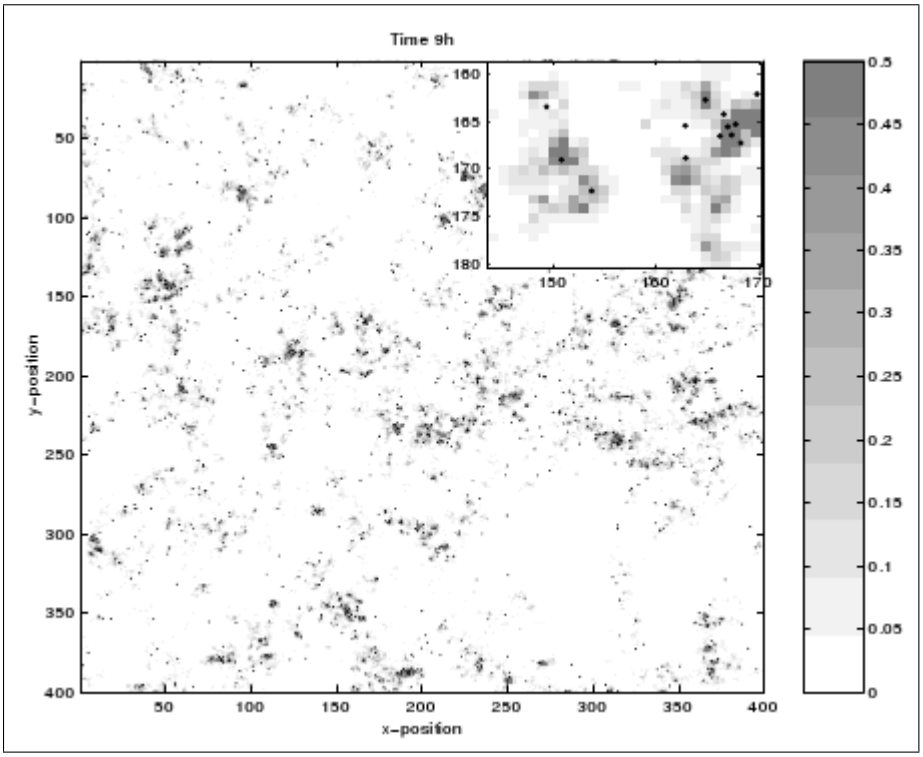

(a) $time = 9hours$

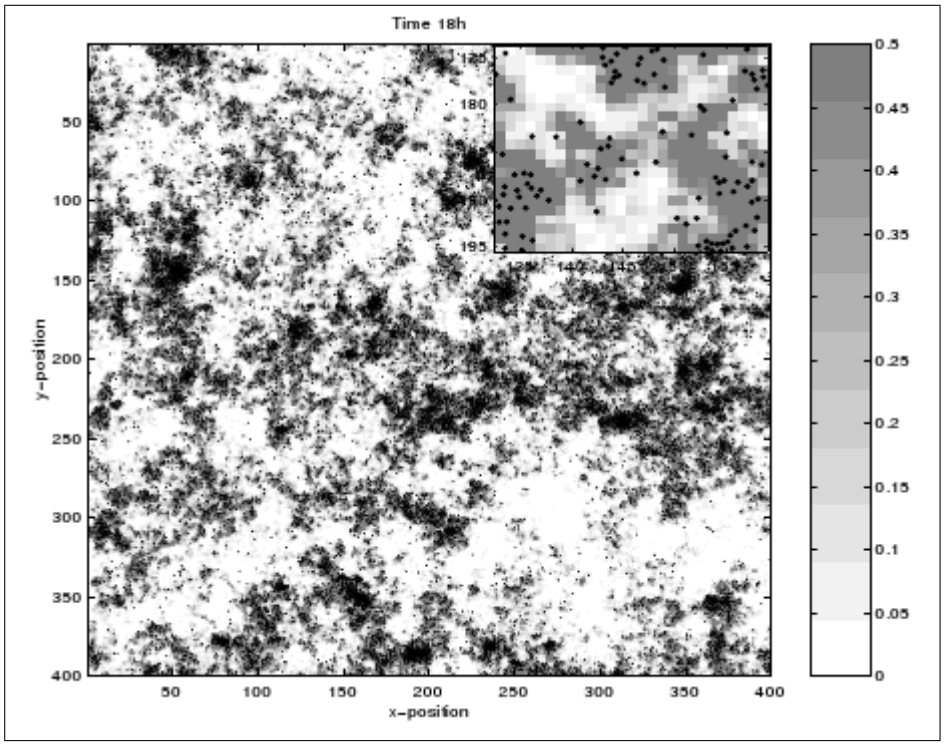

(b) $time = 18hours$

Figure 5.6: Overall and zoomed view of the spatial pattern formed by the bacteria (black dots) and the excreted macromolecules (gray scale) for motile bacteria ($\beta = 100$)

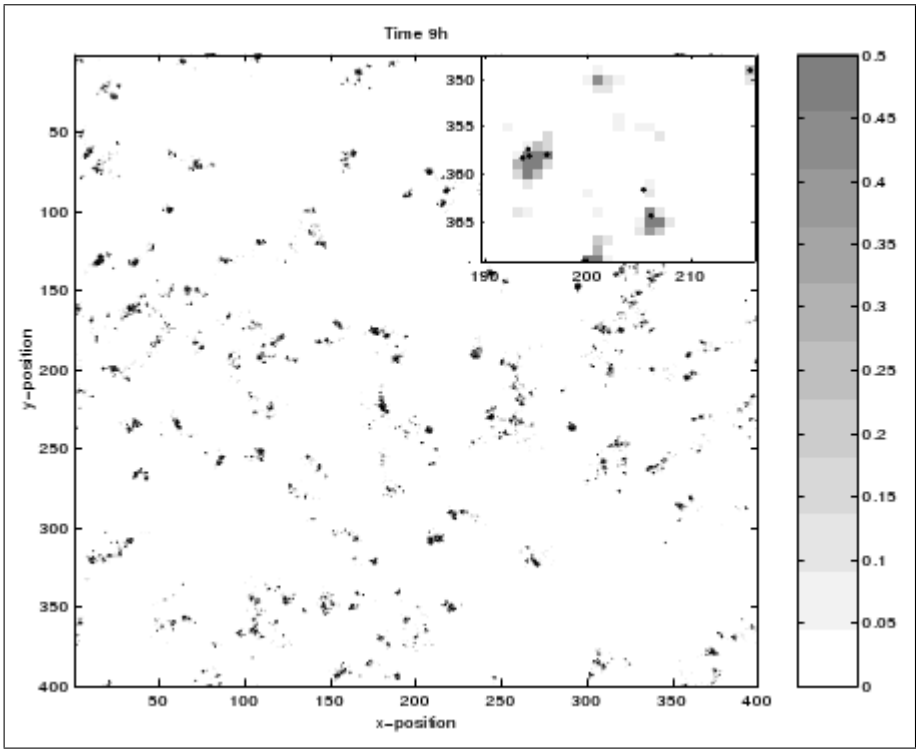

(a) $time = 9hours$

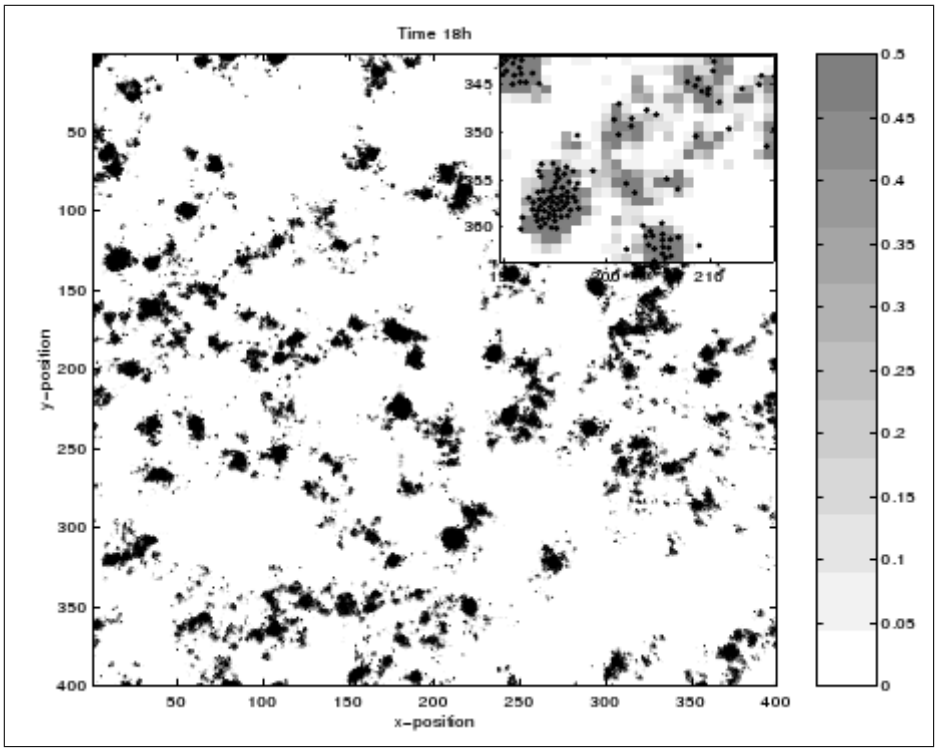

(b) $time = 18hours$

Figure 5.7: Overall and zoomed view of the spatial pattern formed by the bacteria (black dots) and the excreted macromolecules (gray scale) for motile bacteria ($\beta = 500$)

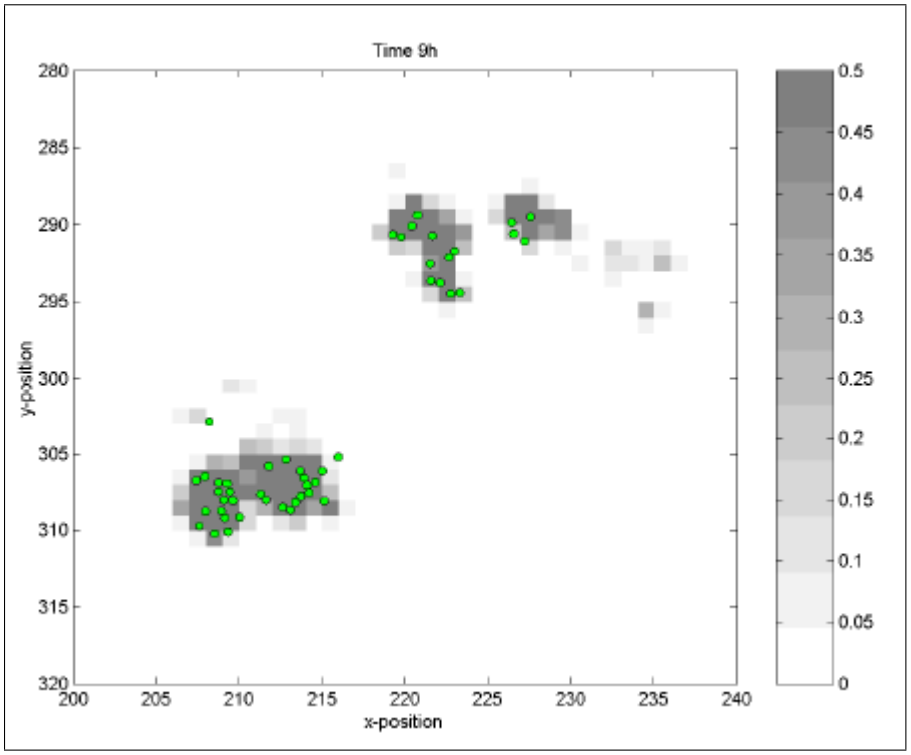

(a) $time = 9hours$

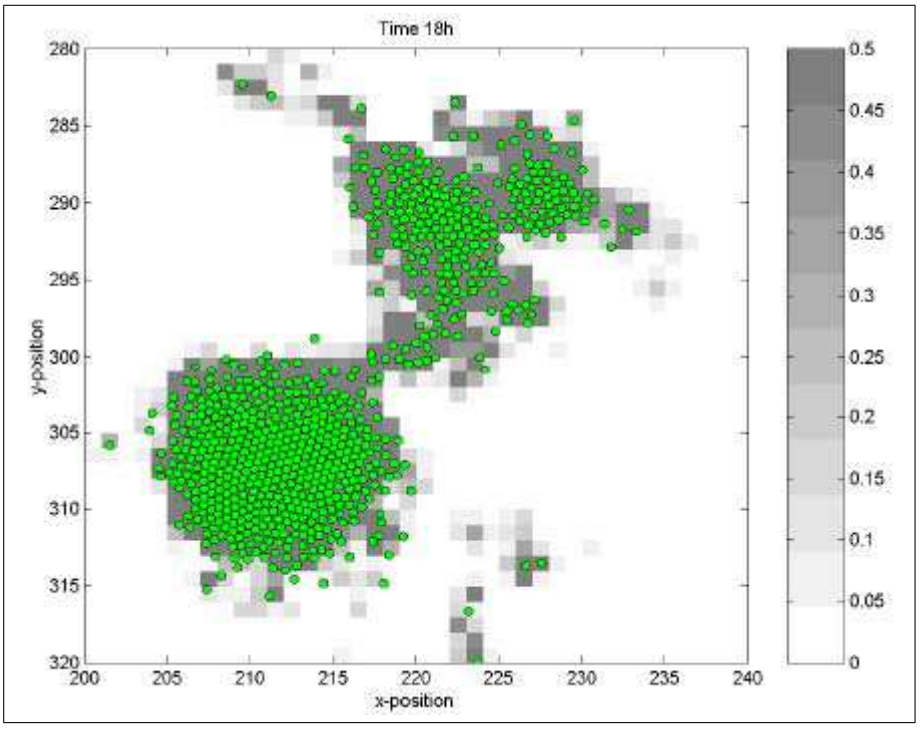

(b) $time = 18hours$

Figure 5.8: Zoomed view of interconnection formation between two microcolonies for a binding affinity $\beta = 500$. Bacteria are represented with green dots and the excreted product concentration with gray scale.

conditions [Parsek 2008][Johnson 2008]. However, recent observations suggest that in some cases the matrix of extracellular DNA (and possibly other products) may guide migration of the cells between microcolonies [Lu 2005][Barken 2008] favoring a type of collaboration between distinct subpopulations within a biofilm. This may be related to studies in landscape ecology where this pattern of interconnected habitats is recognized as particularly important (Burel and Baudry, 2003) [Burel 2003].

Individual-based models are appealing to microbiologists because of the emphasis on the individual cell as the fundamental unit and the richness of their dynamic. However when they are too complex they often become difficult to analyze which limits their practical payoff [Grimm 2005]. Therefore, we have attempted to keep our model as simple as possible and inspired by the phenomenological results mentioned in the introduction, but rich enough to produce patterns of interconnected microcolonies. Johnson [Johnson 2008] proposed a model based on the assumption of the "direct" interaction between individual cells through attractive (and repulsive) forces arguing that forces between cells can be a proxy for the behavior we expect to see due to chemotaxis in response to chemicals released by other cells [Johnson 2008]. The assumption simplifies the model as the dynamic of the excreted product is not considered explicitly. This is a reasonable assumption when the dynamics of the chemical being produced is fast (high diffusion) compared to the dynamic of the bacteria (motility and growth) [Lee 2001]. Our model is based on the assumption that the excreted macromolecules like DNA and exopolymers diffuse at low rates and persist on the path of the motile bacteria. This seems to play a role in the formation of the interconnected microcolonies as microcolonies yielded by Johnson's model through attractive/repulsive forces seem not to be interconnected [Johnson 2008]. Our study included, however, some limitations that should be acknowledged for future research in this area. Examples, inherent to individual-based modeling approach, include the question of how to measure the "goodness" of an IBM. Grimm and Railsback [Grimm 2005] suggested that testing an IBM against multiple observed patterns is a powerful way to assess the IBM capacity to capture system's essential characteristics. In this work we assessed the "goodness" of our IBM through comparison of an observed pattern (connected microcolonies in fig.1) to a simulated one (fig.8). Despite the similarities between the experimental and simulated patterns (thin path of bacteria and product connecting neighboring microcolonies) there are still differences. For example cells surrounded the thin path in figure 1 while they are contained in the area with high amount of product in figure 8. Therefore, additional patterns should be identified and compared to the simulated ones in order to strengthen or falsify the hypothetical implication of self-excreted product in motility reduction and formation of interconnected microcolonies. Another limitation of our model is the determination of parameters like the binding affinity factor (β) and cell diffusion (D_f). These parameters may be difficult to obtain from experimental observations and their impact should be assessed through sensitivity analysis.

Finally, the model can be extended to investigate the effect of other macromolecules like exopolymers on the bacteria motility and microcolonies formation. Another potential extension is to include additional processes like bacteria detachment and substrate feeding which allow investigating the effect of the interactions between cell motility and excreted macromolecules on the architecture of mature biofilms.

Chapter 6

Moment approximation of an individual-based model of a biofilm formed with motile bacteria

Contents

In this chapter we derive a moment approximation model of an individual-based model (IBM) describing the formation of microcolonies due to bacteria motility reduction by a self-produced product. The direct derivation of moment models of the IBM presented in chapter 5 is difficult. thus we start by simplifying the IBM than approximating the simplified IBM with a moment model. The main simplifications consist in representing the individuals (bacteria and product) as point particles.

The moment model aggregates the state variables of the simplified IBM into two type of quantities: the average density of individuals (bacteria and polymer) which correspond to the first spatial moment and the average neighborhood of an individual at different distances, measured by the self and cross pair density correlation functions (second spatial moments). The fluctuation of the local density of individuals observed in the IBM are averaged in the moment model. We show in this chapter that if the individual response to these fluctuations is non-linear or depends

on a threshold value than moment models may fail in capturing the dynamic of the IBM.

The chapter is organized in four sections: first we start by simplifying the IBM presented in the previous chapter. Than we derive the moment approximation model of the simplified IBM in the second section. In the third section we compare the moment and simplified IBM simulations and we discuss the limits of the moment approach in coping with the fluctuation of the local environment of the individuals.

6.1 Description of the simplified IBM

6.1.1 Overview

6.1.1.1 Purpose

The aim of the individual-based model is to investigate the patterns that arise formed by the aggregation of individual motile cells into microcolonies when their motility in reduced by a self-excreted polymer.

6.1.1.2 State variables

The system contains two types of discrete individuals: bacterial cells and polymeric particles. Each individual (bacterium or polymeric particle) is characterized by a continuous position in the two-dimensional domain.

6.1.1.3 Overview

We consider a population of discrete, identical individual bacterial cells inhabiting a two dimensional continuous environment. The bacteria undergo four stochastic processes: they move around the spatial domain, excrete polymeric particles, divide into two identical cells and get detached from the domain. The spatial domain is initially homogeneous but the progressive accumulation of the excreted polymeric particles introduces spatial heterogeneity that affect the detachment and motility rates of the bacteria. Our main assumption is that the accumulation of polymeric particles reduces the motility of the bacteria but increases their probability of being detached. This is a simplified description of the tendency of some bacteria colonizing a surface to excrete extracellular polymeric substances that hold the cells together and attach them to the surface. But when the local density of polymer increases, the microcolony grows in the vertical dimension and its structure is weakened by the hydrodynamic stresses. Finally we suppose that the polymeric particles can also detach from the system and that their detachment rate also increases with the increase of the local density of polymers.

6.1.1.4 Scheduling

The dynamic of the IBM is governed by the following events:

- Division of a bacterial cell
- Production of a polymer particle
- Detachment of bacterial cell
- Detachment of a polymer particle
- Motility of a bacterial cell

We implemented the IBM in the continuous time. To simulate the temporal evolution of the system we need to specify when the next event will occur, what kind of event it will be and which individual will be concerned with the event. We use a procedure adapted from the algorithm of Gillespie [GIllespie 1976] to simulate the evolution of the system. The procedure yields an asynchronous random execution of the events and suppose that one event occurs at a time. It iterates over the following steps:

1. Set the time to $t = 0$
2. Calculate:
   (a) the individual detachment rates of the bacteria
   (b) the individual detachment rates of the polymer
   (c) the individual motility rates of the bacteria
3. Calculate the sums r_1, r_2 and r_3 which are respectively the sums of the individual rates of bacteria detachment, polymer detachment and bacteria motility.
4. Calculate the sums r_4 and r_5 which are respectively the sum of the individual division rates of the bacteria and the individual production rates of polymer
5. Calculate the overall rate of events : $r = r_1 + r_2 + r_3 + r_4 + r_5$
6. Choose the waiting time τ for the next event to occur according to $\tau = -\frac{1}{r} \ln \lambda$ where $0 < \lambda \leq 1$ is a uniformly distributed random number
7. Choose an event with the following probabilities:
   (a) a detachment of a bacterium with a probability r_1/r
   (b) a detachment of a polymer with a probability r_2/r
   (c) a division of a bacteria with a probability r_3/r
   (d) a production of a polymer with a probability r_4/r
   (e) a displacement of a bacterium with a probability r_5/r
8. Select an individual:

(a) If the event is a detachment of polymer than a polymeric particle j is selected with a probability r_{2j}/r where r_{2j} is the detachment rate of the individual j

(b) If the event is a detachment of a bacterium than a bacterium i is selected with a probability r_{1i}/r where r_{1i} is the detachment rate of the individual i

(c) If the event is a production of polymer than bacterium i is selected with a probability r_{4i}/r where r_{4i} is the production rate of the of polymer of the individual i

(d) If the event is a division of a bacterium than a bacterium i is selected with a probability r_{3i}/r where r_{3i} is the division rate of the individual i

(e) If the event is a displacement of a bacterium than a bacterium i is selected with a probability r_{5i}/r where r_{5i} is the motility rate of the individual i

9. Perform the selected event on the selected individual

10. Update time according to $t = t + \tau$

11. Continue from step 2 until $t < t_{end}$

6.1.2 Details

6.1.2.1 Submodels

- **Division:** We suppose that the probability per unit of time that a bacterium i in position x_i produces a new cell located in position x' is given by:

$$B_b(x_i, x') = b_1 K\left(\frac{||x_i - x'||}{w_b}\right) \tag{6.1}$$

The parameter b_1 is density-independent division rate of the bacteria and $K(||x_i - x'||/w_b)$ is a uniform dispersion kernel with a window side w_b. The general form of this kernel for a window side w given by:

$$K\left(\frac{||x - x'||}{w}\right) = \begin{cases} 1/w & \text{if} \quad ||x - x'|| < w \\ 0 & \text{else} \end{cases} \tag{6.2}$$

The dispersion kernel gives the probability that the newly formed individual disperses instantaneously after the division event to the location x'. This probability depends on the distance $||x_i - x'||$ and the size of the dispersion kernel w_b.

- **Polymer production:** We suppose that the probability per unit of time that a bacterium individual i in position x_i produces a new polymeric particle in position x' is given by:

$$B_p(x_i, x') = b_2 K\left(\frac{||x_i - x'||}{w_b}\right) \tag{6.3}$$

The parameter b_2 is density-independent polymer production rate. We use the same dispersion kernel as for the bacteria division.

- **Bacteria detachment:** We suppose that the probability per unit of time that a bacterium i in position x_i detaches depends on the local concentration of polymeric particles in x_i denoted $p_{loc}(x_i)$. This probability is given by:

$$D_b(x_i) = [d_1 + d'_1 p_{loc}(x_i)] \tag{6.4}$$

The parameters d_1 and d'_1 are the density-independent and the density-dependant detachment rates respectively. The term $p_{loc}(x_i)$ is the local density (defined in more details below) as perceived by the individual in x_i.

- **Polymer detachment:** We suppose that the probability per unit of time that a polymeric particle j in position x_j detach depends on the local concentration of polymeric particles in x_j denoted $p_{loc}(x_j)$. This probability is given by:

$$D_p(x_j) = [d_2 + d'_2(p_{loc}(x_j))] \tag{6.5}$$

The parameters d_2 and d'_2 are the density-independent and the density-dependant detachment rates respectively. The term $p_{loc}(x_i)$ is the local density (defined in more details below) as perceived by the individual in x_j.

- **Calculation of the perceived local density:** The contribution of a polymeric particle j located in x_j to the local density of polymer perceived by an individual (bacteria or polymer) i located in x_i is weighted by an interaction kernel $K(||x_i - x_j||/w_d)$. The local density of polymer perceived by the individual in x_i is calculated by summing the weighted contributions of all the polymeric particles in the system:

$$p_{loc}(x_i) = \sum_{j=0}^{j=n_p} K\left(\frac{||x_i - x_j||}{w_d}\right) \tag{6.6}$$

If the particle in x_i is a polymeric particle its contribution to the perceived local density is not counted.

- **Bacteria motility:** The probability per unit of time that a bacterium i in x_i moves to a position x' is given by:

$$M(x_i, x') = [m_1 - m_2 p_{loc}(x_i)] K\left(\frac{||x_i - x'||}{w_m}\right) \tag{6.7}$$

Where m_1 and m_2 are respectively the density-independent and the density dependent motility rates and $K(||x_i - x'||/w_m)$ a uniform motility kernel.

6.1.2.2 Initialization

The model is initialized with $n_b(t = 0) = 1000$ bacterial cells distributed uniformly over the domain. Initially there are no polymer particles in the domain ($n_p(t = 0) = 0$)

6.1.2.3 Model parameters

The individual-based model parameters are summarized in table 6.3. Unless explicitly specified, we use the default parameter values in table 6.3.

6.2 Moment approximation

We propose to develop a deterministic mathematical model that approximate the dynamic of the individual-based model described in the previous section using moment approximation techniques.

6.2.1 First moment dynamics

The dynamic of the first moment (average densities of bacteria and polymer) is given by the following equations:

$$\frac{dN_b}{dt} = (b_1 - d_1)N_b - d_1' \int C_{bp}(\xi) K\left(\frac{||\xi||}{w_d}\right) d\xi \tag{6.8}$$

$$\frac{dN_p}{dt} = b_2 N_b - d_2 N_p - d_2' \int C_{pp}(\xi) K\left(\frac{||\xi||}{w_d}\right) d\xi \tag{6.9}$$

Equations 6.8 and 6.9 describe respectively the dynamic of the average density of bacteria N_b and polymer N_p. The integral terms in the right-hand side are the neighborhood-dependent components of the detachment. They involve respectively the pair densities $C_{bp}(\xi)$ and $C_{pp}(\xi)$ and an interaction kernel $K(||\xi||/w_d)$. These terms encompass the effect of the local density of polymer in the neighborhood of bacteria, as given by $C_{bp}(\xi)$, and in the neighborhood of a polymeric particle, as given by $C_{pp}(\xi)$, weighted by the uniform interaction kernel $K(||\xi||/w_d)$. Note that if the size w_d of uniform interaction kernel is equal to the side of the domain than a bacterium (respectively a polymeric particle) experiences equally the effect of all the polymeric particle within the domain. This reduces equations 6.8 and 6.9 to the following mean-field system:

$$\frac{dN_b}{dt} = (b_1 - d_1)N_b - d_1' N_b N_p \tag{6.10}$$

$$\frac{dN_p}{dt} = b_2 N_b - d_2 N_p - d_2' N_p N_p \tag{6.11}$$

The mean-field equations can also be obtained if the position of the bacterial cells (respectively the polymeric cells) are not correlated with the position of the polymeric particles. In this case the density of pairs formed with a focal bacterium (respectively a focal polymeric particles) with a polymeric particle located at a vectorial distance ξ from the focal particle is equal to the product of the average densities $N_b N_p$ (respectively $N_p N_p$). Spatial patterns formation and small interaction kernel may cause a departure from the mean-field model. The system formed with equations 6.8 and 6.9 is not closed and need to be coupled to the dynamic of $C_{bp}(\xi)$ and $C_{pp}(\xi)$.

6.2.2 Second moment dynamics

The pair correlation functions $C_{bb}(\xi)$, $C_{bp}(\xi)$ and $C_{pp}(\xi)$ characterize the spatial pattern formed by the bacteria and the polymer. They measure respectively the densities of pairs formed with two bacteria, a bacterium and a polymeric particle or two polymeric particles at different vectorial distance ξ. The dynamic of these functions account for the five processes: bacteria division, production of polymeric particles, bacteria detachment, polymer detachment and motility of the bacteria.

6.2.2.1 Dynamic of the bacteria-bacteria pair correlation function

The dynamic of the bacteria-bacteria pair correlation function $C_{bb}(\xi)$ is given by:

$$\frac{dC_{bb}(\xi)}{dt} = \left(\frac{dC_{bb}(\xi)}{dt}\right)_{division} + \left(\frac{dC_{bb}(\xi)}{dt}\right)_{detachment} + \left(\frac{dC_{bb}(\xi)}{dt}\right)_{motility} \tag{6.12}$$

The terms in the right hand side denotes for the effect of three processes that may modify the bacteria pattern and which are the bacteria division, detachment and motility events. The effect of division events on $C_{bb}(\xi)$ is given by the following equation:

$$\begin{aligned}\left(\frac{dC_{bb}(\xi)}{dt}\right)_{division} &= +2b_1 N_b K\left(\frac{||\xi||}{w_b}\right) \\ &\quad +2b_1 \int C_{bb}(\xi+\xi')K\left(\frac{||\xi'||}{w_b}\right) d\xi'\end{aligned} \tag{6.13}$$

- The first term in the right-hand side accounts for the division of a bacterium i producing a new cell j located at a vectorial distance ξ. This event yields a new pair of bacteria separated with a vectorial distance ξ. The rate at which such division events occur is obtained by multiplying the density of average bacteria N_b by the division rate b_1. Then we multiply by the probability $K(||\xi||/w_b)$ that the newly formed cells are located at a distance ξ from the parent cell. The factor 2 accounts for newly formed cells at a vectorial distance $-\xi$ which also form a new par (j,i) at distance ξ.

- The second term focuses on the new pair that the daughter cell of a parent bacterium i form with a bacterium j located at a distance $\xi + \xi'$ from i. The density of (i, j) pairs is $C_{bb}(\xi + \xi)$ and the division rate is b_1. Multiplying these two factors with the probability $K(||\xi'||/w_b)$ that the newly formed cells is located at a distance ξ' from i and integrating over all possible distances ξ' gives the second term. We also take into consideration that analogous event can occur to the individual j by multiplying the second term by a factor 2.

The contribution of the detachment events of bacteria to the dynamic of $C_{bb}(\xi)$ is given by:

$$\begin{aligned}\left(\frac{dC_{bb}(\xi)}{dt}\right)_{detachment} &= -2d_1 C_{bb}(\xi) \\ &\quad -2d_1' \int K\left(\frac{||\xi''||}{w_d}\right) T_{bbp}(\xi, \xi'') d\xi'' \end{aligned} \tag{6.14}$$

- The first term in the right hand side accounts for the detachment of the cell i in the pair (i, j). Such events occur at a rate d_1. Multiplying d_1 by the density $C_{bb}(\xi)$ of (i, j) pairs at distance ξ gives the resulting decrease in that density. The factor 2 accounts that analogous event can occur for the individual j.

- The second term is the density-dependent detachment term that accounts for the presence of polymeric particles in the neighborhood of the bacteria. The detachment of a bacterium i of the (i, j) pair can result from the presence of polymer particle k at a distance ξ'' from i. Such triplet configuration occurs at a density $T_{bbp}(\xi, \xi'')$. The cumulative effect of the polymeric particles k situated at different distances ξ'' from the cell i is obtained by weighting the triplet density with $K(||\xi''||/w_d)$ and integrating over all interaction distances ξ''. Multiplying contribution of the local density of polymer with the density-dependent detachment rate of the bacteria d_1' gives the second term. The factor 2 accounts for the analogous event that can occur for the cell j in the the pair (i, j).

The contribution of the motility to the dynamic of $C_{bb}(\xi)$ is given by the following equation:

$$\begin{aligned}\left(\frac{dC_{bb}(\xi)}{dt}\right)_{motility} &= -2m_1 C_{bb}(\xi) \\ &\quad +2m_1 \int K\left(\frac{||\xi'||}{w_m}\right) C_{bb}(\xi + \xi') d\xi' \\ &\quad +2m_2 \int K\left(\frac{||\xi''||}{w_d}\right) T_{bbp}(\xi, \xi'') d\xi'' \\ &\quad -2m_2 \int\int K\left(\frac{||\xi'||}{w_m}\right) K\left(\frac{||\xi''||}{w_d}\right) T_{bbp}(\xi + \xi', \xi'') d\xi' d\xi'' \end{aligned} \tag{6.15}$$

- When the individual i moves, the original pair (i, j) at distance ξ is destroyed. The first term in the right hand side accounts for this process by multiplying the density-independent motility rate of m_1 by the density of pairs $C_{bb}(\xi)$ of the original pair configuration.

- On the other hand a new (i, j) pair of bacteria is created at distance ξ when the cell i at originally at a distance $\xi + \xi'$ from the cell j moves a distance ξ'. This effect is captured by the second term, which weights the density $C_{bb}(\xi + \xi')$ of the original pair configuration with the motility kernel $UK(||\xi'||/w_m)$ and integrating over all possible motility distances ξ'.

- The third term corrects the first term by accounting for the possible presence of polymeric particles in the neighborhood of the cell in the pair (i, j) originally at a distance ξ. The motility of i in the pair (i, j) is reduced by the presence of polymeric particle k located at a distance ξ'' from i. The density triplet formed with two cells separated with a distance ξ and a polymeric particle at a distance ξ'' from i is $T_{bbp}(\xi, \xi'')$. Weighting this density by the interaction kernel $K(||\xi''||/w_d)$ and integrating over all distances ξ'' gives the third term. The factor 2 accounts for the analogous event that can occur for the cell j.

- The last term corrects the second term by accounting for motility reduction of the cell i originally at a distance $\xi + \xi'$ from the cell j due to the presence of a polymeric particle k at a distance ξ'' from i. The cumulative effect of the polymeric particles k is obtained by multiplying the triplet density $T_{bbp}(\xi + \xi', \xi'')$ by the interaction kernel $K(||\xi''||/w_d)$ and integrating over all distances ξ''. The result is then multiplied by the motility kernel $K(||\xi'||/w_m)$, integrated over all distances ξ' and multiplied by the density dependent motility rate m_2. the factor 2 accounts for analogous event that may be experienced by the cell j in the pair (i, j).

6.2.2.2 Dynamic of the polymer-polymer pair correlation function

The dynamic of the density of pairs of polymeric particles separated with a distance ξ is given buy the following equation:

$$\frac{dC_{pp}(\xi)}{dt} = \left(\frac{dC_{pp}(\xi)}{dt}\right)_{production} + \left(\frac{dC_{pp}(\xi)}{dt}\right)_{detachment} \tag{6.16}$$

The first term in the right-hand side accounts for the contribution of polymer production events and the second term for polymer detachment events . Polymer production events contribute to the creation positively to $C_{pp}(\xi)$ according to the following equation:

$$\left(\frac{dC_{pp}(\xi)}{dt}\right)_{production} = +2b_2 \int K\left(\frac{||\xi'||}{w_b}\right) C_{bp}(\xi + \xi') d\xi' \tag{6.17}$$

- the right hand-side accounts for new pairs of polymers that are formed when the bacterial cell i situated at a distance $\xi + \xi'$ from a polymeric particle j produces a new polymeric particle k at a distance ξ'. The density of pairs (i, j) is $C_{bp}(\xi + \xi')$ and the probability that the newly formed polymer particles is located at a distance ξ' from the cell i is given by $K(||\xi'||/w_b)$. Multiplying these two factors with the polymer production rate b_2 and integrating over all possible distances ξ' gives the term in the right-hand side.

The contribution of the detachment of polymer to the dynamic of $C_{pp}(\xi)$ is given by:

$$\begin{aligned}\left(\frac{dC_{pp}(\xi)}{dt}\right)_{detachment} &= -2d_2C_{pp}(\xi) \\ &\quad -2d_2'C_{pp}(\xi)K\left(\frac{||\xi||}{w_d}\right) \\ &\quad -2d_2'\int K\left(\frac{||\xi''||}{w_d}\right)T_{ppp}(\xi,\xi'')d\xi'' \qquad (6.18)\end{aligned}$$

- The first term in the right-hand side translates the destruction of pair of polymer (i, j) is one of the particles i or j detach.

- The second term accounts for the effect of the particle j in the pair (i, j) on the detachment rate of the particle i. This is obtained by multiplying the density of pairs $C_{pp}(\xi)$ by the interaction kernel $K(||\xi||/w_d)$. Multiplying by d_2' gives the contribution of this process.

- The third term accounts for polymeric particles k that are neighbors of a particle i in the pair (i, j). The density of particles in this configuration is given by $T_{ppp}(\xi, \xi'')$. Where ξ'' is the distance between the particles k and i. This density is weighted by the interaction kernel $K(||\xi''||/w_d)$ and multiplied by the density dependent detachment rate. Integrating over all distances ξ'' gives the third term.

The factor 2 in the right hand side of equation 6.18 accounts for analogous detachment events that may be experienced by the particle j in the pair i, j.

6.2.2.3 Dynamic of the bacteria-polymer pair correlation function

The dynamic of the bacteria-polymer pair correlation function $C_{bp}(\xi)$ is more complex. All processes affecting the bacteria and the polymer contributes to this dynamic as can be shown from the following equation:

$$\begin{aligned}\frac{dC_{bp}(\xi)}{dt} &= +\left(\frac{dC_{bp}(\xi)}{dt}\right)_{division} \\ &\quad +\left(\frac{dC_{bp}(\xi)}{dt}\right)_{production} \\ &\quad +\left(\frac{dC_{bp}(\xi)}{dt}\right)_{detachment\ bact} \\ &\quad +\left(\frac{dC_{bp}(\xi)}{dt}\right)_{detachment\ poly} \\ &\quad +\left(\frac{dC_{bp}(\xi)}{dt}\right)_{motility} \end{aligned} \tag{6.19}$$

The contribution of bacteria division to the dynamic of $C_{bp}(\xi)$ is given by:

$$\left(\frac{dC_{bp}(\xi)}{dt}\right)_{division} = +b_1 \int K\left(\frac{||\xi'||}{w_b}\right) C_{bp}(\xi+\xi')d\xi' \tag{6.20}$$

- the term in the right-hand side accounts for the case where a new pair that a daughter cell k resultant from the division of a parent cell i forms with a polymeric particle j located at a distance $\xi+\xi'$ from i. The per capita bacteria division rate is b_1, the density of (i,j) pairs is $C_{bp}(\xi+\xi')$ and the spatial density of daughter cells at distance ξ' is $K(||\xi'||/w_b)$. Multiplying these factors and integrating over all distances ξ' gives the term on the right-hand side.

The contribution of polymer production to the dynamic of $C_{bp}(\xi)$ is given by the following equation:

$$\begin{aligned}\left(\frac{dC_{bp}(\xi)}{dt}\right)_{production} &= +b_2 N_b K\left(\frac{||\xi||}{w_b}\right) \\ &\quad +b_2 \int K\left(\frac{||\xi'||}{w_b}\right) C_{bb}(\xi+\xi')d\xi' \end{aligned} \tag{6.21}$$

- The first term in the right-hand side accounts for new pairs (k,j) formed by a bacterium k and a produced polymer particle j located at a distance ξ. The polymer production rate is $b_2 N_b$ and the density of self-produced polymer particles at a distance ξ from a focal bacterium i is $K(||\xi||/w_b)$. Multiplying these factors gives the first term.

- In the second term we focus on pairs (i,j) formed with two bacteria at a distance $\xi+\xi'$. If the bacteria i produces a polymer particle k at distance ξ' than a new pair bacteria polymer (j,k) is formed at distance ξ. The density of pairs (i,j) is $C_{bb}(\xi+\xi')$ and the probability that the polymer particle produced by the cell i is located at a distance ξ' is $K(||\xi'||/w_b)$. Multiplying these two factors by the per capita polymer production rate and integrating over all distances ξ' gives the second term.

The contribution of bacteria and polymer detachment processes is given respectively by the two following equations which have a comparable structure:

$$\begin{aligned}\left(\frac{dC_{bp}(\xi)}{dt}\right)_{detachment\ bact} &= -d_1 C_{bp}(\xi) \\ &\quad -d_1' \int K\left(\frac{||\xi''||}{w_d}\right) T_{bpp}(\xi,\xi'')d\xi'' \\ &\quad -d_1' K\left(\frac{||\xi||}{w_d}\right) C_{bp}(\xi) \end{aligned} \tag{6.22}$$

$$\begin{aligned}\left(\frac{dC_{bp}(\xi)}{dt}\right)_{detachment\ poly} &= -d_2 C_{bp}(\xi) \\ &\quad -d_2' \int K\left(\frac{||\xi''||}{w_d}\right) T_{bpp}(\xi,\xi+\xi'')d\xi'' \end{aligned} \tag{6.23}$$

The first two terms of the right-hand side of both equations are comparable:

- the first term takes into account the effect of the neighborhood-independent detachment events of a bacterium (equation 6.22) or a polymeric particle (equation 6.23).

- the second term takes into account the effect of the neighborhood dependent detachment of a bacterium (equation 6.22) or a polymeric particle (equation 6.23). For the calculation of this term triplets of individuals formed with a pair bacterium-polymer (i, j) and a polymeric particle k need to be considered. In equation 6.22 we account for the effect of the polymer k on the bacterium detachment and use the density of triplet $T_{bpp}(\xi, \xi'')$ while in equation 6.23 we account for the effect of the polymer k on the detachment of the polymeric particle j in the pair (i,j) and use the density of triplet $T_{bpp}(\xi, \xi + \xi'')$.

- the third term in the right-hand side of equation 6.22 accounts for the effect of the polymer particle j in the bacterium-polymer pair (i, j) on the detachment rate of the bacterium i.

Finally the motility process of the bacteria also contributes to the dynamic of the pair correlation function $C_{bp}(\xi)$ according to the following equation:

$$\begin{aligned}\left(\frac{dC_{bp}(\xi)}{dt}\right)_{motility} &= -m_1 C_{bp}(\xi) \\ &\quad +m_1 \int K\left(\frac{||\xi'||}{w_m}\right) C_{bp}(\xi+\xi')d\xi' \\ &\quad +m_2 \int K\left(\frac{||\xi''||}{w_d}\right) T_{bpp}(\xi,\xi'')d\xi'' \\ &\quad -m_2 \int\int K\left(\frac{||\xi''||}{w_d}\right) K\left(\frac{||\xi'||}{w_m}\right) T_{bpp}(\xi+\xi',\xi'')d\xi' d\xi'' \\ &\quad +m_2 C_{bp}(\xi) K\left(\frac{||\xi||}{w_d}\right) \\ &\quad -m_2 \int K\left(\frac{||\xi'||}{w_m}\right) K\left(\frac{||\xi+\xi'||}{w_d}\right) C_{bp}(\xi+\xi')d\xi' \qquad (6.24)\end{aligned}$$

- When the bacterium i, in a bacterium-polymer pair (i,j) at distance ξ, moves, the original pair (i,j) is destroyed. This is accounted for with the first term.
- On the other hand, when a new pair (i,j) at distance ξ is formed is the bacterium originally at a distance $\xi+\xi'$ from the polymeric particle j moves with a distance ξ'. This process is considered by the second term.
- The third term corrects the first term by accounting for the possible presence of polymeric particles in the neighborhood of the bacterium in the bacterium-polymer pair (i,j) originally at a distance ξ. The motility of i in the pair (i,j) is reduced by the presence of polymeric particle k located at a distance ξ'' from i. The density triplet formed with the pair (i,j) separated with a distance ξ and a polymeric particle at a distance ξ'' from i is $T_{bpp}(\xi,\xi'')$. Multiplying this density by the per capita density dependent motility rate m_2, weighting by the interaction kernel $K(||\xi''||/w_d)$ and integrating over all distances ξ'' gives the third term.
- The fourth tern corrects the second term by accounting for motility reduction of the bacterium i originally at a distance $\xi+\xi'$ from the a polymeric particle j due to the presence of a polymeric particle k at a distance ξ'' from i. The cumulative effect of the polymeric particles k is obtained by multiplying the triplet density $T_{bpp}(\xi+\xi',\xi'')$ by the interaction kernel $U(||\xi''||/w_d)$ and integrating over all distances ξ''. The result is then multiplied by the motility kernel $K(||\xi'||/w_m)$, integrated over all distances ξ' and multiplied by the density dependent motility rate m_2.
- The fifth term accounts for the effect of the polymeric particle in the bacterium-polymer pair (i,j) at a distance ξ on the motility of i. The density of pairs (i,j) is $C_{bp}(\xi)$. Weighted by the interaction kernel $K(||\xi||/w_d)$ and multiplied by the density dependent per capita motility rate m_2 yields the fifth term

- The sixth term corrects the second term in which a bacterium polymer pair originally at a distance $\xi + \xi'$ yields a new pair at a distance ξ after the bacterium has moved with a distance ξ'. The sixth term account for the effect of the polymeric particle in this pair on the motility of the bacterium. The density of the original pairs is $C_{bp}(\xi + \xi)$ that we weight by the interaction kernel $K(||\xi + \xi'||/w_d)$. Multiplying by $K(||\xi'||/w_m)$ which represents the probability to move with a distance ξ' and the per capita density dependent motility rates than integrating over all distances ξ' yields the sixth term.

6.2.3 Closure of the moment hierarchy

The dynamic of the first moment involves second moment terms and the dynamic of the second moment involves the third moment terms. To truncate the hierarchy of the moment we suppose that the position of triplet particles are not correlated and can be expressed as the product of the second moment terms. This yields the following closure expressions:

$$T_{ppp}(\xi, \xi'') = \frac{C_{pp}(\xi)C_{pp}(\xi'')}{N_p} \tag{6.25}$$

$$T_{bpp}(\xi, \xi'') = \frac{C_{bp}(\xi)C_{bp}(\xi'')}{N_b} \tag{6.26}$$

$$T_{bbp}(\xi, \xi'') = \frac{C_{bb}(\xi)C_{bp}(\xi'')}{N_b} \tag{6.27}$$

6.2.4 Solving the moment model

The state variables of the moment model are the average densities of bacteria (N_b) and polymer (N_p) and the three pair correlation functions $C_{bb}(\xi)$, $C_{pp}(\xi)$ and $C_{bp}(\xi)$. The pair correlation function are discretized with regards to space with spatial resolution $d\xi = (d\xi_1, d\xi_2)$ and they are transformed into three matrices. We discretize time derivatives according to an Euler explicit scheme and we use a fixed time step $\Delta t = 0.1$.

6.3 Results and discussion

In this section we compare the IBM and the moment model. All parameters take the values listed in table 6.1 unless otherwise stated. In the first part we turn off all the density dependent processes and assess how density-independent motility affects the spatial pattern. We show that motility promotes the dispersion of the bacteria and prevents colony formation. In the second part we turn on the motility dependence on the local polymer density and compare the pattern to the previously obtained ones. We show that the reduction of motility due to the produced polymer promotes colony formation. Finally, we turn on the density-dependent detachment processes. The detachment rate increases with the increase of the local density

Parameters	Description	Value
L	Domain size	101×101
ΔL	Spatial discretization	1
b_1	Density-independent bacteria division rate	0.1
b_2	Density-independent polymer production rate	0.1
d_1	Density-independent bacteria detachment rate	0.1
d_2	Density-independent polymer detachment rate	0.1
d_1'	Density-dependent bacteria detachment rate	0.0
d_2'	Density-dependent polymer detachment rate	0.0
m_1	Density-independent motility rate	1.0
m_2	Density-dependent motility rate	2.0
w_b	Uniform division and polymer production kernel side	5
w_d	Uniform Interaction kernel side	5
w_m	Uniform motility kernel side	5

Table 6.1: Model parameters

of polymer. We investigate how this process affect the aggregated pattern formed by density-dependent motility. All along this section we compare the simulation of the IBM with the results of the moment model and assess the validity of the approximation made in the moment approach.

Density-independent model

In the absence of density-dependent processes ($m_2 = 0$, $d_1' = 0$, $d_2' = 0$) the spatial pattern has no effect on the average densities of bacteria and polymer. For a system formed with immotile bacteria ($m_1 = 0$) spatial pattern forms as a result of the short-range dispersion of the daughter cells. Figure 6.1 shows two snapshots of the state of the system for the cases of short-range ($w_b/L \sim 0.05$) and long-range dispersion ($w_b/L \sim 0.1$) of the daughter cells (L is the domain size). The formation of colonies is less marked for larger daughter cells dispersion. This result is well captured by the moment approximation function as can be seen in figure 6.2. For low dispersion of the daughter cells, the density of pairs of bacteria increases at short distances suggesting the existence of a bacteria-bacteria aggregation at these distances. Large dispersion range yields pairs density function that takes values close to 1, indicating a uniform pattern. The moment model captures well the dynamic of the pair correlation function.

Now how density-independent bacteria motility affects the aggregated pattern yielded in the case of short range dispersion? Figure 6.3 shows snapshots of the simulated system when density-independent motility of the bacteria is added. The motility range is varied by varying the size w_m of the motility kernel. Increasing the motility range of the bacteria disperse daughter cells and their parents preventing

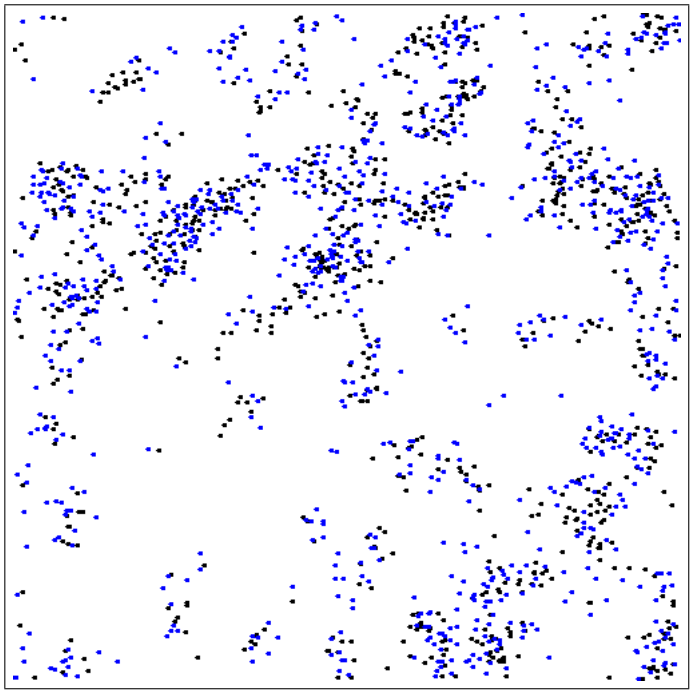

(a) $w_b = 5$

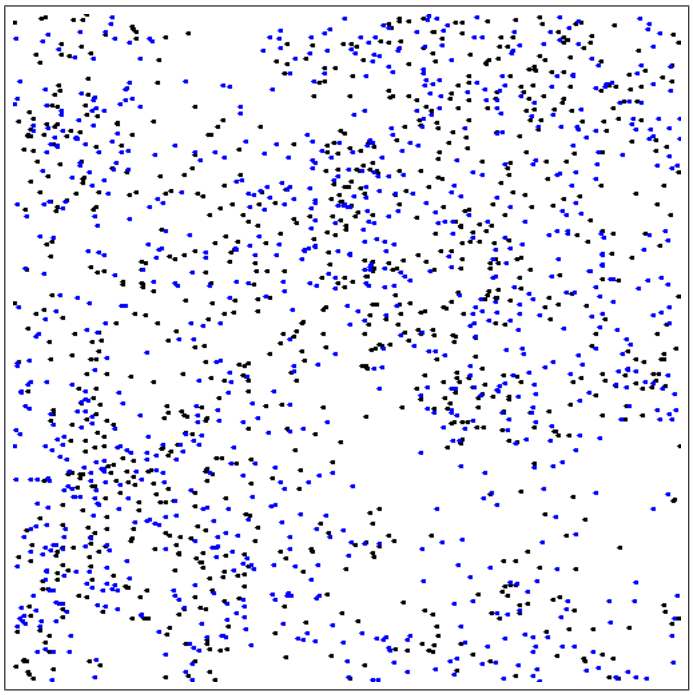

(b) $w_b = 11$

Figure 6.1: IBM snapshots of the state of the system at time $t = 100$ for the case of immotile bacteria $m_1 = 0.0$. (a) short-range dispersion, (b) long-range dispersion. The value of the other parameters are $b_1 = d_1 = 0.1$, $b_2 = d_2 = 0.1$, $d_1' = d_2' = m_2 = 0.0$ (no density-dependent processes)

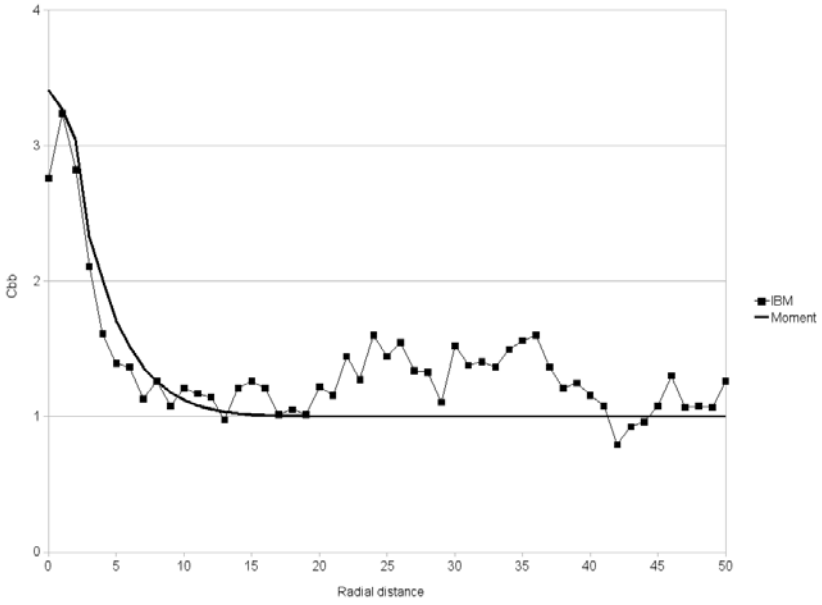

(a) $w_b = 5$

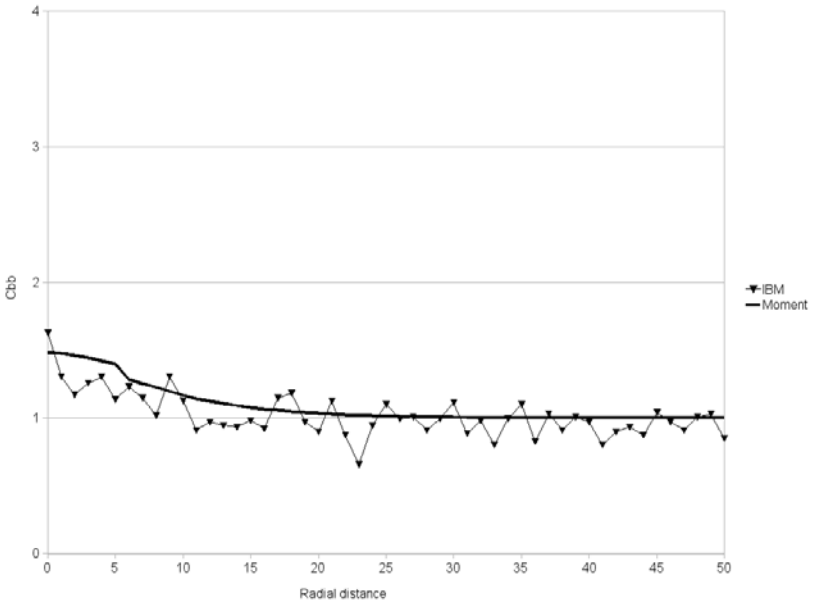

(b) $w_b = 11$

Figure 6.2: Comparison of the radial pair correlation functions obtained by the IBM and the moment model at time $t = 100$ for the case of immotile bacteria $m_1 = 0.0$. (a) short-range dispersion, (b) long-range dispersion. The value of the other parameters are $b_1 = d_1 = 0.1$, $b_2 = d_2 = 0.1$ (no polymer), $d_1' = d_2' = m_2 = 0.0$ (no density-dependent processes)

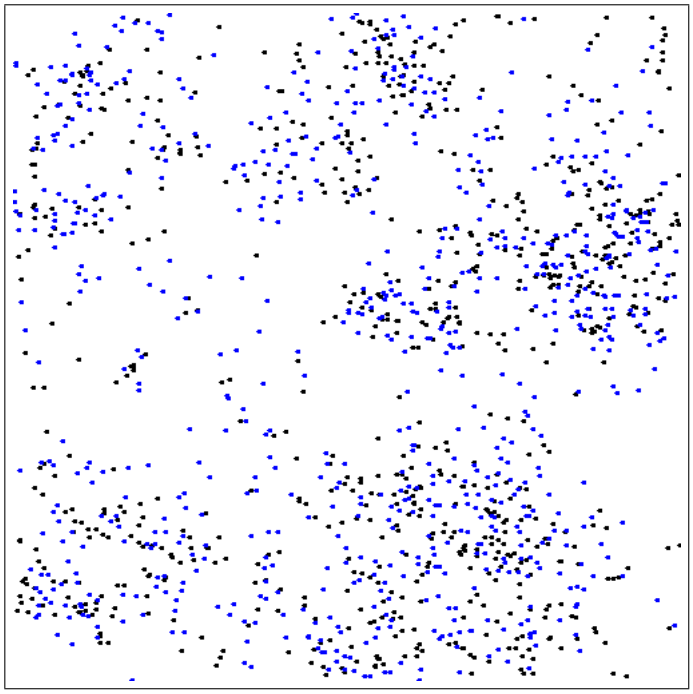

(a) $s_m = 3$

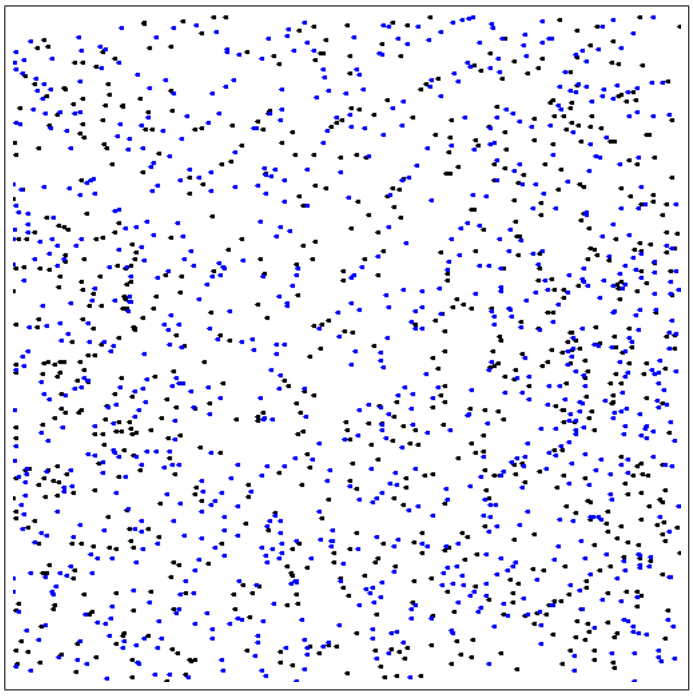

(b) $s_m = 15$

Figure 6.3: IBM snapshots of the state of the system at time $t = 150$ for the case of density-independent motile bacteria $m_1 = 0.0$. (a) short-range motility, (b) long-range motility. The value of the other parameters are $b_1 = d_1 = 0.1$, $b_2 = d_2 = 0.1$, $d_1' = d_2' = m_2 = 0.0$ (no density-dependent processes) and $w_b = 5$

the formation of colonies. In essence, the motility acts as the dispersal kernel and tend to mix the bacteria yielding uniform patterns. This is also demonstrated by the pair correlation function in figure 6.4. The pair correlation function in the IBM and moment models take values close to 1 for long-range motility indicating a uniform spatial pattern. We show in the next section that long-range motility plays the inverse role and promotes aggregated patterns formation in the case of density-dependent motility

Density-dependent motility

In the IBM, the density-dependent motility process is described by equation 6.7. The probability per unit of time that a bacterium moves to any other position within the domain is given by $m_1 - m_2 p_{loc}(x)$ where $p_{loc}(x)$ is the local density of polymer perceived by the bacterium in location x. The value of the local density of polymer is not bounded as a bacterium can hypothetically have any number of neighboring polymeric particles. In order to avoid negative probabilities we fix a threshold for the local densities of polymer above which the motility probability is set to zero. The threshold value corresponds to m_1/m_2. While in the IBM the local density of polymer perceived by an individual fluctuates due to the different stochastic processes, the dynamic of the moment model relies on the average value of the local density of polymer which is, for the parameters used in this chapter, always below the threshold value m_1/m_2.

Figure 6.5 shows snapshots of the state of the system for different values of m_2. In the IBM, increasing the value of m_2 promotes the formation of colonies due to the decrease of the immobilization threshold. This can also be observed from figure 6.6 showing the radial pairs correlation function (at time $t = 400$) simulated with the IBM and withe moment model. The pair correlation function peaked at short distance with the increase of the value of m_2. Surprisingly, comparison with the moment model shows that the later fail in capturing the formation of colonies (figure 6.6(b)). The pair correlation function yielded by the moment model remains close to 1 indicating a uniform pattern. To explain this difference we extracted the time course of the local polymer densities experienced by the bacteria in the IBM and the moment model. The local density experienced by the bacteria in the IBM differ from an individual to another depending on the location of the individual and its neighborhood. At each time step we calculate the average local density of polymer and the maximum value experienced by the bacteria. In the moment model, only the average local polymeric density is considered in the model and is given by:

$$p_{loc} = \int K\left(\frac{||\xi||}{w_d}\right) C_{bp}(\xi) d\xi \tag{6.28}$$

Figure 6.7 compares the average and maximum values of the local polymer density experienced by the individuals in the IBM with the average local density of

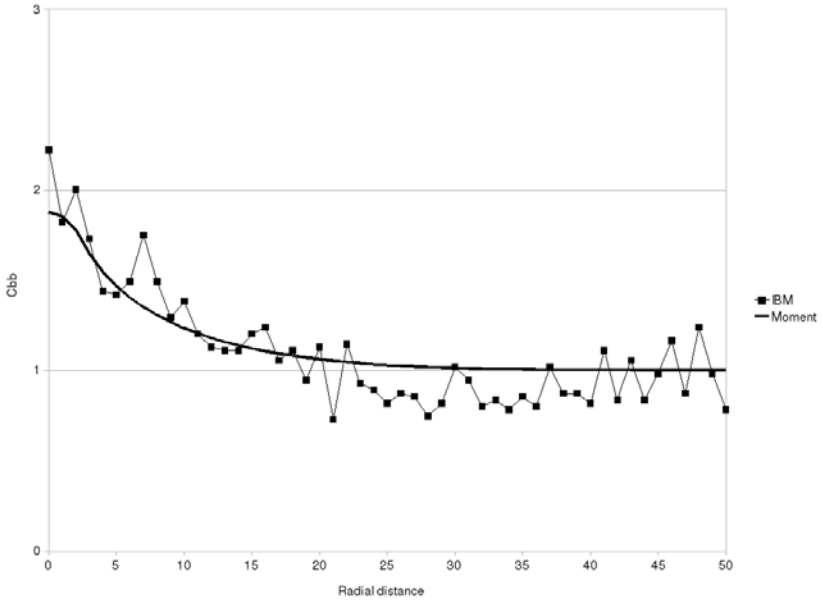

(a) $s_m = 3$

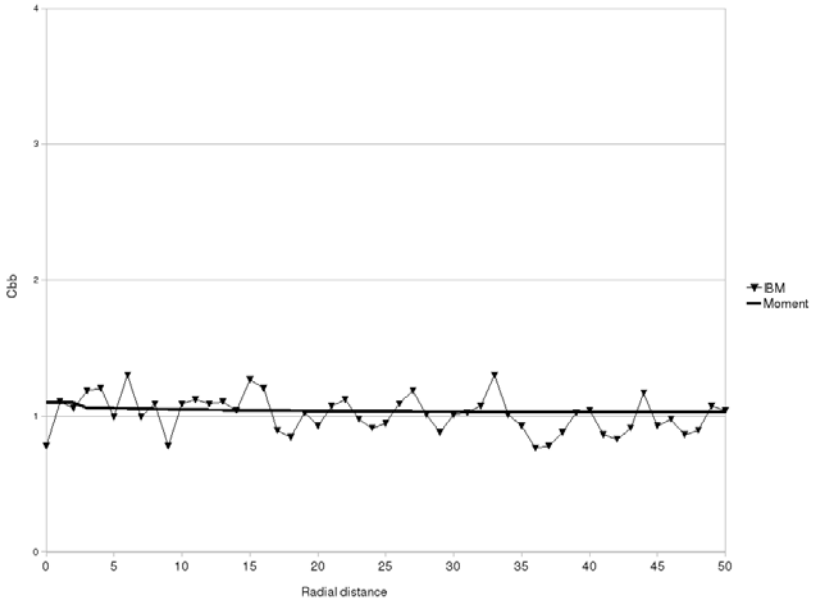

(b) $s_m = 151$

Figure 6.4: Comparison of the radial pair correlation functions obtained by the IBM and the moment model at time $t = 150$ for the case of motile bacteria $m_1 = 1.0$ (a) short-range motility, (b) long-range motility. The value of the other parameters are $b_1 = d_1 = 0.1$, $b_2 = d_2 = 0.1$, $d_1' = d_2' = m_2 = 0.0$ (no density-dependent processes) and $w_b = 5$

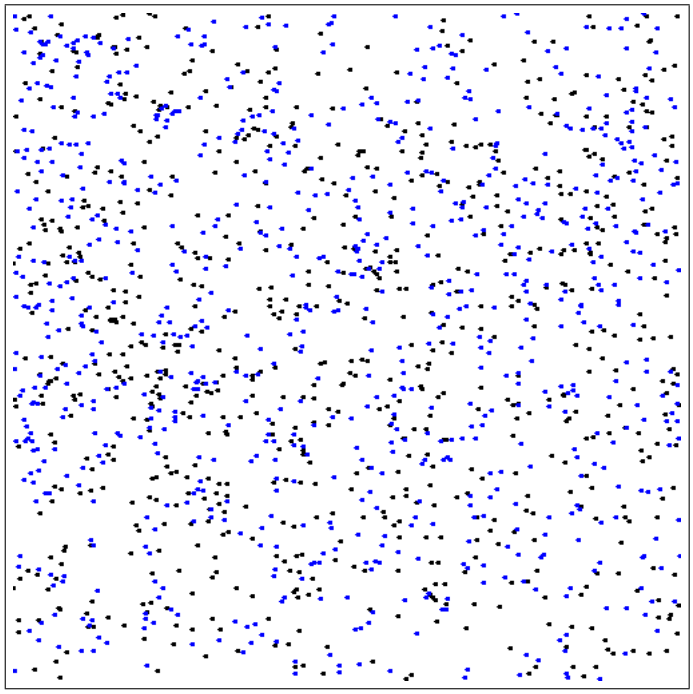

(a) $m_2 = 1.0$

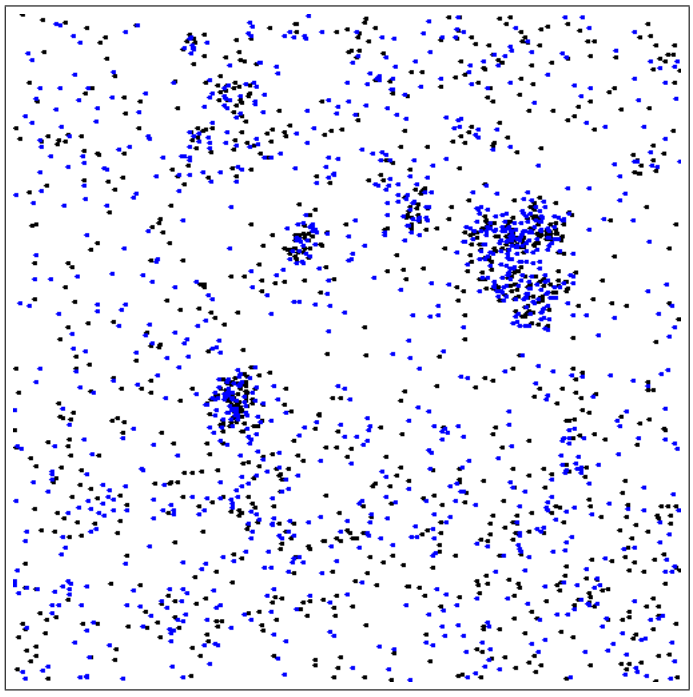

(b) $m_2 = 2.0$

Figure 6.5: IBM snapshots of the state of the system at time $t = 400$ for the case of density-dependent motile bacteria. The value of the other parameters are $b_1 = d_1 = 0.1$, $b_2 = d_2 = 0.1$, $d_1' = d_2' = 0.0$ (no density-dependent detachment) and $w_b = 5$, $w_m = 15$, $w_d = 5$

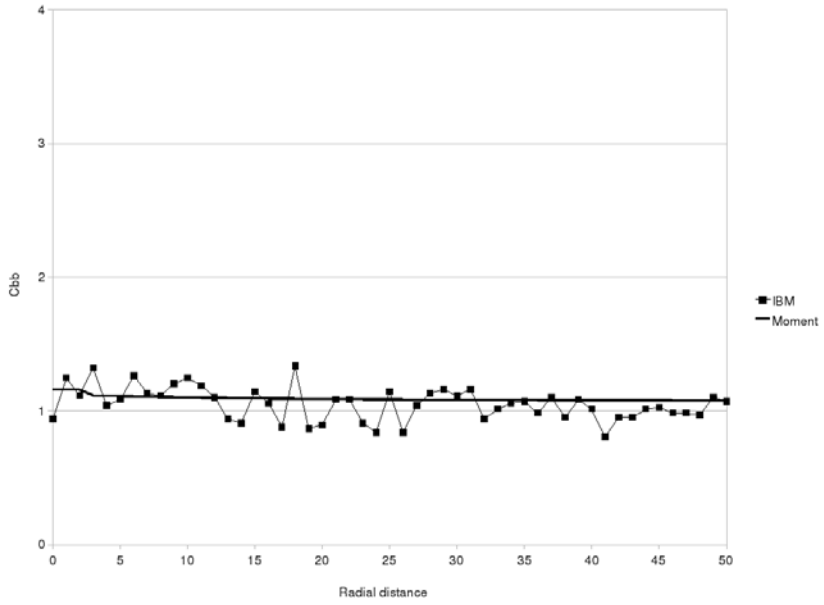

(a) $m_2 = 1.0$

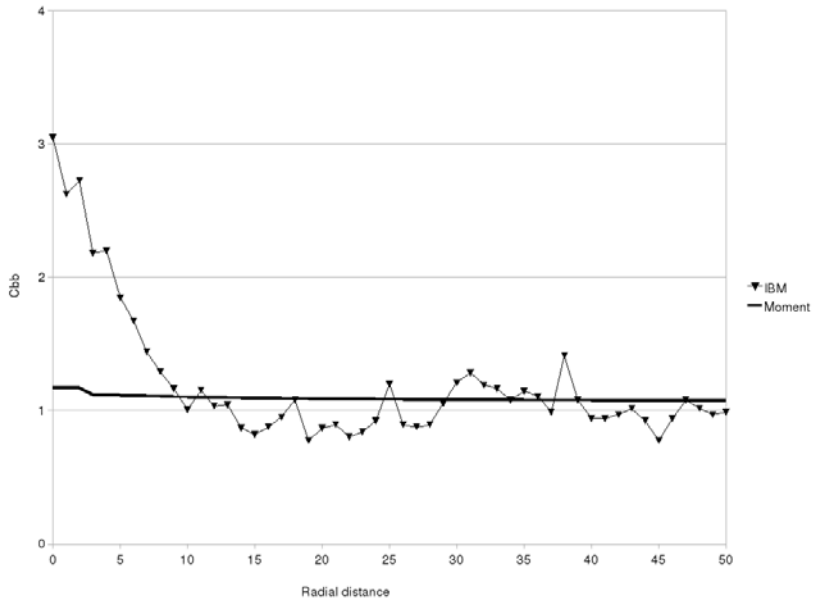

(b) $m_2 = 2.0$

Figure 6.6: Comparison of the radial pair correlation functions obtained by the IBM and the moment model at time $t = 400$ for the case of density-dependent motile bacteria. The value of the other parameters are $b_1 = d_1 = 0.1$, $b_2 = d_2 = 0.1$, $d_1' = d_2' = 0.0$ (no density-dependent detachment) and $w_b = 5$, $w_m = 15$, $w_d = 5$

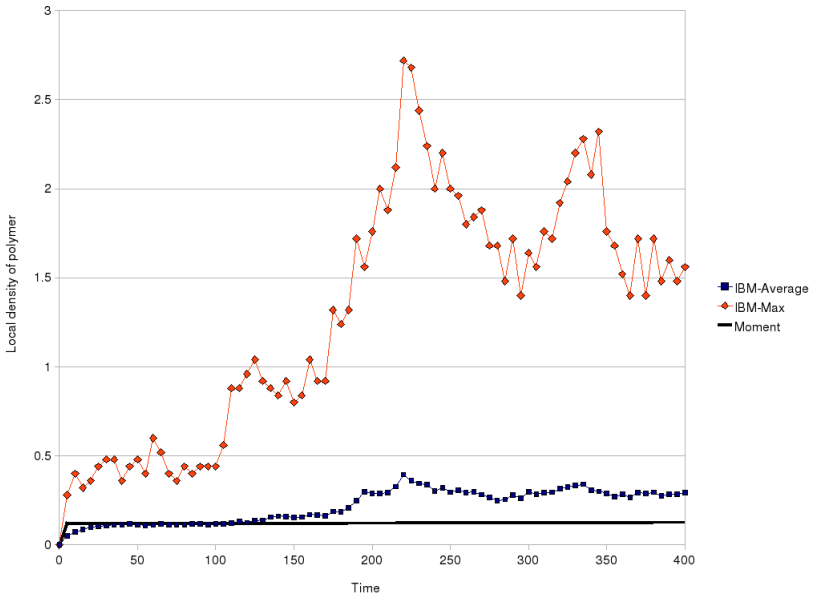

Figure 6.7: Comparison of the local densities of polymer as perceived by the bacteria in the IBM (average and max) and in the moment model. The model parameters are $b_1 = d_1 = 0.1$, $b_2 = d_2 = 0.1$, $d_1' = d_2' = 0.0$ (no density-dependent detachment) and $w_b = 5$, $w_m = 15$, $w_d = 5$

polymer calculated in the moment model. Figure 6.7 shows that as long as the maximum value of the local polymer density experienced by the individual in IBM is smaller than the immobilization threshold, both models yield similar results with respect to the average local density of polymer (and the correlation function - data not shown). At time $t \sim 100$ and due to stochastic fluctuations the maximum value of the local density of polymer in the IBM increases beyond the immobilization threshold (given by $m_1/m_2 = 0.5$). This means that in some region of the domain at least one bacterium experienced a local density of polymer higher than the immobilization threshold value. The bacterium than becomes immotile and may initiate the formation of a colony. It may happen that the stochastic polymer detachment removes one or more polymeric particles from the neighborhood of the immobilized bacterium which reduces the local density of polymeric particles below the threshold value and the immobilized bacterium recover its motility (see the small peak in figure 6.7 at instant 0). But it may also happen that additional polymeric particles are produced in the neighborhood of the immobilized bacteria which yield the formation of a colony. The moment model do not capture these phenomena because it relies on the average local density of polymer which is still below the threshold immobilization value (see figure 6.7).

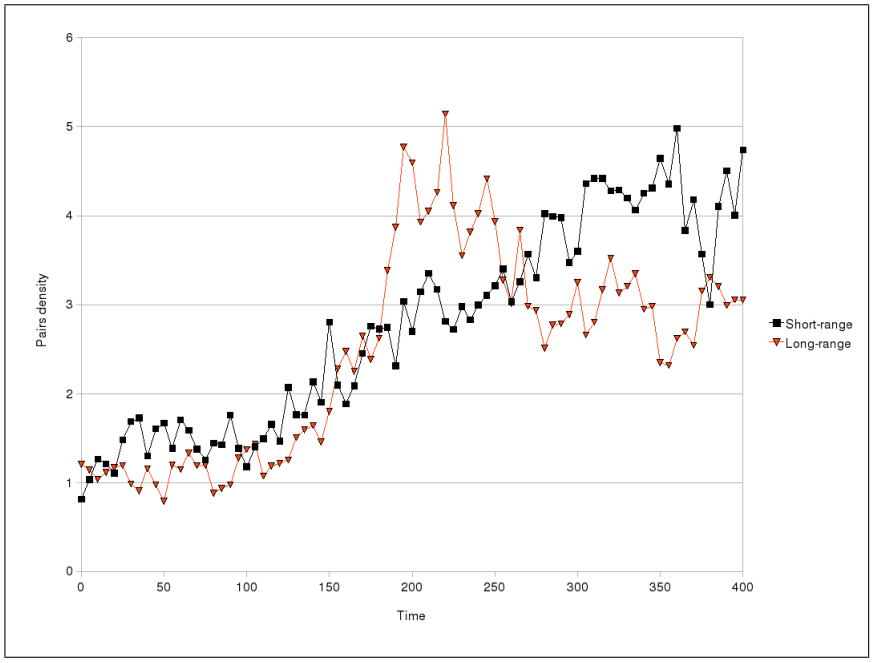

Figure 6.8: Effect of motility range w_m on colony formation. Short-range corresponds to $w_m = 5$ and long-range to $w_m = 15$. Other parameters are $b_1 = d_1 = 0.1$, $b_2 = d_2 = 0.1$, $d_1' = d_2' = 0.0$ (no density-dependent detachment), $m_2 = 2.0$, $w_b = 5$ and $w_d = 5$

The formation of colonies in the IBM induces significant changes of the spatial pattern and the further evolution of the system. Other processes may reinforce the formation of the colony like the division of the immobilized bacterium or the entrapment of motile bacteria in the region where the local polymer density increased beyond the immobilization threshold value. We investigated the effect of increasing the motility range (w_m) on the colony formation for $m_2 = 2.0$. Figure 6.8 reports the impact of increasing the motility range on the bacteria pair correlation function at the shortest distance $\xi = d\xi$ (where $d\xi$ is the spatial resolution) simulated using the IBM. The formation of colonies is translated by the increase of the value of the pair correlation function at distance $d\xi$. It can be seen from figure 6.8 that in the case of long-range motility, the peak in the pair correlation function occurs at $t = 200$ while the same peak occurs at time $t = 350$ in the case of short-range motility. The formation of colonies seems to be faster in the case of long-range motility. While increasing the motility range of the bacteria prevented the formation of colonies in the case of the density-independent model, it is likely to have the inverse effect in the case of density-dependent motility. The increase of the motility range accelerate the formation of colonies. A possible explanation is that motile bacteria traveling over long distance have more chance to be trapped in a location with high density of polymer than bacteria traveling over short distances.

Density-dependent detachment

So far, we considered that detachment of the bacteria and polymer occurs at a fixed density-independent rate ($d_1 = d_2 = 0.1$ and $d'_1 = d'_2 = 0$). Now we investigate the case where the detachment rates of polymer and bacteria increase with the local density of polymer. This means that bacteria and polymer enclosed within colonies will experience higher detachment rates that their dispersed counterparts. Figure 6.9 shows IBM snapshots of the pattern for two different values of density-dependent detachment rates $d'_1 = d'_2 = 0.05$ and $d'_1 = d'_2 = 0.1$. Increasing the effect of the density-dependent detachment prevents the formation of the colonies. This is confirmed by the pair correlation functions in figure 6.10 where the peak reached by the pair correlation function is lower in the case of higher density-dependent detachment rates, indicating a lower level of aggregation of the bacteria. The moment model fails in capturing the colonies formation and the effect of the density-dependent detachment is under-estimated in the moment model.

Density-dependent detachment has an impact on the average-density of the bacteria and polymer. Figure 6.11 shows the time course of the density of bacteria and polymer calculated with the IBM and the moment model. For high density-dependent detachment rates, the equilibrium densities yielded by the IBM are lower than the densities that results from the moment model. The formation of colonies increases the detachment rate experienced by the bacteria which yields lower equilibrium densities. The difference between both models vanishes for higher density-detachment rates because of the absence of colonies formation.

6.4 Conclusion

We derived a moment approximation equations of a simplified IBM that describes colonies formation due to to bacteria motility reduction by a self-produced polymer. Both models account for five processes taking place at the level of the individuals. To analyze these models we proceed progressively starting with a density independent model obtained by setting the motility and detachment density dependent factors to zero. We show that in the absence of motility, colonies form as a result of the low dispersion of the daughter cells and that density-independent motility tend to increase this dispersion range preventing the formation of colonies. Moment model and the IBM compare very well in the case of density independent model. The pair correlation function of the bacteria positions yielded by the IBM simulation captured the main features of the simulated patterns and are in a good agreement with those yielded by the moment model.

Starting from the case of bacteria with a long-motility range (no colonies formation) we then introduced density-dependent motility. Our results showed that colonies form due to the immobilization of bacteria in the location where the local density of polymer increases above a threshold value. While in average, the local

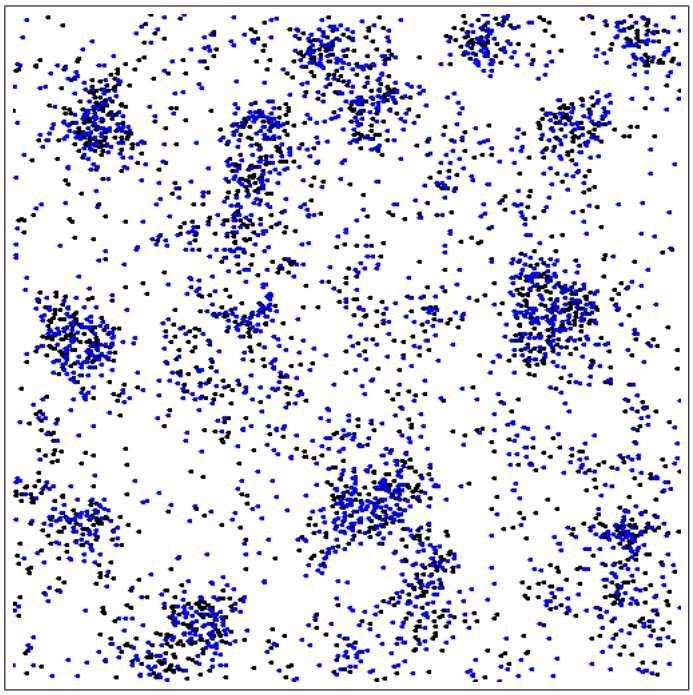

(a) $d_1 = d_2' = 0.05$

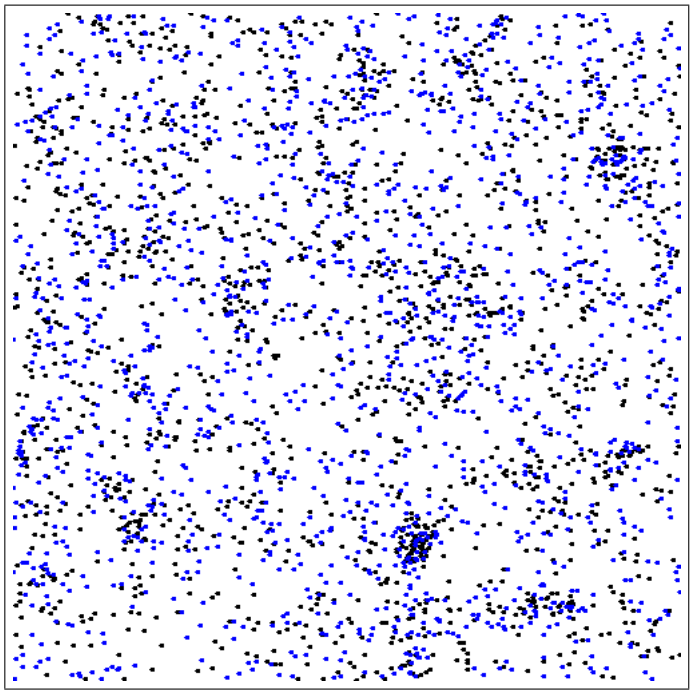

(b) $d_1' = d_2' = 0.1$

Figure 6.9: IBM snapshots of the state of the system at time $t = 400$ for the case of density-dependent detachment. $b_1 = b_2 = 0.12$, $d_1 = d_2 = 0.1$, $m_1 = 1.0$, $m_2 = 2.0$,$w_b = 5$, $w_m = 15$ and $w_d = 5$

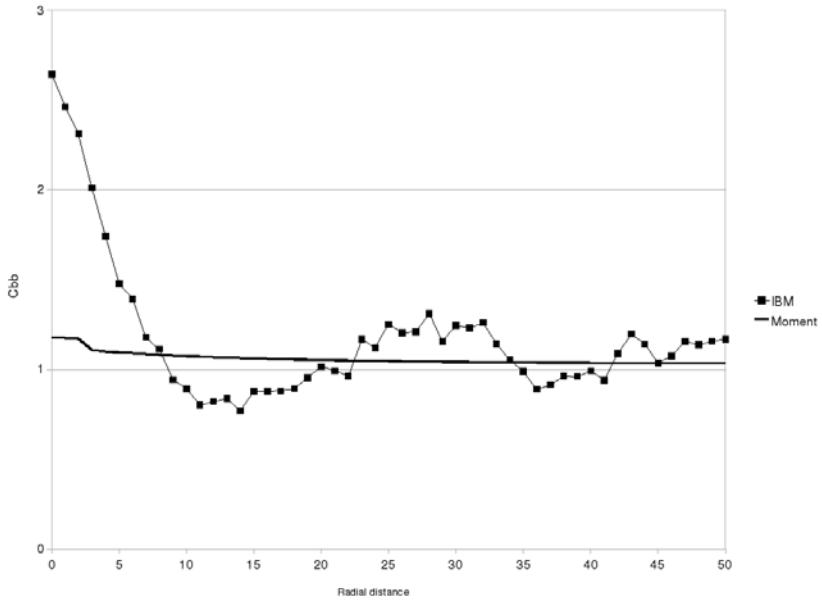

(a) $d_1 = d_2' = 0.05$

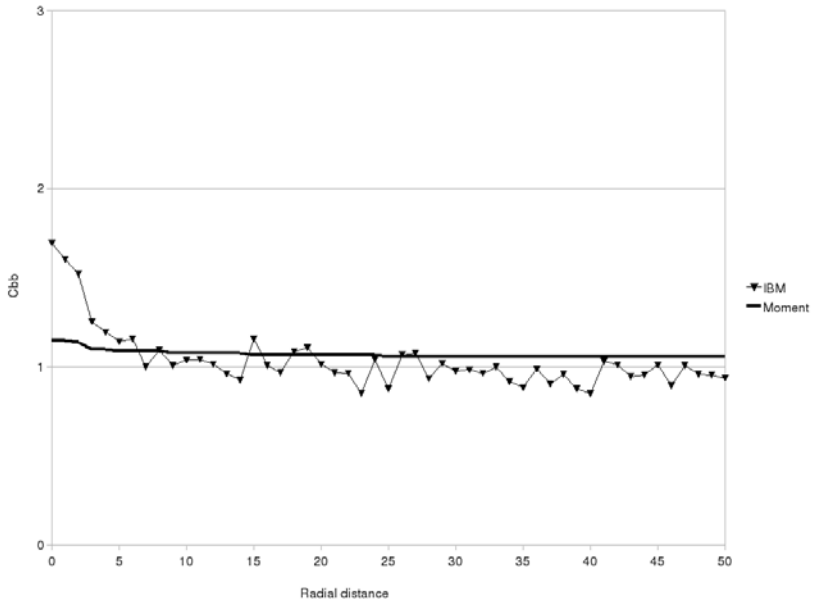

(b) $d_1 = d_2' = 0.1$

Figure 6.10: Comparison of the radial pair correlation functions obtained by the IBM and the moment model at time $t = 400$. The models parameters are:$b_1 = b_2 = 0.12$, $d_1 = d_2 = 0.1$, $m_1 = 1.0$, $m_2 = 2.0$,$w_b = 5$, $w_m = 15$ and $w_d = 5$

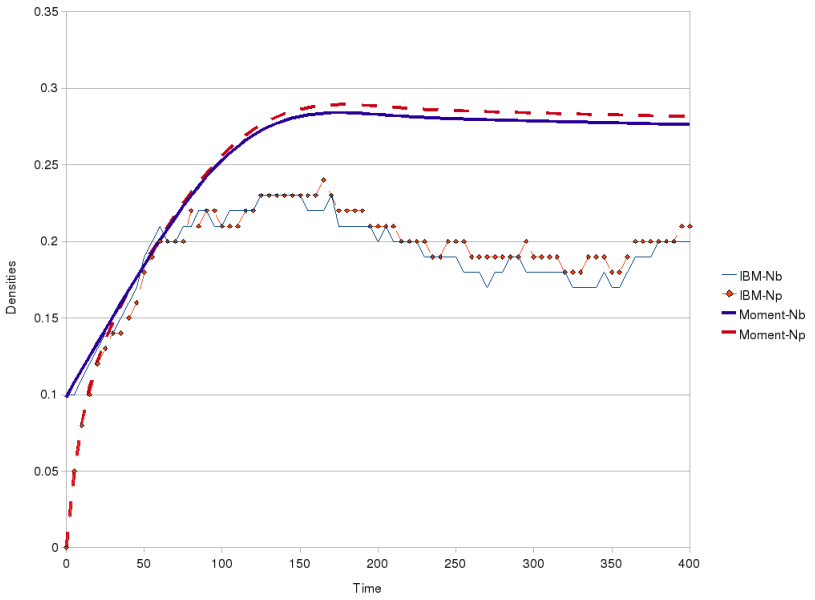

(a) $d_1 = d_2' = 0.05$

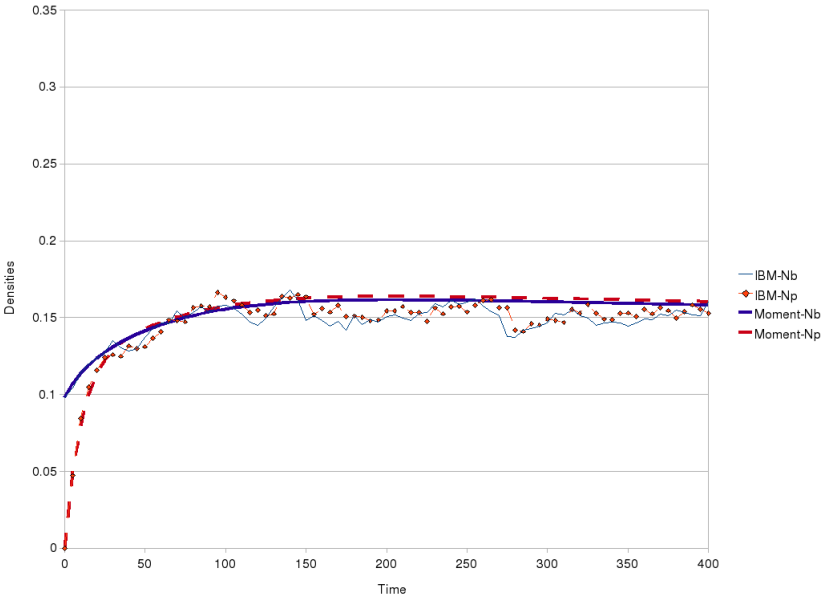

(b) $d_1 = d_2' = 0.1$

Figure 6.11: Comparison of the time course of the densities of bacteria N_b and polymer N_p yielded by the IBM and the moment model. The models parameters are:$b_1 = b_2 = 0.12$, $d_1 = d_2 = 0.1$, $m_1 = 1.0$, $m_2 = 2.0$,$w_b = 5$, $w_m = 15$ and $w_d = 5$

density experienced by the individuals remain below the immobilization threshold, fluctuations in local polymer densities would have pushed the value of the local density above the immobilization threshold which initiated the formation of colonies. The moment model do not capture this process, as the dynamics of the moments is based on the average local density.

Furthermore, we investigated how the formation of colonies in the case of density dependent motility is affected by the size of the motility kernel s_m. Surprisingly increasing the motility range of the bacteria tend to promote the formation of colonies. Long range motility, allowing motile bacteria to travel over longer distances, increases their chance to cross locations where the polymer density exceeds the immobilization threshold value.

Finally, the influence of density-dependent detachment of polymer and bacteria goes the other direction of density-dependent motility. Detachment is assumed to increase with the local density of polymer experienced by the individuals. Thus depending on the value of the density-dependent detachment parameters colonies may or may not form.

Chapter 7

Exploring the labyrinth-like patterns in a simplified IBM of a microbial biofilm formed with motile bacteria

Contents

We propose to further simplify the individual-based model (IBM) presented in the previous chapter and discuss its approximation using moment models. The main simplification is that individuals motility and detachment depend now directly on the local density of the individuals rather than on the excreted polymer. Hence we do not consider polymer dynamic in this chapter.

The chapter is organized in four sections: in the first section we describe the simplified IBM. In the second section we explore the pattern yielded by the IBM and compare these patterns qualitatively to experimental biofilm patterns and to the pattern obtained with the IBM including the polymer (chapter 6). Finally we discuss the approximation of the IBM using moment approach assess the technical difficulties in solving moment equations with motility.

7.1 Simplified IBM for biofilm formed with density-dependent motile bacteria

The IBM that we describe in this section is an extension of the IBM presented in chapter 4 that includes division and density dependent detachment. In addition to these processes , we include a density-dependent motility process. The resultant IBM considers the following three processes:

- Division process: an individual in location $x = (x_1, x_2)$ has a probability (per unit of time) $B(x, x')$ to produce a newborn located in x' given by:

$$B(x, x') = b_1 \tag{7.1}$$

where b_1 is a constant division rate.

- Detachment process: an individual in location x detaches with a density-dependent probability $D(x)$ given by:

$$D(x) = d_1 + d_1' p_d^{loc}(x) \tag{7.2}$$

where d_1 and d_1' are the density-independent and the density-dependent detachment rates and $p_d^{loc}(x)$ is the local density perceived by the individual in x. $p_d^{loc}(x)$ measures the impact of the neighboring individuals on the detachment probability of the individual in x. We calculated this local density using the detachment kernel $K(||x - x'||/w_d)$ given by:

$$\frac{K(||x - x'||}{w_d} = \begin{cases} 1/w_d & \text{if} \quad ||x - x'|| < w_d \\ 0 & \text{else} \end{cases} \tag{7.3}$$

- Motility: we model individuals motility as density-dependent process such that the probability per unit of time for an individual located in x to move to a location x' decreases with the increase of the local density of individuals in x. Thus, in this model the neighbor of a focal individual tend to reduces its motility and increase its detachment rate. The probability per unit of time of an individual to move from x to x' is given by:

$$M(x, x') = [m_1 - m_2 p_{loc}(x, w_v)] K((x - x')/w_m) \tag{7.4}$$

where m_1 and m_2 are respectively the density independent and the density dependent motility parameters, $p_{loc}(x, w_v)$ is the local density of bacteria perceived by an individual in x and calculated using a uniform interaction kernel with a size w_v and $m(x - x')$. The expression $[m_1 - m_2 p_{loc}(x, w_v)]$ corresponds to the motion probability (per unit of time) of the individual in x. This expression should be positive. If the local perceived density $p_{loc}(x, w_v)$ is higher that the value of m_1/m_2 than the motion probability of the individual in x is set to zero.

A simulation is initialized with a number N_0 individual cells uniformly distributed over the domain. The model parameters are summarized in table 7.1.

Parameters	Description	Value
L	Domain size	201×201
ΔL	Spatial discretization	1
b_1	Density-independent bacteria division rate	0.1
d_1	Density-dependent detachment rate	0.0
d_2	Density-dependent detachment rate	0.4
m_1	Density-independent motility rate	0.0 or 1.0
m_2	Density-dependent motility rate	0.0 or 3.0
w_b	Uniform division and polymer production kernel side	variable
w_d	Uniform detachment interaction kernel side	variable
w_v	Uniform motility interaction kernel side	variable
w_m	Uniform motility kernel	variable

Table 7.1: Model parameters

A major difference of this simplified IBM with the IBM presented in the previous chapter (Chapter 6) is that the detachment and the motility probabilities depend on the density of the individuals themselves rather than on the density of the excreted product. The implicit assumption behind this simplification is that the excreted products and the individuals spatial distributions are correlated such that the local accumulation of the first induces (and/or results from) the accumulation of the second.

7.2 Numerical exploration of the IBM

Though simple, the IBM described above yields a diversity of patterns ranging from uniform distribution of the individuals to isolated colony and labyrinth-like patterns. In a recent paper Xavier *et al.* [Xavier 2009] showed that similar patterns arise in laboratory culture of the biofilm forming strain *P. aeruginosa* (figure 7.1). They explained the formation of these patterns by scale-dependent interactions between nutrient competition and mechanical pushing. At low nutrient densities the bacteria formed isolated colonies. The increase of the nutrient concentration induced a transition to the labyrinth-like patterns then to the dense biofilm pattern.

Our simplified model can reproduce similar transitions from the isolated colony pattern to the labyrinth-like pattern, as illustrated in figures 7.2 and 7.3, either by increasing progressively the division rate of the individuals (figure 7.3) or by increasing the value of the density-dependent parameter m_2. We identify bacteria motility and detachment as two potential processes that may yield labyrinth-like patterns.

Figure 7.4 shows the patterns yielded by the simplified model are comparable to those that may be obtained with the IBM including the dynamic of the polymer

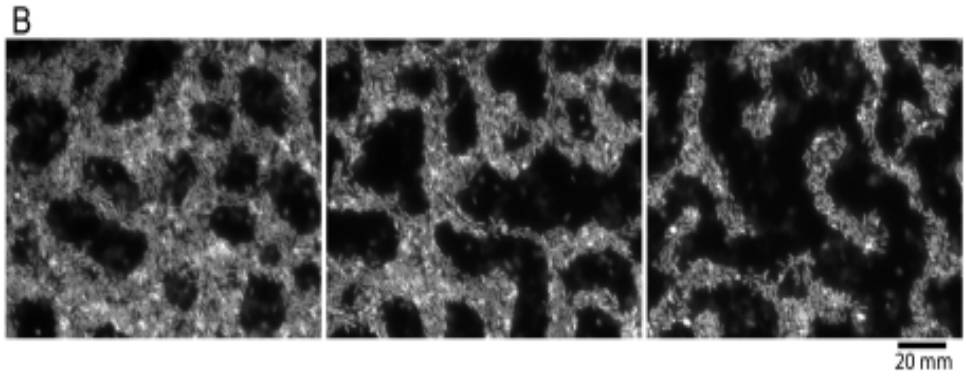

Figure 7.1: [Xavier 2009]

(Chapter 6). These results that the explicit consideration of the polymer may not be necessary for the formation of these spatial patterns.

In order to understand how these labyrinth-like patterns form in our model we propose to examine in details an IBM simulation through pattern observation and measuring spatial moments. Figure 7.5 shows the snapshots of the formation of the labyrinth-like pattern. The simulation is initiated with $n_0 = 100$ individuals distributed uniformly. The individuals divide and disperse due to the large motility kernel. As the density of individuals increases in the systems the motility of the individuals decreases progressively and colonies start to form. The formation of colonies in not due to the total immobilization of the individuals but rather to local equilibrium between division which tend to promote the local accumulation due to the small birth kernel ($w_b = 3$) and motility that tends to disperse the individuals.

Figure 7.8 reports the time evolution of the average density of individuals and shows a rapid first phase where the average density increases before decreasing towards an equilibrium value (0.25). The equilibrium average density of individuals yielded by the IBM is lower than the value calculated using the mean-field model (0.35) indicating that the individuals in average detach at a higher rate than what would be expected in the absence of any spatial pattern.

7.3 Deriving the moment approximation model

We derive the dynamical equations of the first spatial moment (average density of the individuals) and the second spatial moment (pair density correlation function) approximating the dynamic of the IBM. The dynamic of the first moment is influenced by division and detachment events. The motility of an individual from a location x to a location x' has no impact on the average density of individuals. The dynamic of the first moment is given by:

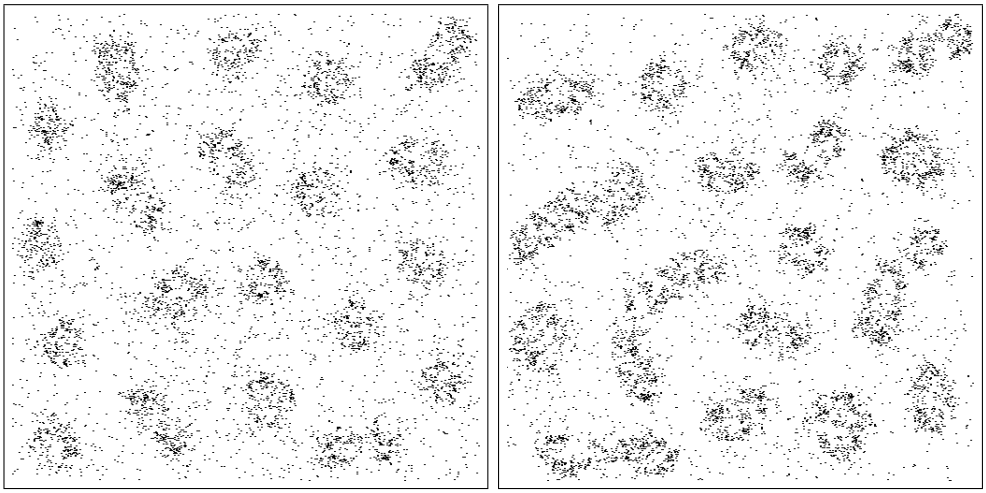

(a) $b_1 = 0.10$ (b) $b_1 = 0.13$

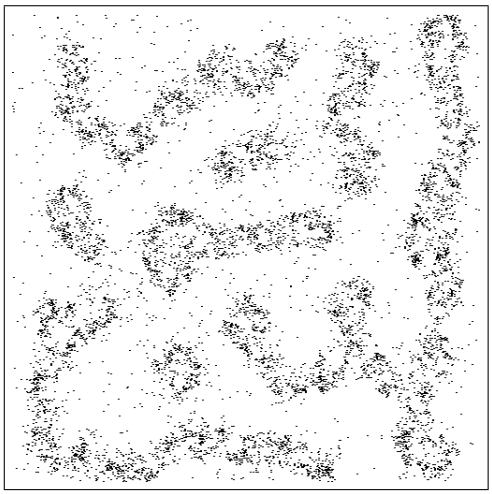

(c) $b_1 = 0.15$

Figure 7.2: Examples of patterns yielded by the simplified IBM and the IBM with extracellular product

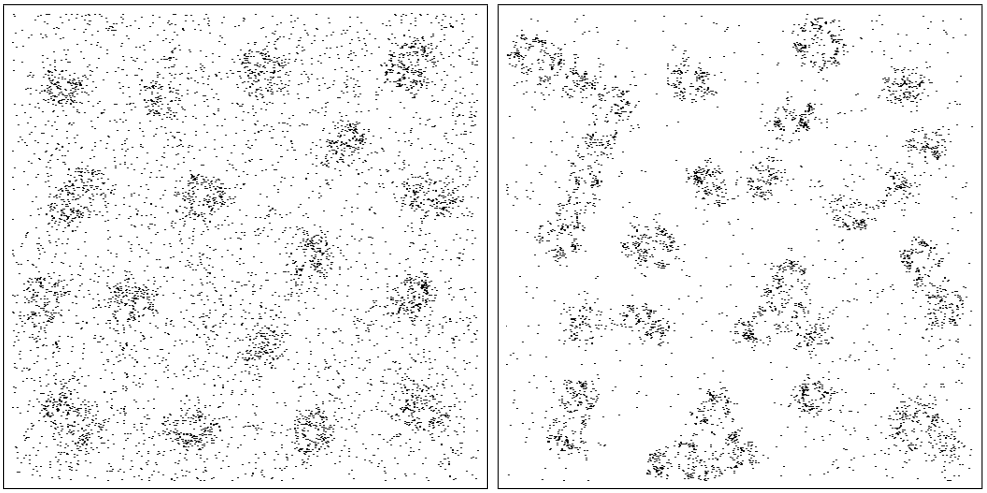

(a) $m_2 = 3.0$ (b) $m_2 = 2.0$

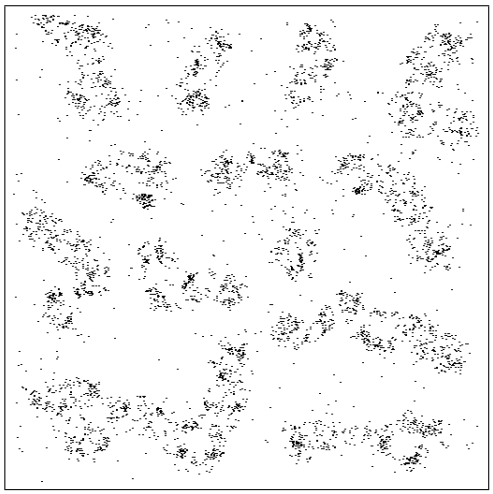

(c) $m_2 = 4.0$

Figure 7.3: Examples of patterns yielded by the simplified IBM and the IBM with extracellular product

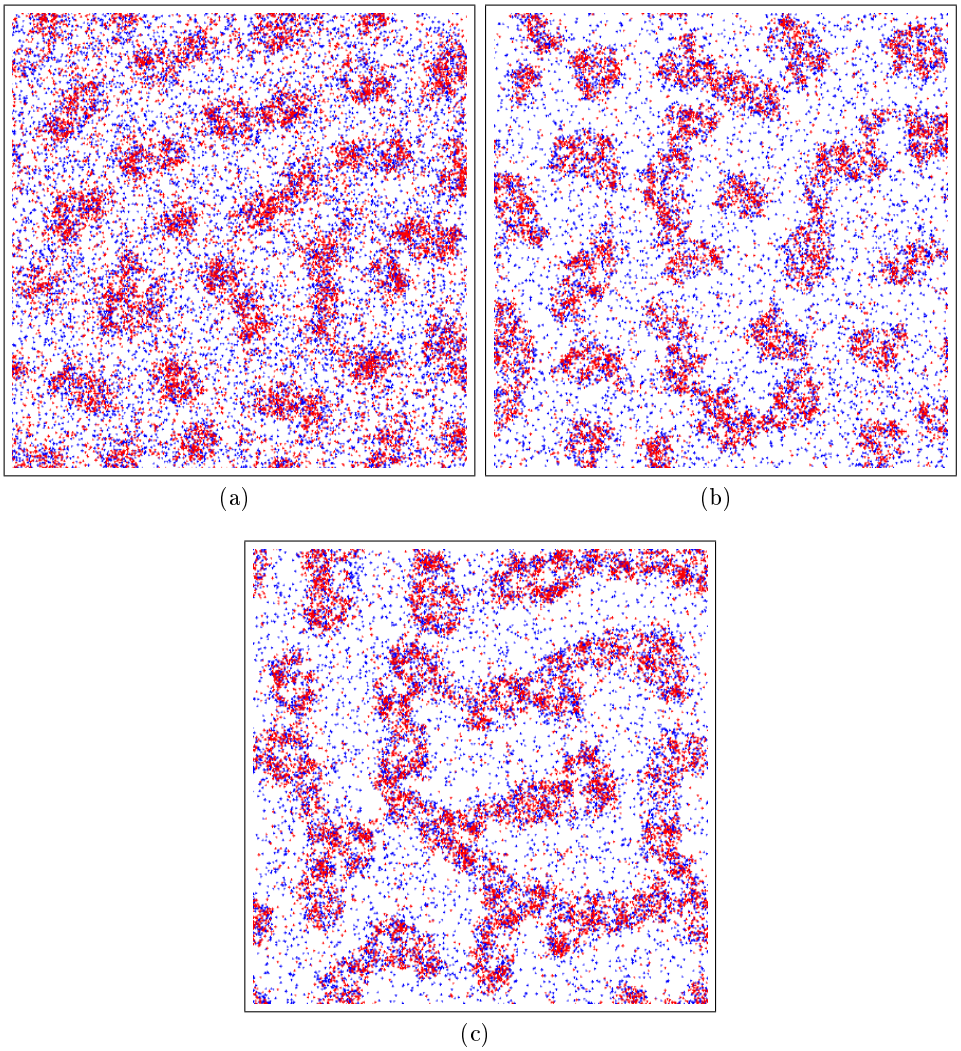

Figure 7.4: Pattern yielded by the IBM with product dynamic (bacteria: red and polymeric particles: blue)

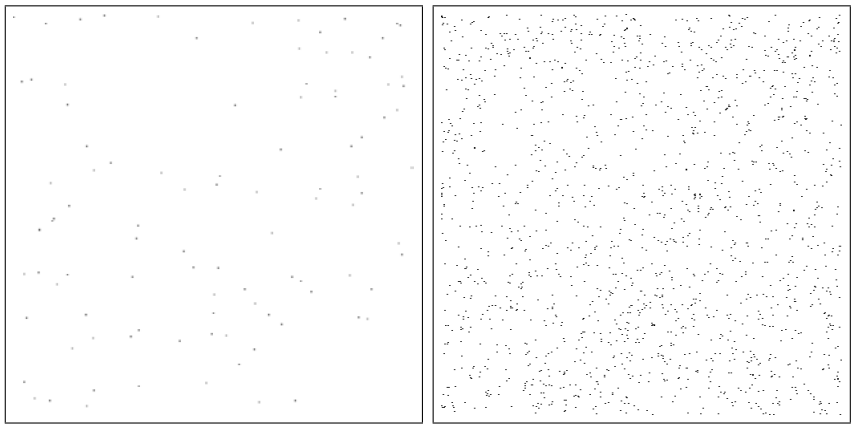

(a) $t = 0$ (b) $t = 20$

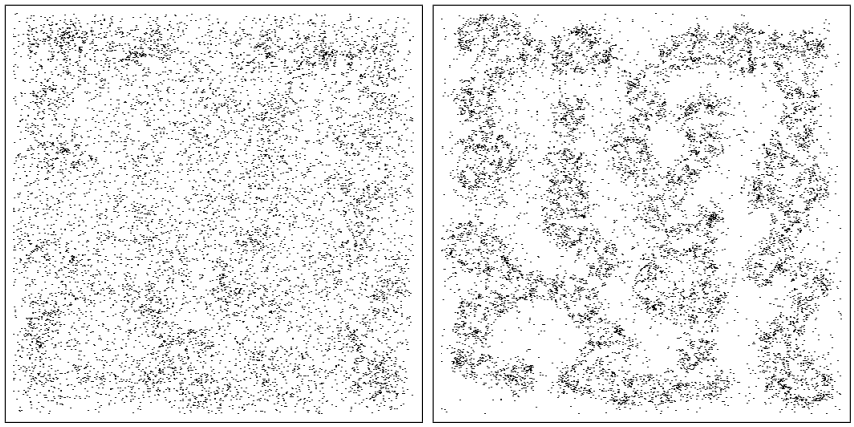

(c) $t = 40$ (d) $t = 60$

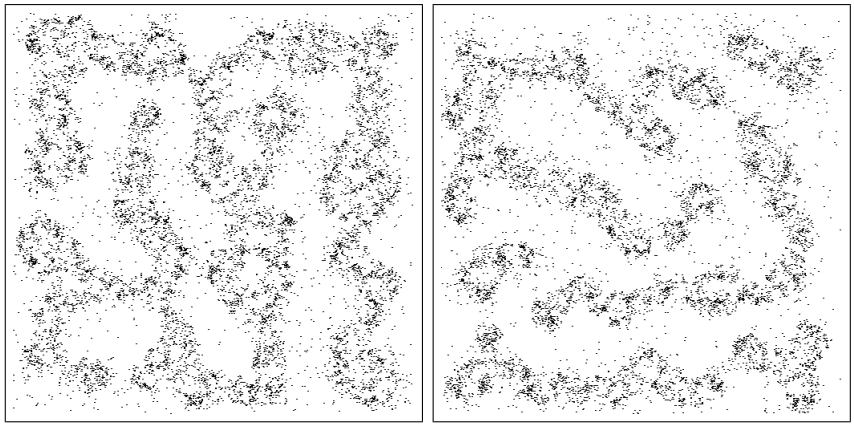

(e) $t = 80$ (f) $t = 740$

Figure 7.5: Snapshots of the spatial pattern yielded by the IBM at different times. The parameters are $b_1 = 0.15$, $w_b = 3$, $w_d = 19$, $w_m = 31$, $w_v = 19$, $m_1 = 1.0$ and $m_2 = 3.0$

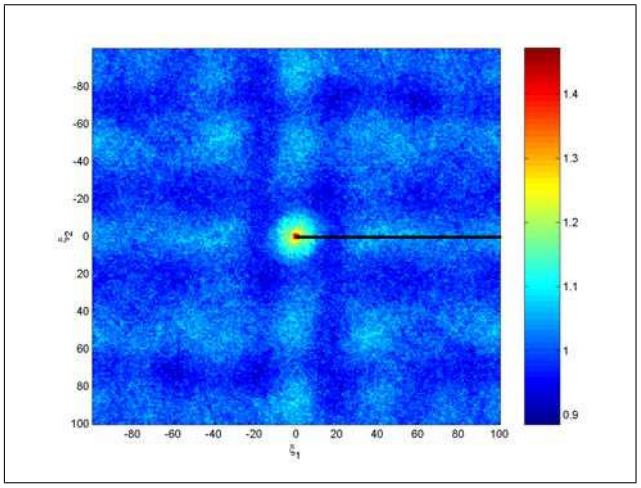

(a) $t = 40$

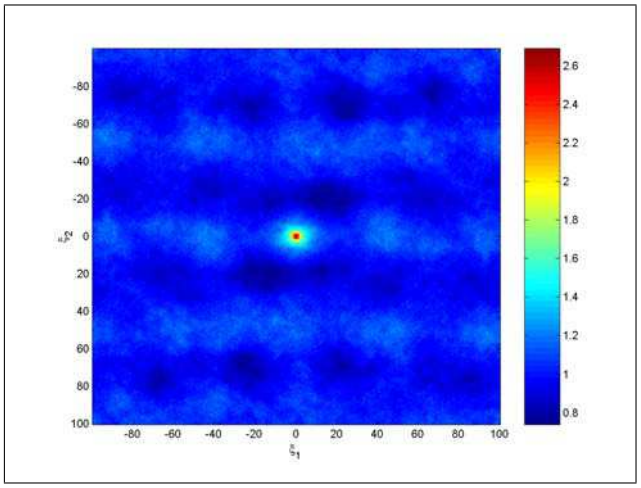

(b) $t = 80$

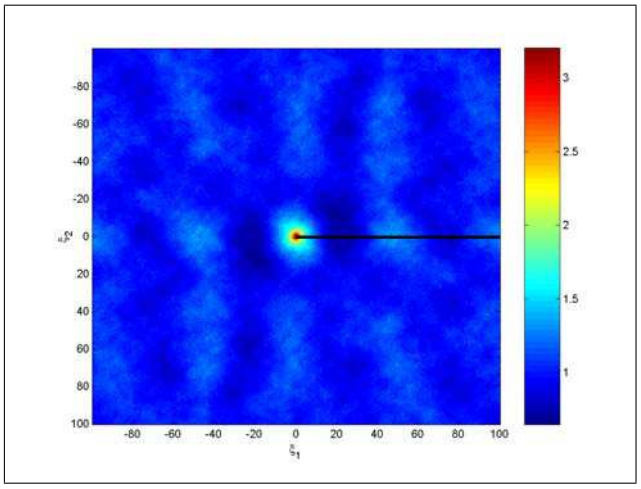

(c) $t = 740$

Figure 7.6: Time evolution of the cartesian pair correlation function. The parameters are $b_1 = 0.15$, $w_b = 3$, $w_d = 19$, $w_m = 31$, $w_v = 19$, $m_1 = 1.0$ and $m_2 = 3.0$

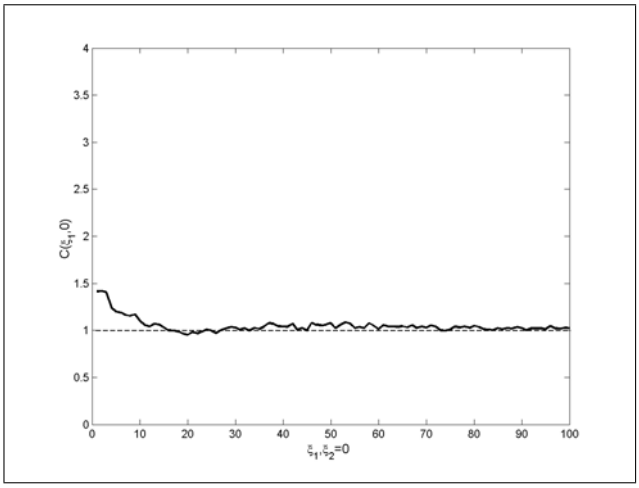

(a) $t = 40$

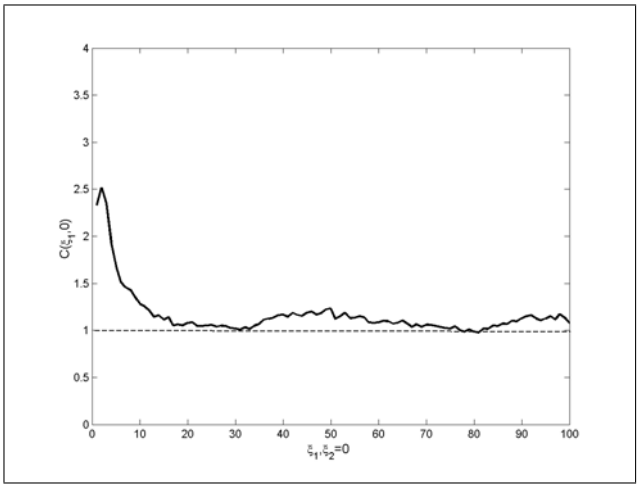

(b) $t = 80$

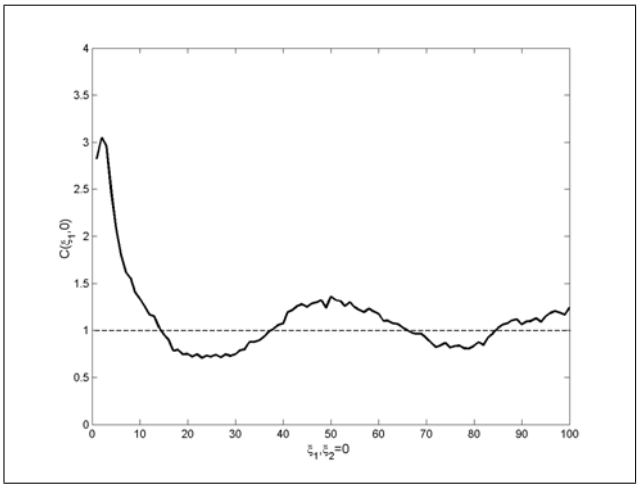

(c) $t = 740$

Figure 7.7: Time evolution of the 'radial' pair correlation function. The parameters are $b_1 = 0.15$, $w_b = 3$, $w_d = 19$, $w_m = 31$, $w_v = 19$, $m_1 = 1.0$ and $m_2 = 3.0$

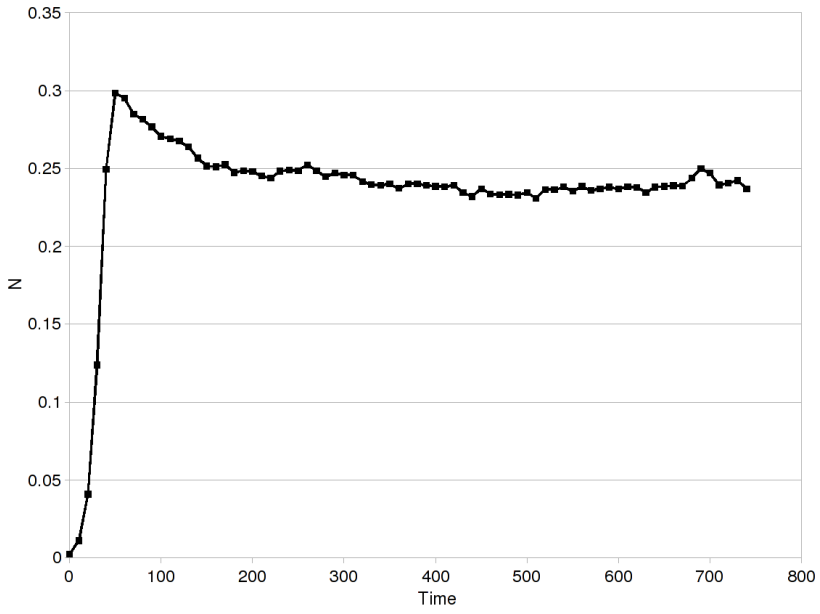

Figure 7.8: Time evolution of average density of individual N

$$\frac{dN}{dt} = b_1 N - d_1 N - d_1' \int C(\xi) K\left(\frac{||\xi||}{w_d}\right) d\xi \tag{7.5}$$

Note that the motility is not involved in equation 7.5 as the motility of an individual from one position to another does not affect the total number of individuals. However, motility may affects the average number of individuals indirectly by modifying the spatial distribution of the individuals and consequently their detachment rates.

The second moment measures the density of pairs of individuals separated with a vectorial distance ξ. This density is affected by division, detachment and motility events:

$$\frac{dC(\xi)}{dt} = \left(\frac{dC(\xi)}{dt}\right)_{division} + \left(\frac{dC(\xi)}{dt}\right)_{detachment} + \left(\frac{dC(\xi)}{dt}\right)_{motility} \tag{7.6}$$

The first two terms on the right hand side have already been detailed in chapter 4. The first terme accounts for the net variation of $C(\xi)$ due to division events while the second term accounts for the net variation of $C(\xi)$ due to detachment events. The third term in the right hand side of equation 7.6 accounts for the net variation of density of pairs at distance ξ. This term is given by:

$$\left(\frac{dC(\xi)}{dt}\right)_{motility} = \tag{7.7}$$

$$- \; m_1 C(\xi) + m_2 K\left(\frac{||\xi||}{w_v}\right) C(\xi) \tag{7.8}$$

$$+ \; m_2 \int K\left(\frac{||\xi''||}{w_v}\right) T(\xi, \xi'') d\xi''$$

$$+ \; m_1 \int K\left(\frac{||\xi'||}{w_m}\right) C_{bb}(\xi + \xi') d\xi'$$

$$- \; m_2 \int\int K\left(\frac{||\xi'||}{w_m}\right) K\left(\frac{||\xi''||}{w_v}\right) T(\xi + \xi', \xi'') d\xi' d\xi''$$

$$- \; m_2 \int K\left(\frac{||\xi + \xi'||}{w_v}\right) K\left(\frac{||\xi'||}{w_m}\right) C(\xi + \xi') d\xi'$$

The right-hand side is formed with 5 terms:

- the first term denotes for the pairs ij lost due to the migration of the individual i
- the second term corrects the first term by adding the effect of the individual j within the pair ij on the motility probability of the individual i
- the third term accounts for the effect of neighbors of a focal individual i on the its motility motility probability. This implies to consider the density of triplet formed with the pair ij and a neighbor k located at a distance ξ''
- the fourth term accounts for pairs ij created when the individual i originally located at a distance $\xi + \xi'$ from j moves with a distance $-\xi'$.
- the fifth term corrects the fourth term by including the effect of neighbors of i (other than the individual j on its motility probability
- finally the sixth term account for the effect of the individual j in the pair ij at distance $\xi + \xi'$ on the motility of the individual i

We attempt to solve the moment model as in the previous chapter by discretizing the distances ξ with a spatial step $d\xi = (d\xi_1, d\xi_2)$ and time with a constant timestep $\Delta t = 1$ using an explicit Euler scheme. However the resultant discretized system diverged after few steps. The decrease of the time step to 0.1 and to 0.01 did not prevent the divergence of the algorithm nor did the implementation of Runge-Kutta scheme (RK4). We presume that the difficulty in solving these equation is due to the rapid dynamic of the motility in comparison to division and detachment dynamic from one side and the discrepancy between the scale over which motility and birth occurs play.

7.4 Discussion and conclusion

In this chapter we show that the simplification of the polymer dynamic (IBM of chapter 6) still allow the obtainment of diversity of patterns including the labyrinth-like pattern that have been observed in laboratory biofilm experiments. In a system formed with a density-independent motile bacteria, the individuals tend to disperse and produce no spatial structure. Our model suggest that the formation of colonies in such system may result from density-dependent motility reduction process. The spatial pattern of the colonies seems to be influenced by local equilibrium between individuals 'entering' the colony through migration or division and individuals 'leaving' the colony through migration and detachment. In the absence of motility the yielded pattern is formed with isolated colony. However when density-dependent motility is considered the colonies may connect yielding the labyrinth-like patterns. The detachment kernel seems to play a role in maintaining the strips of the labyrinth separated. This structure yielded a cartesian correlation matrix with a peak in the center (indicating the tendency of the individual to aggregate due to the reduction of their motility) and a wavy structure due to the labyrinth-like pattern.

There are few attempts in the literature of approximating individual-based models with density-dependent motility using moment models. Murrell and Law [Murrell 2000] approximated an IBM of Beetles migration in a fragmented woodland. They considered a fixed landscape pattern and assumed that beetles are attracted by the locations corresponding to woodland. In their model, Murrell and Law considered only the motility process(no birth and death processes). In their paper, the size of the migration kernel was relatively small compared to the size of the domain. The interaction kernel (the equivalent of $K(||\xi||/w_v)$ in our work) is not specified explicitly in their work as they assumed that interaction occur exclusively when an individual enters a woodland patch. Implicitly, they consider an interaction kernel with a size corresponding to the size of a patch (equivalent to the spatial resolution $d\xi$ in our work). Though simpler than our model, Murrell and Law highlighted that there may be practical problems in the numerical integration of the dynamical system due, in their work, to the discrepancy between the scale of movement and the space scale of the woodland patterns.

In this work we meet comparable difficulties in the numerical integration of the moment model. We presume that in part the instability of our numerical scheme is due to the discrepancy between the spatial scales over which the different processes occur combined with the significant difference in the motility rate and birth and detachment rates. We hope to address these issues in a future work.

Chapter 8

Conclusion

Contents

This thesis takes place in the context of the debate between complex individual based models (IBMs) and more traditional differential equation models with a low number of variables. The use of individual-based models (IBMs) in microbial ecology has been growing rapidly during the last two decades, encouraged by the fast increase in computing power and advances in laboratory observation techniques. IBMs expand the toolbox of theoretical ecologists providing a valuable means to investigate how system-level properties emerge out of local interactions. However several reviews and textbooks on the use of IBMs in ecology (but also in other fields) pointed out some of the limitation of the approach. The complexity and limited generality are often quoted as the main limitations of individual-based modeling [Uchmanski 1996] [Grimm 1999]. IBMs evolve in a large state space as the description of the system requires the description of the state of all the individuals. A key question is whether all these state variables are necessary for the purpose of an investigation. A smaller model with a small number of aggregated state variables wouldn't be more appropriate ?

In this work, we try to reconcile these opposite points of view. Indeed, we investigate how practical and productive it is to approximate the dynamic of IBMs used in microbial ecology with aggregated mathematical models involving a small number of state variables. In particular, we assess whether these 'simpler' models capture successfully the spatio-temporal patterns yielded by the IBM. Several aggregated models of the literature describe complex microbial systems without referring explicitly to individuals, and as a first approach we compare in chapter 2 one of these models (a diffusion-reaction model) to an IBM of bacterial colony growth. The IBM explicitly represents the individual microbial cells and their variability. Comparisons of this type can be helpful as the deterministic model can provide us with a reference to which the IBM results can be compared. However, we show that the comparison can be difficult (even meaningless) when the aggregated model is derived independently of the IBM. One of the main difficulties is to assign appropriate values to the parameters of both models, especially when some of these parameters

have no clear physical meaning. In our example, we had to tune the parameters of the diffusion-reaction model empirically to obtain the best fit with the IBM.

Then we adopted a general approach involving two steps: (i) simplifying IBMs to transform them into clearer mathematical objects and (ii) deriving deterministic mathematical models which approximate some aggregated dynamics of this simplified IBM. We focused on moment approximation techniques which provide a valuable means to derive deterministic models on the middle ground between over-simplified mean-field models and intractable IBMs. In particular, this approach allows one to capture some important aspects of spatial dynamics. Chapter 3 and 4 illustrated how such models are derived on the example of the colony growth and planar biofilm development. The moment approach captures the main features of spatial pattern dynamics yielded by the IBM. The originality of the moment approach is in projecting the complexity of the IBM into a new state space where the variables are the average number of individuals (first spatial moment) and the average neighborhood of the individuals at different distances (second spatial moment given by the pair correlation function). The heterogeneities of the individual properties (mass and diameter) and their spatial extent are not considered by the moment model. The nutrient dynamic is also simplified and considered indirectly through density-dependent growth function (chapter 3). These substantial simplifications of the original IBM that did not prevent the moment model to reproduce the main statistical features of the IBM simulation.

In the second part of this thesis (chapter 5 to 7) we investigate how the full approach applies to a new individual-based model of biofilm formation involving motile bacteria, which motility is reduced by a self-excreted product (exopolymeric substances). The IBM attempts to explain the formation of patterns with interconnected microcolonies observed in recent biofilm experiments. Chapter 5 gives a detailed description of the IBM and qualitative comparison of the simulated patterns with those observed in experimental laboratory setting of *P. aeruginosa* cultivation., a model bacterium in biofilm research. In this part, the moment approach provided some interesting insights on the studied dynamics, but we also encountered some of its limitations and also some practical difficulties of implementation.

In chapter 6 we proposed a simplified version of the IBM obtained by neglecting the spatial extent of the bacteria and the dynamic of the nutrient. The excretion of extracellular product is considered in this first simplified model. We approximated the resultant IBM using moment approach and compared the patterns dynamics yielded by both models. The moment model captured the dynamic of the IBM in the case of immotile bacteria but failed in capturing the formation of colonies and the subsequent resultant transformation of the patterns. The detailed analysis of the IBM patterns shows that the colonies form when the local density of polymer reaches a threshold value causing the quasi immobilization of the individuals. This

may happens in few location within the domain due to the stochastic fluctuations of the individuals neighborhood but not necessary in average. As the moment model is based on the average neighborhood it misses this process. The example illustrates well one of the major limitation of the moment approach in dealing with the fluctuations especially if the individuals response to these fluctuations are non-linear or ruled by threshold values. In such a situation the aggregation of the IBM using first and second moment measures as state variable may not be appropriate.

Chapter 7 illustrates some of the technical limitations that may be encountered when implementing and solving moment models. We simplify further the IBM with motile bacteria by dropping the polymer dynamics and assuming that the bacteria motility is reduced by the increase of their local density. The resultant model is simpler to analyze though numerical experimentation and still reproduces the rich patterns that can be observed with the polymer. We discretized the moment model using either Euler scheme and RK4 but both time discretization schemes are unstable for the parameters that we considered. The discrepancy between the motility and birth kernel size and the significant difference between the time scale and mobility and the other processes are probably at the origin of these instabilities. We shall note however that the moment equations still miss a solid mathematical framework that allow the analysis of their properties.

8.1 Perspectives

The aggregation of individual-based models that arise in ecology, and microbial ecology in particular, is still in its infancy as a research field. There are few attempts in the microbial ecological literature to simplify the detailed IBMs and approximate their dynamics using a small number of aggregated state variables. The approach is more encountered in physics through the derivation of the master equation and its further reduction to simpler models. The difficulty to extend this approach to ecology lies in the richness and complexity of the ecological interactions. Living organisms, unlike inert interacting particles, have the capacity to adapt and evolve which may confer to the population new emergent properties. We believe that much research effort are still needed to develop reliable techniques for the aggregation and reduction of IBMs that arise in ecology.

Moment approximation can be useful in deriving new models where the local neighborhood of the individuals is considered explicitly as a state variable. They however have some limitations that may be overcome with an additional research effort. In particular tools and methods to analyze moment models are needed.

There are other techniques for deriving aggregated mathematical models that can be explored in future work. In particular, models of probability densities provide some average behaviors which are interesting to compare with the different runs of

the IBM, and can be complementary with the moment approximation. It can also be interesting to compute the second moment of these density models, and compare it with the second moment approximation.

Finally IBM simplification may yield "unrealistic" models but it seems to us necessary if we would like to generalize the IBM results and elaborate new theories, and explore how complex structures can emerge form interactions. Moreover, we hope that our work brought some convincing evidences that differential equation models approximating these IBMs can bring some insight about this process of emergence.

Bibliography

[Aas 2002] F. E. Aas, M. Wolfgang, S. Frye, S. Dunham, C. Lvold and M. Koomey. *Competence for natural transformation in Neisseria gonorrhoeae: components of DNA binding and uptake linked to type IV pilus expression.* Molecular Microbiology, vol. 46, no. 3, pages 749–760, 2002. 68

[Allesen-Holm 2006] M. Allesen-Holm, K. B. Barken, L. Yang, M. Klausen, J. S. Webb, S. Kjelleberg, S. Molin, M. Givskov and T. Tolker-Nielsen. *A characterization of DNA release in Pseudomonas aeruginosa cultures and biofilms.* Molecular Microbiology, vol. 59, no. 4, pages 1114–1128, 2006. 68, 79

[Alpkvist 2006] E. Alpkvist, C. Picioreanu, M.C.M. Van Loosdrecht and A. Heyden. *Three-dimensional biofilm model with individual cells and continuum EPS matrix.* Biotechnology and Bioengineering, vol. 94, pages 961–979, 2006. 79

[Alpkvist 2007] E. Alpkvist and I. Klapper. *A multidimensional multispecies continuum model for heterogenuous biofilm development.* Bulletin of Mathematical Biology, vol. 69, pages 765–789, 2007. 12, 13

[Arthur 1997] B. Arthur W., N. Durlauf S. and A. Lane D., editeurs. The economy as an evolving complex system ii. Santa Fe Institute Studies in the Science of Complexity, Readings, MA: Addison-Wesley, 1997. 1

[Aumann 2007] Craig A. Aumann. *A methodology for developing simulation models of complex systems.* Ecological Modelling, vol. 202, no. 3-4, pages 385–396, April 2007. 1, 4

[Barken 2008] K. B. Barken, S. J. Pamp, L.g Yang, M. Gjermansen, J. J. Bertrand, M. Klausen, M.l Givskov, C. B. Whitchurch, J. N. Engel and T. Tolker-Nielsen. *Roles of type IV pili, flagellum-mediated motility and extracellular DNA in the formation of mature multicellular structures in Pseudomonas aeruginosa biofilms.* Environmental Microbiology, vol. 10, no. 9, pages 2331–2343, 2008. 68, 79, 84

[Ben-Jacob 2000] E. Ben-Jacob, I. Cohen and H. Levine. *The Cooperative Self-Organization of Microorganisms.* Adv. Phys., vol. 49, pages 395–554, 2000. 12

[Birch 2006] A. Birch D. and R. Young W. *A master eaquation for a spatial population model with pair interactions.* Theoretical Population Biology, vol. 70, pages 26–42, 2006. 51, 56

[Bolker 1997] B. Bolker and S.W . Pacala. *Using Moment Equations to Understand Stochastically Driven Spatial Pattern Formation in Ecological Systems.* Theoretical Population Biology, vol. 52, no. 3, pages 179–197, December 1997. 6

[Brehm-Stecher 2004] B.F. Brehm-Stecher and E.A. Johnson. *Single-cell microbiology: tools, technologies and applications.* Microbial Molecular Biology Review, vol. 68, pages 538–559, 2004. 4

[Burel 2003] F. Burel and J. Baudry. Landscape ecology. Science Publishers, 2003. 84

[Button 1993] D.K. Button. *Nutrient-limited microbial growth kinetics: overview and recent.* Antonie van Leeuwenhoek, vol. 63, pages 225–235, 1993. 16

[Cogan 2004] N. Cogan and J.P. Keener. *The role of the biofilm matrix in structural development.* Math. Med. and Biol, vol. 21, pages 147–166, 2004. 12, 13

[Costerton 1995] JW Costerton, Z Lewandowski, DE Calcwell, DR Korber and HM Lappin-Scott. *Microbial biofilms.* Annu Rev Microbiol, vol. 49, pages 711–745, 1995. 12, 68

[Crawford 2005] W. Crawford J., K. Ritz Harris and M. Young I. *Towards an evolutionnary ecology of life in soil.* Trends Ecol. Evol., vol. 20, pages 81–87, 2005. 1

[Dalton 1994] H.M. Dalton, L.K. Poulsen, P. Halaz, M.L. Angles and A.E. Goodman. *Substratum-induced morphological changes in a marine bacterium and their relevance to biofilm structure.* Journal of Bacteriology, vol. 176, pages 6900–6906, 1994. 79

[Dalton 1996] H M Dalton, A E Goodman and K C Marshall. *Diversity in surface colonization behavior in marine bacteria.* Journal of Industrial Microbiology and Biotechnology, vol. 17, no. 3, pages 228–234, September 1996. 79

[Davey 2000] M.E. Davey and G.A. O'Toole. *Microbial Biofilms: from Ecology to Molecular Genetics.* Microbiology And Molecular Biology Reviews, vol. 12, pages 847–867, 2000. 68

[Deffuant 2004] G. Deffuant. *Modeliser la complexite: quelques pistes pour relever le defi.* Rapport technique, Memoire d'Habilitation a Diriger des Recherches. Ecole Doctorale SPI. Universite Blaise Pascal de Clermont-Ferrand, 2004. 1, 5

[Deffuant 2005] G. Deffuant, S. Huet and F. Amblard. *An individual-based model of innovation diffusion mixing social value and individual benefit. American Journal of Sociology 110-4, 1041-1069.* American Journal of Sociology, vol. 110, pages 1041–1069, 2005. 1

[Dens 2005] E.J. Dens, K. Bernaerts, A.R. Standaert, J.U. Kreft and J.F. Van Impe. *Cell division theory and individual-based modelling of microbial lag. Part II. Modeling lag phenomena induced by temperature shifts.* Journal of Food Microbiology, vol. 101, pages 319–332, 2005. 2

[Dieckmann 1999] U. Dieckmann. *From Individuals to Populations: Systematic Model Reduction in Evolutionary Theory and Spatial Ecology.* Rapport technique, Habilitation report - Wien University, 1999. 31

[Dieckmann 2000] U. Dieckmann, R. Law and J.A.J Metz. The geometry of ecological interactions: simplifying spatial complexity. Cambridge University Press, 2000. 2, 6, 29, 37, 42, 43, 61

[Dockery 2001] J. Dockery and I. Klapper. *Finger formation in biofilm layers.* SIAM J. APPL. Math., vol. 62, pages 853–869, 2001. 13

[Eberl 2001] J. Eberl H., D.F. Parker and M.C.M. Van Loosdrecht. *A new deterministic spatio-temporal continu mode for biofilm development.* Journal of Theoretical Medicine, vol. 3, pages 161–175, 2001. 8, 11, 12, 13, 18, 21, 22

[Emonet 2005] T. Emonet, C.M. North, C.E. Wickersham and P. Cluzel. *AgentCell: a digital single-cell assay for bacterial chemotaxis.* Bioinformatics, vol. 21, pages 2714–27, 2005. 2

[Ferrer 2008] J. Ferrer, C. Prats and D. Lopez. *Individual-based Modelling: An Essential Tool for Microbiology.* J Biol Phys, vol. 34, pages 19–37, 2008. 2, 69

[GIllespie 1976] T. GIllespie D. *A general method for numerically simulating the stochastic time evolution of coupled chemical reactions.* Journal of Computational Physics, vol. 22, pages 403–434, 1976. 31, 89

[Ginovart 2002] Marta Ginovart, Daniel Lopez and Joaquim Valls. *INDISIM, An Individual-based Discrete Simulation Model to Study Bacterial Cultures.* Journal of Theoretical Biology, vol. 214, no. 2, pages 305–319, January 2002. 2, 69

[Grimm 1999] Volker Grimm, Tomasz Wyszomirski, David Aikman and Janusz Uchmanski. *Individual-based modelling and ecological theory: synthesis of a workshop.* Ecological Modelling, vol. 115, no. 2-3, pages 275–282, February 1999. 2, 131

[Grimm 2005] Volker Grimm and Steven F. Railsback. Individual-based modeling and ecology. Princeton University Press, 2005. 4, 5, 84

[Grimm 2006] Volker Grimm, Uta Berger, Finn Bastiansen, Sigrunn Eliassen, Vincent Ginot, Jarl Giske, John Goss-Custard, Tamara Grand, Simone K. Heinz, Geir Huse, Andreas Huth, Jane U. Jepsen, Christian Jorgensen, Wolf M. Mooij, Birgit Muller, Guy Pe'er, Cyril Piou, Steven F. Railsback, Andrew M. Robbins, Martha M. Robbins, Eva Rossmanith, Nadja Ruger, Espen Strand, Sami Souissi, Richard A. Stillman, Rune Vabo, Ute Visser and Donald L.

DeAngelis. *A standard protocol for describing individual-based and agent-based models.* Ecological Modelling, vol. 198, no. 1-2, pages 115–126, September 2006. 3, 5, 7, 8, 12, 69

[Grimson 1994] M. Grimson and G. Barker. *Continuum model for the spatiotemporal growth of bacterial colonies.* Phys Rev E, vol. 49, pages 1680–1684, 1994. 12

[Gujer 2002] W. Gujer. *Microscopic versus macroscopic biomass models in activated sludge systems.* Water Science and Technology, vol. 46, pages 1–11, 2002. 2

[Hellweger 2009] F.L. Hellweger and V. Bucci. *A bunch of tiny individuals - Individual-based modeling for microbes.* Ecological Modelling, vol. 220, pages 8–22, 2009. 2, 4, 69

[Hernàndez-Garcià 2004] López C. Hernàndez-Garcià E. *Clustering, advection and patterns in a mode of population dynamics with neighborhood-dependent rates.* Phys Rev E, vol. 70, 2004. 56

[Johnson 2008] Leah R. Johnson. *Microcolony and biofilm formation as a survival strategy for bacteria.* Journal of Theoretical Biology, vol. 251, no. 1, pages 24–34, March 2008. 84

[Klausen 003a] M. Klausen, A. Heydorn, P. Ragas, L. Lambertsen, A. Aaes-Jorgensen, S. Molin and T. Tolker-Nielsen. *Biofilm formation by Pseudomonas aeruginosa wild type, flagella and type IV pili mutants.* Molecular Microbiology, vol. 48, no. 6, pages 1511–1524, June 2003a. 68, 79

[Klausen 003b] M. Klausen, A. Aaes-Jorgensen, S. Molin and T. Tolker-Nielsen. *Involvement of bacterial migration in the development of complex multicellular structures in Pseudomonas Aeruginosa biofilms.* Molecular Microbiology, vol. 50, no. 1, pages 61–68, October 2003b. 68, 77, 79

[Koch 1993] L. Koch A. *Biomass growth rate during the prokaryote cell cycle.* Crit Rev Microbiol, vol. 19, pages 17–42, 1993. 16

[Kreft 1998] J.U. Kreft, G. Booth and Wimpenny J.W.T. *Bacsim, a simulator for individual-based modelling of bacterial colony growth.* Microbiology, vol. 144, pages 3275–3278, 1998. 1, 8, 11, 13, 16

[Kreft 1999] J U Kreft, G Booth and J W T Wimpenny. *Applications of individual-based modelling in microbial ecology.* In Johnson Green Bell C R Brylinsky M, editeur, Microbial Biosystems: New Frontiers. Proceeding of the 8th International Symposium on Microbial Ecology, 1999. 2

[Kreft 2001] Jan-Ulrich Kreft, Cristian Picioreanu, Julian W.T. Wimpenny and Marck C.M. van Loosdrecht. *Individual-based modelling of biofilms.* Microbiology, vol. 147, pages 2897–2912, 2001. 2, 3, 11, 12, 16, 69, 71, 75

[Lacasta 1999] A.M. Lacasta, I.R. Cantalapiedra, C.E. Auguet, A. Pearanda and L. Ramirez-Piscina. *Modelling of spatio-temporal patterns in bacterial colonies.* Phys. Rev. E, vol. 59, pages 7036 – 7041, 1999. 12

[Laspidou 2009] C.S. Laspidou, A. Kungolos and P. Samaras. *Cellular-automata and individual-based approaches for the model of biofilm structure: Pros and cons.* Desalination, vol. Article in Press, 2009. 3

[Law 2000] R. Law and U. Dieckmann. Moment approximations of individual-based models, chapitre 14, pages 252–270. Cambridge University Press, 2000. 38

[Lee 2001] C. Lee, M. Hoopes, J. Diehl, W. Gilliland, G. Huxel, E. Leaver, K. McCann, J. Umbanhowar and A. Mogilner. *Non-local concepts and models in biology.* Journal of Theoretical Biology, vol. 210, pages 201–219, 2001. 84

[Levin 1998] S. A. Levin. *Ecosystems and the biosphere as complex adaptative systems.* Ecosystems, vol. 1, pages 431–436, 1998. 1

[Lobry 2003] C. Lobry. *Modèles mathématiques et modèles informatiques, sur la théorie du modèle.* Annales des Ponts et Chaussées, vol. 107-108, pages 10–18, 2003. 1

[Lu 2005] Ann Lu, Kyunyung Cho, Wesley P. Black, Xue-yan Duan, Renate Lux, Zhaomin Yang, Heidi B. Kaplan, David R. Zusman and Wenyuan Shi. *Exopolysaccharide biosynthesis genes required for social motility in Myxococcus xanthus.* Molecular Microbiology, vol. 55, no. 1, pages 206–220, 2005. 84

[Luke 2004] S. Luke, C. Cioffi-Revilla, L. Panait and K. Sullivan. *MASON : A Java Multi-Agent Simulation Toolkit.* Proceedings of the 2004 SwarmFest Workshop, 2004. 8, 76

[McKane 2004] A. J. McKane and T. J. Newman. *Stochastic models in population biology and their deterministic = analogs*, October 2004. 4

[Morgenroth 1997] E. Morgenroth, T. Sherdena, M. C. M. Van Loosdrecht M.C.M., J.J. Heijnen and P.A. Wilderer. *Aerobic granular sludge in a sequencing batch reactor.* Water Research, vol. 31, pages 3191–3194, 1997. 12

[Morgenroth 2000] E. Morgenroth and P.A. Wilderer. *Influence of detachment mechanisms on competition in biofilms.* Water Research, vol. 34, pages 417–426, 2000. 54

[Murphy 2008] T. Murphy J., R. Walshe and M. Devocelle. *An Agent Based Approach to Modelling Microbial Ecosystems.* ERCIM News, vol. (april), 2008. 2

[Murray 2001] J.D. Murray. Mathematical biology: I. an introduction. Springer, 3rd ed. 2001. 11

[Murrell 2000] D.J. Murrell and R. Law. *Beetles in fragmented woodlands: a formal framework for dynamics of movement in ecological landscapes.* Journal of Animal Ecology, vol. 69, no. 3, pages 471–483, 2000. 5, 6, 129

[O'Toole 2000] G. O'Toole, H. Kaplan and R. Kolter. *Biofilm formation as microbial development.* Annu Rev Microbiol, vol. 54, pages 49–79, 2000. 2

[Parsek 2008] Matthew R Parsek and Tim Tolker-Nielsen. *Pattern formation in Pseudomonas aeruginosa biofilms.* Current Opinion in Microbiology, vol. 11, no. 6, pages 560–566, December 2008. 68, 84

[Picioreanu 2004] Cristian Picioreanu, Jan-Ulrich Kreft and Mark C. M. van Loosdrecht. *Particle-Based Multidimensional Multispecies Biofilm Model.* Appl. Environ. Microbiol., vol. 70, no. 5, pages 3024–3040, 2004. 2, 3, 11, 12

[Picioreanu 2005] C. Picioreanu, D.J. Batstone and M.C.M. Van Loosdrecht. *Multidimensional modelling of anaerobic granules.* Water Science and Technology, vol. 53, pages 501–507, 2005. 2

[Picioreanu 2007] C. Picioreanu, J-U Kreft, M. Klaussen, J.A.J. Haagensen, T. Tolker-Nielsen and S. Molin. *Microbial mobility involvement in biofilm structure formation - a 3D modelling study.* Water Science & Technology, vol. 55, pages 337–343, 2007. 69, 76, 77, 79

[Railsback 2001] F. Railsback Steven. *Concepts from Complex Adaptative Systems as a Framework for Individual-based Modelling.* Ecological Modelling, vol. 139, pages 47–62, 2001. 1

[Rammel 2007] C. Rammel, S. Stagl and H. Wilfing. *Managing Complex Adaptive systems: A Co-Evolutionary Perspective on Natural Resource Management.* Ecological Economics, vol. 63, pages 9–21, 2007. 1

[Schmid 2003] M. Schmid, A. Thill, U. Purkhold, M. Walcher, J.-Y. Bottero, P. Ginestet, P.H. Per Halkjaer Nielsen, S. Wuertz and M. Wagner. *Characterization of activated sludge flocs by confocal laser scanning microscopy and image analysis.* Water Research, vol. 37, pages 2043–2052, 2003. 12

[Stewart 1993] P. S. Stewart. *A Model for Biofilm Detachment.* Biotech Bioeng, vol. 41, pages 111–117, 1993. 54

[Tolker-Nielsen 2000] Tim Tolker-Nielsen, U. C. Brinch, P. C. Ragas, J. B. Andersen, Carsten Suhr J. and S. Molin. *Development and Dynamics of Pseudomonas sp. Biofilms.* J. Bacteriol., vol. 182, no. 22, pages 6482–6489, November 2000. 54

[Treuil 2008] J.P. Treuil, D. Zucker and A. Drogoul. Modélisation et simulation à base d'agents. 2008. 3

[Uchmanski 1996] Janusz Uchmanski and Volker Grimm. *Individual-based modelling in ecology: what makes the difference?* Trends in Ecology & Evolution, vol. 11, no. 10, pages 437–441, October 1996. 3, 131

[Van Baalen 2000] M. Van Baalen. The geometry of ecological interactions: Simplifying spatial complexity,, chapitre Pair approximations for different spatial geometries, pages 359–387. Cambridge University Press, 2000. 7

[Van Schaik 2005] E.J. Van Schaik, C.L. Giltner, G.F. Audette, D.W. Keizer, D.L. Bautista, C.M. Slupsky, B.D. Sykes and R.T. Irvin. *DNA Binding: a Novel Function of Pseudomonas aeruginosa Type IV Pili.* Journal of Bacteriology, vol. 187, no. 4, pages 1455–1464, February 2005. 68

[Vlachos 2006] C. Vlachos, R.C. Paton, J.R. Saunders and Q.H. Wu. *A rule-based approach to the modelling of bacterial ecosystems.* Biosystems, vol. 84, pages 49–72, 2006. 3

[Whitchurch 2002] C.B. Whitchurch, T. Tolker-Nielsen, Paula C. Ragas and John S. Mattick. *Extracellular DNA required for bacterial biofilm formation.* Science, vol. 295, pages 1487–1487, 2002. 68, 79

[Xavier 2005] Joao B. Xavier, Cristian Picioreanu and Mark C. M. van Loosdrecht. *A framework for multidimensional modelling of activity and structure of multispecies biofilms.* Environmental Microbiology, vol. 7, pages 1085–1103, 2005. 2, 11, 69

[Xavier 2009] J.B. Xavier, E. Martinez-Garcia and K.R. Foster. *Social Evolution of Spatial Patterns in Bacterial Biofilms: when conflict drives disorder.* The American Naturalist, vol. 174, pages 1–12, 2009. 119, 120